



UNIVERSITÀ
DEGLI STUDI
DI PADOVA

University of Padua
Department of Agronomy, Food, Natural resources, Animals, Environment

PhD School In Crop Science
Cycle: XXVIII

***Integration of proximal sensing and crop modelling to optimize N
variable fertilization on cereals***

Head of the School : Ch.mo Prof. Antonio Berti

Supervisor: Ch.mo Prof. Giuliano Mosca

Co-supervisor: Ch.mo Prof. Francesco Morari

PhD student : Valentina Zanella

Declaration

I hereby declare that this submission is my own work and that, to the best of my knowledge and belief, it contains no material previously published or written by another person nor material which to a substantial extent has been accepted for the award of any other degree or diploma of the university or other institute of higher learning, except where due acknowledgment has been made in the text.

February 1st 2016

Valentina Zanella

A copy of the thesis will be available at <http://paduaresearch.cab.unipd.it/>

Dichiarazione

Con la presente affermo che questa tesi è frutto del mio lavoro e che, per quanto io ne sia a conoscenza, non contiene materiale precedentemente pubblicato o scritto da un'altra persona né materiale che è stato utilizzato per l'ottenimento di qualunque altro titolo o diploma dell'università o altro istituto di apprendimento, a eccezione del caso in cui ciò venga riconosciuto nel testo.

1 Febbraio 2016

Valentina Zanella

Una copia della tesi sarà disponibile presso <http://paduaresearch.cab.unipd.it>

Table of contents

Riassunto	9
Summary	11
List of abbreviations	13
Chapter I	15
General introduction	15
1.1. Challenges in cereal production	15
1.2. Causes of low NUE in N fertilization management	16
1.3. Precision agriculture as a way to improve NUE.....	17
1.4. Fundaments of site-specific fertilization	18
1.5. Benefit of site-specific N management	20
1.6. Aims of the work	20
1.7. References	22
Chapter II	29
Understanding the effect of site-specific fertilization on yield and protein content in durum wheat: prodrome to site-specific harvest	29
2.1. Introduction	29
2.2. Materials and methods	31
2.2.1 Study Site.....	31
2.2.2 Identification of management zones and VR fertilization.....	32
2.2.3 Data collection.....	36
2.2.3.1 NDVI measurements	36
2.2.3.2 Grain harvest and post-harvest analysis	36
2.2.4 Statistical analysis	37
2.3 Results	37
2.3.1 NDVI measurements	37
2.3.2 Yield and protein content	42
2.3.4 Grain quality	46
2.3.5 N balance and N efficiency	48
2.4. Discussion and conclusions	49

2.5. References	52
Chapter III.....	57
Coupling proximal sensing, medium weather forecasts an crop modelling to optimize in nitrogen variable rate application in durum wheat	57
3.1 Introduction	57
3.2 Materials and methods.....	59
3.2.1 Study Site description and management	59
3.2.2 Site- specific fertilization	61
3.2.3 Yield and protein content data	66
3.2.3 Data processing and statistical analysis	67
3.3 Results	68
3.3.1 Model calibration	68
3.3.2 Medium term weather forecast and crop response to N fertilization	70
3.3.3 Identification of the optimum N rate.....	70
3.3.3 NDVI – N uptake relation and NDVI measurements across the field	72
3.3.4 Prescription map.....	74
3.3.4 Yield and protein content maps.....	74
3.3.5 Environmental and economic indicators	76
3.3.6 N rich strips	76
3.4 Discussions and conclusions	78
3.5 References	81
Chapter IV	87
Combining proximal sensing and simulation modelling to assess within-field corn N stress	87
4.1. Introduction	87
4.2. Materials and methods.....	90
4.2.1 Study Site	90
4.2.2 Weather data and soil sampling	94
4.2.3 NDVI collection	95
4.2.4 LAI measurements	95
4.2.5. Data processing	96

4.2.6	Model calibration.....	97
4.2.6	Model validation and statistical methods for performance assessment.....	101
4.2.7	Identification of the optimum N rate	101
4.3.	Results and discussions	103
4.3.1	Calibration of the model to simulate yield	103
4.3.2	NDVI variability.....	104
4.3.3	Calibration of the model to simulate LAI variability	110
4.3.4	Nitrogen stress simulation	113
4.3.5	Evaluation of the optimum N rate	115
4.4.	Conclusions	121
4.5.	References.....	122
Chapter V.....	127
Overall conclusions	127
5.1	References	129

Riassunto

Nonostante i recenti progressi della tecnica agronomica, la fertilizzazione azotata riporta ancora una bassa efficienza (NUE), con conseguenti ingenti perdite di N nell'ambiente. Questo problema è di particolare importanza in zone vulnerabili ai nitrati, come il bacino scolante della Laguna di Venezia.

Somministrando azoto in maniera sito-specifica in base ai bisogni della coltura, la N-VRA (*variable rate application*) rappresenta una strategia per incrementare l'efficienza della fertilizzazione. Nonostante i provati benefici economici ed ambientali derivanti da questa tecnica, una limitazione deriva dalla difficoltà nella stima della resa finale al momento della concimazione. Questo può causare casi di sottostima o sovrastima o delle dosi che causano da un lato perdite economiche e dall'altro un elevato surplus di N nel suolo.

In questa tesi sono state valutate differenti strategie di N-VRA nel bacino scolante della Laguna di Venezia.

Nel primo esperimento di campo (Capitolo III) è stata applicata una N-VRA basata su zone omogenee in grano duro e ne sono stati studiati gli effetti sulla produzione. Inoltre, l'uso di sensori montati sulla mietitrebbia e le analisi spettrofotometriche della composizione del glutine hanno permesso di studiare l'effetto della concimazione azotata tardiva e della N-VRA sulla qualità della granella e di valutare l'attuabilità di una raccolta sito-specifica.

Due diversi metodi di integrazione di misure spettrali e modellistica colturale sono state proposti nei Capitoli III e IV.

Nel capitolo III è stato studiato un approccio innovativo per l'assimilazione di *proximal sensing*, previsioni meteorologiche e modelli colturali per ottimizzare la concimazione al grano duro. Dopo aver condotto una calibrazione con dati raccolti nel precedente esperimento, è stata simulata la dose ottimale per ogni zona omogenea, che è stata corretta successivamente in base ai valori di NDVI misurati su tutto l'appezzamento.

Nel capitolo IV i dati spettrali sono stati integrati al modello per migliorare l'accuratezza della simulazione della carenza di N in mais, e valutare la dose ottimale di N da distribuire in grado di minimizzare lo stress. Il modello è stato inizialmente calibrato per simulare

correttamente la resa e successivamente per far coincidere il LAI (leaf are index) simulato con quello ricavato dalle misurazioni di NDVI.

Nel capitolo V vengono riportate le conclusioni generali, sottolineando sia in benefici derivanti da queste strategie di N-VRA, sia le limitazioni.

Summary

Despite recent advances in agronomical techniques, N fertilization still shows low efficiency (NUE), with consequently high N loss in the environment. This could be particularly relevant in nitrate vulnerable zones, as the Venice Lagoon watershed, in which N leaching represents a serious risk for water pollution. Applying N site specifically accordingly to crop need, N -VRA (variable rate application) represents a strategy to increase NUE. Although this approach has been proved to provide environmental benefit, a drawback in its application arises from the difficulties to predict precisely final crop yield at the time of fertilizing. This can result in under or over- fertilization which results on one hand in economic loss and on the other in a large N balance on the soil.

In this dissertation different approaches N-VRA application were evaluated in the Venice Lagoon Border, and their benefits in term of enhancing grain production and economic and environmental sustainability were evaluated.

In the first experiment (Chapter II), a two-years field trial was managed to investigate the effect of N-VRA based on management zones on durum wheat final production. Furthermore, the use of real time sensors on a combine- harvester and the spectrophotometric analysis of gluten composition allowed to evaluate the influence of late N foliar fertilization and N-VRA on grain quality and to verify the feasibility of zone-harvesting.

In Chapters III and IV two different strategies of integration of spectral measurements and crop modelling were proposed.

An innovative approach of coupling proximal sensing, medium weather forecasts and crop modelling to optimize N-VRA in durum wheat was proposed in Chapter III. After calibration with data collected in the first experiment, the model was run in each management zone with weather forecasts to evaluate N optimum rate, which was then corrected based on NDVI data.

In Chapter IV proximal sensing and crop modelling were integrated in order to improve within-field estimation of N stress on corn and therefore optimize N fertilization. In this case model accuracy in N stress prediction was improved optimizing the model to properly predict the yield and subsequently to match the simulated and the NDVI-derived

LAI (leaf area index). The optimized model was subsequently run to evaluate optimum N rates able to minimize N stress.

General conclusions were drawn in Chapter V, underlining both the benefits and the limitations of these N-VRA approaches.

List of abbreviations

CEC	Cation exchange capacity
DAS	Days After Sowing
DUL	Drained Upper Limit
EC _a	Electrical conductivity
GDD	Growing Degree Days
GDU	Growing Degree Units
HMW-GS	High Molecular Weight Glutenin Subunit
LAI	Leaf Area Index
LL	Lower limit
LMW-GS	Low Molecular Weight Glutenin Subunit
MZ	Management Zone
NDVI	Normalized Difference Vegetation Index
N _{in}	N input
NIR	Near Infrared
N _{out}	N output
N _{up}	N Uptake
NST	Nitrogen Stress
N - VRA	Nitrogen Variable Rate Application
NUE	Nitrogen Use Efficiency
NVZ	Nitrate Vulnerable Zone
PHINT	Phyllochron
SOM	Soil Organic Matter
ss	Sostanza Secca
VI	Vegetation Index

Chapter I

General introduction

1.1. Challenges in cereal production

The drastic increase in global population since '60s has been supported by a more than double increasing in food supply. Cereals production showed an extraordinary growth: in 1961 agriculture fed 3.075 billion people producing 0.876 billion t of cereals, while in 2011 more than double the population (7.013 billion people) was fed with an amount of cereals more than three times greater (2.852 billion tons). Among cereals nowadays wheat is the most cultivated cereal (711 Mt in 2013), while corn is the first in terms of total production (1017.536 Mt). This trend was paired by a decrease in arable land pro capita (-52.70%) (FAOSTAT, 2015), and a subsequent intensification of agricultural systems, which almost triplicated the yields of the major cereals, but led to negative consequences for the environment, such as air and water pollution and decrease in biodiversity (Matson et al., 1997). The largest environmental issues are related to the high amount of synthetic N supplied: nowadays agriculture emissions are quantified in more than 5 millions Gg of CO₂ equivalent and more than 770000 Gg of CO₂ came from synthetic N use and production (FAOSTAT, 2015). Furthermore, N cycle in the soil leads to gaseous emissions: N₂O produced by nitrification and denitrification contributes to greenhouse effects and pollution, (Sahrawat and Keeney, 1986), as well as ammonia volatilization (Bosch-Serra et al., 2014). The massive N application leads also to N leaching, responsible for water eutrophication and drinking water pollution

This dangerous environmental contamination is due also to current N management strategies with low N Use efficiency (NUE) (Cassman et al., 2002; Fageria and Baligar, 2005; Shanahan et al., 2008).

In 1999 Raun and Johnson estimated that NUE (Nitrogen Use Efficiency) in cereal production was close to 33%. This means that 67% of the applied N was not converted into

grain N, and got lost in the environment. Even though agronomical techniques have recently improved, N balance in the soil is still largely positive. In 2011 in European Union 132 kg N ha⁻¹ were distributed and only 32% of this total amount was removed from the system harvesting the crops, leaving in the soil a gross balance of 47 kg N ha⁻¹, which 61% are represented by N emissions (EUROSTAT, 2015).

Recognizing modern agriculture as the major source of N discharge in the environment, in 1991 European Union signed the European Nitrate Directive (91/676/CEE), aiming to protect waters against pollution caused by nitrates from agricultural sources and forcing each member state to take measures (Action Plans) to achieve this goal. The Nitrate Directive underlined as causes of nitrate pollution risk the large positive N balance in the soil, agricultural practices as the excessive distribution of N under organic forms, the low level of crop growth, and environmental factors influencing the formation of nitrates by mineralization. Since 2011 46.7% of the EU land area has been subjected to the Action Plans, and considered as NVZ (Nitrate Vulnerable Zone). Even if the Nitrate Directive has been shown to contribute to reduce ammonia and nitrate oxide emissions, due to better manure management and optimal fertilizer application based on crop need, 14.4% of the groundwater stations still exceeded the limit of 50 mg l⁻¹ and 5.9% were between 40 and 50 mg l⁻¹ (Report from the period 2008-11).

In some cases Nitrate Directive failed in its aims, and was always not accomplished by farmers (MacGregor and Warren, 2006; Worrall et al., 2009; Barnes et al., 2009; Mouratiadou et al., 2010). Furthermore, the recent diffusion of organic farming has worsened the nitrate water pollution risk (Mondelaers et al., 2009).

1.2. Causes of low NUE in N fertilization management

Shanahan et al (2008) reviewed the causes for low NUE in current management systems. The poor synchrony between N application and crop demand increases the opportunity for N loss. In both wheat and corn, N pre-plant application has been proved to be the most inefficient N fertilization method (Mahler et al., 1994; Randal et al., 2003). Many studies showed that split N amount increased NUE and consequently reduced N loss (Sowers et al., 1994; Martin et al., 1994; Power et al., 2000; Woolfolk et al., 2000). Even if

the benefits of in-season N fertilization are well known, current limits to its adoption are due to a lack of cost-effective and practical technologies (Cassman et al., 2002).

Uniform rate application was identified as a further factor of low NUE. In many fields a spatially variable fertility justifies in terms of economic and environmental benefits the adoption of site-specific fertilization (Sharf et al., 2005; Mamo et al., 2003; Cambardella et al., 1993; Stewart et al., 2002).

A further reason for low NUE was found on the derivation of N recommendation from yield goal. Following this mass-balance approach farmers set N rates before planting, based on the yield they want to reach and N in grain, correcting for a N efficiency coefficient, and giving some credit for other N sources. For example, in Oklahoma fertilization recommendations for wheat suggested to consider as a yield goal the production of the previous 5 years, and apply 33 kg N ha⁻¹ for 1000 kg of wheat, and subtract soil NO₃ level grain (Schmitt et al., 1998). Similarly, Johnson et al. (1977) suggested to distribute 20 kg N ha⁻¹ for 1000 kg of corn. This approach assumed a constant NUE over time and locations, which was proved to vary (Arnall et al., 2009). Long term experiments conducted by Miao et al. (2006) and Johnson and Raun (2003) showed that the demand for N fertilizer is unpredictable, due to environment influence. In addition, spatial variability influences N need, indeed different N rates are needed to reach the same yield level across the field (Sharf, 2005).

In-season N fertilization could also be managed adjusting soil N availability, using PSNT (pre-side-dress soil NO₃ test) to evaluate available N mineralized in soil. (Magdoff et al., 1994; Schröder et al., 2000; Bundy and Andraski, 2013), but this method does not take into account environmental fluctuation affecting yield potential, and a soil sampling campaign able to identify soil spatial variability is required.

1.3. Precision agriculture as a way to improve NUE

When N amount in the soil and factors driving N availability for the crop vary among the field, a precision N management can be applied, supplying VR (variable rate) N accordingly to crop specific needs. The aim of precision agriculture (PA) is defined by Pierce et al. (1994) as the matching of agronomical inputs and techniques to localize condition within a field to do the right thing, in the right place, at the right time, in the right way. Nowadays, the available technology offers the chance to manage site- specifically

sowing and tillage (Basso et al., 2001), irrigation (Bronson et al., 2005; Vellidis et al., 2008), crop protection (Christensen et al., 2009) and fertilization.

1.4. Fundamentals of site-specific fertilization

As in traditional farming systems, N application can be managed following two strategies. In the prevention approaches N supply is determined early on the season, or before plant rapid N uptake, in order to avoid deficiencies. A second approach is based on the evaluation of the actual plant N status at the moment of maximum N uptake. In addition, mixed strategies can be applied, supplying a first N rate early in the growing season, and a second one later, according to plants requirements (Pierce and Nowark, 1999).

Prescription maps for site-specific fertilization can be produced bases on the management zone approach, or on the go crop sensing. Management zones (MZ) are units in the field homogenous for some yield limiting factors for which the application of a single rate or specific input is justified (Franzen and Kitchen, 2000). MZs could be created based on soil properties (Johnson et al., 2000; Fleming et al., 2000), landscape position, (Fridgen et al., 2000), crop aerial photographs (Long et al. 1994) or on previous production maps. Yield maps provide information of the integrated effect of physical, chemical and biological processes under certain weather conditions (van Uffelen et al., 1997). Harvest maps provide also a quantification of the nutrient removal and the re-establishment of the N amount taken off could be a criteria guiding VR fertilization. This N maintenance application presumes that the N amount supplied to the previous crop was sufficient. N is the only factor of soil depletion (Heege, 2013).

The MZs approach assumes that yield is greatly influenced by the factors chosen in the zone delineations and spatial variability is high, but it is static year to year. Furthermore, homogenous zones could be not able to completely explain spatial variability: information about temporal and spatial variability could be not sufficient (van Uffelen et al., 1997).

Sensing of crop properties on the go and real time control offers great potentiality for VR N application, providing an estimation of the interactions between plant and soil and of the actual N uptake (Heege et al., 2008). Different approaches have been applied: use of reflectance sensors, introduced by Heege and Reusch (1996); chlorophyll fluorescence,

induced by laser radiation (Gunther et al., 1999) and mechanical pendulum (Ehlert et al., 2004).

Nitrogen has a double effect on plant reflectance: on one hand the increasing in chlorophyll concentration caused by N leads to a decrease in reflectance in the PAR (Photosynthetic Active Radiation) wavelengths; on the other, the higher plant biomass and specifically LAI (Leaf Area Index), supported by N uptake, causes an increase in reflectance in the NIR (near infrared region) (Brooge and LeBlanc, 2000; Daughtry et al., 2000; Gitelson, 2004; Yoder and Pettigrew-Crosby, 1995). The red edge inflection point expresses the transition between red and infrared reflectance, and moves to longer wavebands where higher N amounts are distributed. Many bands are needed to have data in the red and infrared region are available with high definition. Vegetation index (VI derived from a mathematical calculation involving spectral reflectance in two or more wavelengths, more responsive to changes in biomass than individual wavelengths (Wanjura and Hatfield, 1987). NDVI expresses the normalized ratio between red and infrared reflection (Rouse, 1973). It has been widely used in site specific N rate optimization algorithms (Raun et al., 2002; Holland and Schepers, 2010), relating this VI to potential yield and/or crop responsiveness to N application.

Even if the application of these algorithms have shown an improvement of NUE and consequently environmental benefits (Raun, 2002; Tubana et al., 2008), some drawbacks have been observed.

Firstly, they have to be robust for different field conditions and this requires data collection over multiple years and locations (Raun, 2005), which require time and resources consuming (Raun, 2004).

In addition, spectral indexes are not stress- specific and their use should be limited to situations where N is the only limiting factor, and reasons for low plant grow are completely understood before application (Zillman et al., 2006).

Furthermore, to optimize the benefit of the algorithms, sensing and N application have to be done at the finest spatial resolution (Legnick et al. 1997), but this is limited by the resolution of available information and technical characteristics of the sprayers.

Thus, the more important issue is that crop response after sensing is not taken into account, and this could lead to cases of over or under fertilization, due to unpredictable weather conditions affecting final yield (Holland, 2013).

1.5. Benefit of site-specific N management

Over 20 years of VR N application, researcher have found discordant results in terms of economic and environmental advantages.

Bongiovanni and Lonwenberg-Deboer (2004) revised the contributions of precision farming in improving the sustainability of production agriculture. Even if in some cases no differences between VR and uniform N fertilization were observed probably due to low spatial variability (Redulla et al., 1996; Roberts et al., 2001), several studies showed that site specific N fertilization could reduce nitrate leaching and improve NUE. Delgado et al (2005), for example, proved that a reduction of 25% in N₀₃-N leaching occurred during the first year after VR N application, while Larson et al (1997) reported a reduction of 50%. Casa et al. (2011) showed than a management zones fertilization approach based on nitrogen balance allowed to distribute a lower N amount, but did not differ from a uniform application in terms of grain yield, nitrate content in the soil profile and economic return above N cost.

Biermachet et al. (2009) evaluated the feasibility of site-specific optimal sensing for managing N fertilization in winter wheat based on the algorithm developed by Raun et al. (2002) which related spectral data, yield potential, and crop responsiveness to fertilization; they proved that the economic advantage was small and the system was a breakeven in respect to uniform pre-plant N application. Similar results were obtained by Boyer et al., (2011), but economic and environmental advantages are supposed to increase with the advantages of fertilization technology (Biermacher et al. 2009)

1.6. Aims of the work

This work aimed to evaluate the application of site-specific N management for improving cereals production. Environmental and economic benefits were evaluated for durum wheat and maize grown in nitrate vulnerable zones.

Firstly, the effects of VR N application based on MZs on durum wheat yield and protein content were studied, and the possibility to exploit the site-specific input for a subsequent differentiated harvest was evaluated. The high intra-variability shown in MZs suggested the application of VR fertilization based on on the go crop sensing at a finest scale. Furthermore, unpredictable water conditions occurred led to over fertilization due to reduced crop growth a final production lower than expected.

For these reasons, the integration of proximal sensing, crop modeling and medium-term weather forecasts were evaluated in order to optimize N rate in response to crop growth forecasts and spectral measurements.

Eventually, a different approach for combining proximal sensing and crop models were evaluated, using data from a previous PA experiment on maize. Spectral measurements were used to spatially optimize the model in order to increase its accuracy in N stress simulation, and subsequently improve estimation of in-season N rate..

1.7. References

- Arnall, D.B., Tubaña, B.S., Holtz, S.L., Girma, K. And Raun, W.R. 2009. Relationship between nitrogen use efficiency and response index in winter wheat. *J. Plant. Nutr.* 32, 502-515.
- Basso, B., Sartori, L., Bertocco, M., Cammarano, C., Martin, E.C. and Grace, P.R. 2011. Economic and environmental evaluation of site-specific tillage in a maize crop in NE Italy. *Eur. J. Agron.* 35, 83–92.
- Biermacher, J.T., Epplin, F.M., Brorsen, B.W., Solie, J.B. and Raun, W.R. Economic feasibility of site-specific optical sensing for managing nitrogen fertilizer for growing wheat. *Precis. Agric.* 10, 213-230.
- Bongiovanni, R. and Lowenberg-DeBoer, J. 2004. Precision agriculture and sustainability. *Precis. Agric.* 5, 359–387.
- Bosch-Serra, A.D., Yague M.R. and Teira-Esmatger, M.R. 2014. Ammonia emissions from different fertilizing strategies in Mediterranean rainfed winter cereals. *Atmos Environ.* 84, 204-212.
- Boyer, C.N., Brorsen, B.W., Solie, J.B. and Raun, W.R. 2011. Profitability of variable rate nitrogen application in wheat production. *Precis. Agr.* 12, 473-487.
- Broge, N. H., Leblanc, E. 2000. Comparing prediction power and stability of broadband and hyperspectral vegetation indices for estimation of green leaf area index and canopy chlorophyll density. *Remote Sens. Environ.* 76, 156-172.
- Bronson, K.F., Booker, J.D., Bordovsky, J.P., Keeling, J.W., Wheeler, T.A., Boman, R.K., Parajulee, M.N., Segarra, E. and Nichols, R.L. 2005. Site-specific irrigation and nitrogen management for cotton production in the Southern High Plains. *Agron. J.* 98, 212-129.
- Bundy, L.G. and Andraski, T.W. 2013. Soil yield potential effects on performance of soil nitrate tests. *J. Prod. Agric.* 8, 561-568.
- Cambardella, C.A, Moorman, T.B., Parkin, T.B., Karlen, D.L, Novak, J.M., Turco, R.F. and Konopka, A.E. 1993. Field-scale variability of soil properties in Central Iowa soils. *Soil Sci. Soc. Am. J.* 58 (5), 1501-1511.
- Casa, R., Cavalieri, A. and Lo Cascio, B. 2011. Nitrogen fertilization management in precision agriculture: a preliminary application example on maize. *Ital. J. Agron.* 6, 23-27.

- Cassman, K. G., Dobermann, A., and Walters, D. T. 2002. Agroecosystems, nitrogen-use efficiency, and nitrogen management. *Ambio* 31, 132–140.
- Christensen, S., Sjøgaard H.T., Kudsk, P., Nørrenmark, M., Lund, I., Sadimi, E.S. and Jørgensen, R. 2009. Site-specific weed control technologies. *Weed Res.* 49, 233-241.
- Daughtry, C.S.T., Walthall, C.L., Skim, M.S., Brown de Colstoun, E. and McMurtrey, J.E. 2000. Estimating corn leaf chlorophyll concentration from leaf and canopy reflectance. *Remote Sens Environ* 74, 229-239.
- Delgado, J. A., Koshla, R., Bausch, W. C., Westfall, D. G. and Inman, D. J. 2005. Nitrogen fertilizer management zones reduces potential for nitrate leaching. *J Soil Water Conserv.* 60, 402-410.
- EC-Council Directive, 1991. Council Directive 91/676/EEC Concerning the Protection of Waters Against Pollution Caused by Nitrates from Agricultural Sources.
- Ehlert, D., Schmerler, J. and Voelker, U. 2004. Variable nitrogen fertilization in winter wheat based on a crop density sensor. *Precis. Agric.* 5 (3), 263–273.
- Fageria, N.K and Baligar, V.C. 2005. Enhancing nitrogen use efficiency in crop plants. *Adv. Agron.* 88, 97–185.
- Fleming, K.L., Heermann, D. F. and Westfall, D. G. 2004. Evaluating soil color with farmer input and apparent soil electrical conductivity for management zone delineation. *Agron. J.* 96,1581–1587.
- Franzen, D.W., Kitchen, N.R., 1999. Developing management zones to target nitrogen applications. SSMG-5. Site-specific Management Guidelines Series. Potash Phosphate Institute.
- Fridgen J.J., Kitchen, N.R. and Sudduth, K.A. Variability of soil and landscape attributes within sub-field management zones. In Robert PC, Rust RH, Larson WE, editors. Proc. of the 5th International Conference on Precision Agriculture and Other Source Management; Madison, WI, USA: ASA, CSSA, SSSA; 2000.
- Gitelson, A. 2004. Wide dynamic range vegetation index for remote quantification of biophysical characteristics of vegetation. *J. Plant Physiol.* 161, 165-173.
- Günther ,K.P, Dahn, H.G and Lüdeker, W. 1999. Laser-induced-fluorescence, a new method for precision farming. In: Sensor system in precision farming. Workshop,

- University of Rostock, 27–28 Sept 1999, Rostock. Institut für Geodäsie und Geoinformatik, Bill R et al. (eds) 133–144.
- Heege H.J., and Reusch, S. 1996. Sensor for on-the-go control of site-specific nitrogen top dressing. In: International meeting in Phoenix. American Society of Agric Engineering, St. Joseph, Paper No. 961018
- Heege, H.J., Reusch, S. and Thiessen, E. 2008. Prospects and results for optical systems for site-specific on-the-go control of nitrogen-top-dressing in Germany. *Precis. Agric.* 9, 115-131.
- Heege, H.J. 2013. Site-specific fertilizing. In: *Precision in Crop Farming. Site specific concepts and sensing methods: application and results.* Heege, H.J., Ed.; Springer: Kiel, Germany, 356.
- Holland, K.H. and Schepers, J. S. 2010. Derivation of a variable rate nitrogen application model for in-season fertilization of corn. *Agron. J.* 102, 1415–1424.
- Johnson, C.K., Doran, J.W., Duke, H.R., Wienhold, B.J., Eskridge, K.M and Shanahan, J.F. 2001. Field-scale electrical conductivity mapping for delineating soil condition. *Soil Sci. Soc. Am. J.* 65, 1829–1837.
- Johnson, G.V. and Raun, W.E. 2003. Nitrogen index as a guide to fertilizer management. *J. Plant Nutr.* 26, 249-262.
- Johnson, G.V., Raun, W.R., Zhang, H. and Hattey, J.A. 1997. *Soil fertility handbook.* Okla. Agric. Exp. Stn., Stillwater.
- Larson, W., Lamb, J., Khakural, B., Ferguson, R. and Rehm, G. 1997. Potential of site-specific management for non point environmental protection. In: *The State of Site-Specific Management for Agriculture.* edited by F. Pierce and E. Sadler, ASA-CSSA-SSSA, Madison, Wisconsin, 1997, 337–367
- Lengnick, L.L 1997. Spatial variation of early season nitrogen availability indicators in corn. *Commun. Soil Sci. Plant Anal.* 28, 1721-1736.
- Long, D.S., Carlson, G.R and DeGloria, S.D. 1994. Quality of field management maps. *Proceedings of the 2nd International Conference on Site-Specific Management for Agricultural Systems;* Madison, WI, USA: ASA, CSSA, SSSA; 1994. pp. 251–271.

- MacGregor, C.J., and Warren, C.R. 2006. Adopting sustainable farm management practices within a Nitrate Vulnerable Zone in Scotland: The view from the farm. *Agr. Ecosyst. Environ.* 113, 108-119.
- Magdoff, F.R., Ross, D. and Amadon, J. 1984. A soil test for nitrogen availability to corn. *Soil Sci. Soc. Am. J.* 48, 1301–1304.
- Mahler, R., Koehler, F.E. and Lutcher, L.K. 1994. Nitrogen source, timing of application, and placement: effects on winter wheat production. *Agron. J.* 86(4), 637-642.
- Mamo, M., Malzer, G.L., Mulla, D.J., Huggins, D.R. and Strock, J. 2003. Spatial and temporal variation in economically optimum nitrogen rate for corn. *Agron. J.* 95, 958–964.
- Martin, E. C., Loudon, T. L., Ritchie, J. T. and Werner, A. 1994. Use of drainage lysimeter to evaluate nitrogen and irrigation management strategies to minimize nitrate leaching in maize production. *Trans. ASAE* 37, 79–83.
- Matson, P.A., Parton, W.J., Power, A.G. and Swift, M.J. 1997. Agricultural intensification and ecosystem properties. *Science* 277, 504-509
- Miao, Y., Mulla, D.J., Robert, P.C. and Hernandez, J.A. 2006. Within-field variation in corn yield and grain quality responses to nitrogen fertilization and hybrid selection. *Agron. J.* 98, 129-40
- Mondelaers, K., Aertsens, J. and van Huylenbroeck, G. 2009. A meta-analysis of the differences in environmental impacts between organic and conventional farming. *Brit. Food J.* 111, 1098-119.
- Mouratiadou, I., Russell, G., Topp, C, Louhichi, K. And Moran, D. 2010. Modelling common agricultural policy–Water Framework Directive interactions and cost-effectiveness of measures to reduce nitrogen pollution. *Water Sci. Technol.* 61, 2689-2697.
- Power, J. F., Wiese, R., and Flowerday, D. 2000. Managing nitrogen for water quality: Lessons from management systems evaluation area. *J. Environ. Qual.* 29, 355–366.
- Pierce, F.J. and P. Nowak. 1999. Aspects of precision agriculture. *Adv. in Agron.* 67, 1-85.
- Pierce, F. J., Robert, P. C. and Mangold, G. 1994. Site-specific management: The pros, the cons, and the realities. In “Proceedings of the International Crop Management Conference, Iowa State University pp. 17-21.

- Randall, G.W., Vetsch, J.A. and Huffman, J.R. 2003. Corn production on a subsurface-drained mollisol as affected by time of nitrogen application and nitrapyrin. *Agron. J.* 95, 1213-1219.
- Raun, W.E. and Johnson, G.V. 1999. Improving nitrogen use efficiency for cereal production. *Agron. J.* 91, 357-367.
- Raun, W. R., Solie, J. B., Johnson, G. V., Stone, M. L., Mullen, R. W., Freeman, K. W., Thomason, W.E. and Lukina, E. 2002. Improving nitrogen use efficiency in cereal grain production with optical sensing and variable rate application. *Agron. J.* 94, 815–820.
- Raun, W. R., Solie, J. B., Stone, M. L., Martin, K. L., Freeman, K. W., Mullen, R. W., Zhang, H., Schepers, J.S. and Johnson, G.V. 2005. Optical sensor-based algorithm for crop nitrogen fertilization. *Commun. Soil Sci. Plant Anal.* 36, 2759–2781.
- Redulla, C., Havlin, J., Kluitenberg, G., Zhang, N. and Schrock, M. 1996. Variable N management for improving groundwater quality. In: *Proceedings of the 3rd International Conference on Precision Agriculture*. edited by P. C. Robert, R. H. Rust and W. E. Larson. ASA-CSSA-SSSA. Madison, WI,USA: 1101–1110.
- Report from the Commission to the Council and the European Parliament on the implementation of Council Directive 91/676/EEC concerning the protection of waters against pollution caused by nitrates from agricultural sources based on Member State reports for the period 2008–2011.
- Roberts, R., English, B. and Mahajanashetti, S. 2001. Environmental and economic effects of spatial variability and weather. In: *Proceedings of the 3rd European Conference on Precision Agriculture* . edited by S. Blackmore and G. Grenier (AGRO, Montpellier, France), 545–550.
- Rouse, J.W., Haas, R.H., Schell, J.A., Deering, D.W. 1973. Monitoring vegetation systems in the Great Plains with ERTS. In: *Third ERTS symposium*. NASA SP-3 51, 309–317.
- Sahrawat, K.L., and Keeney, D.R. 1986. Nitrous oxide emission from soils. *Ad. Soil S.* 4, 103–148.
- Scharf, P.C., Kitchen, N.R., Sudduth, K.A., Davis, G.J., Hubbard, V.C. and Lory, J.A. 2003. Field-scale variability in optimal nitrogen fertilizer rate for corn. *Agron. J.* 97, 452–461.

- Schmitt, M.A, Randall, G.W. and Rehm, G.W. 1998. A soil nitrogen test option for N recommendation with corn. Univ. of Minnesota Ext. Srv. FO-06514-GO.
- Schröder, J.J., Neeteson, J.J., Oenema, O. And Struik, P.C. 2000. Does the crop or the soil indicate how to save nitrogen in maize production?: Reviewing the state of the art. *Field Crop Res* 66 (2), 151-154.
- Shanahan, J.F., Kitchen, N.R., Raun, W.R. and Schepers, J.S. 2008. Responsive in-season nitrogen management for cereals. *Comput. Electron. Agr.* 61, 51-62.
- Sowers, K. E., Pan, W. L., Miller, B. C., and Smith, J. L. 1994. Nitrogen use efficiency of split nitrogen applications in soft white winter wheat. *Agron. J.* 86, 942–948.
- Stewart, C.M., McBratney, A.B., Skerritt, J.H. 2002. Site-specific durum wheat quality and its relationship to soil properties in a single field in Northern New South Wales. *Precis. Agric.* 3 (2), 155-168.
- Tubaña, B.S., Arnall, D.B., Walsh, O., Chung, B., Solie, J.B., Girma, K. and Raun, W.R. 2008. Adjusting midseason nitrogen rate using a sensor-based optimization algorithm to increase use efficiency in corn. *J. Plant Nutr.* 31 (8), 1393-1419
- van Uffelen, C.G.R., Verhagen, J. and Bouma, J. 1997. Comparison of Simulated Crop Yield Patterns for Site-specific Management. *Agric. Sys.* 54, 207-222.
- Vellidis, G. Tucker, M., Perry, C., Kvien, C, and Vednarz, C. 2008. A real-time wireless smart sensor array for scheduling irrigation. *Comput. Electron. Agr.* 61, 44-50.
- Wanjura, D. F. and Hatfield, J. L. 1987. Sensitivity of spectral vegetative indices to crop biomass, *Trans ASAE* 30:810-816.
- Woolfolk, C. W., Raun, W. R., Johnson, G. V., Thomason, W. E., Mullen, R. W., Wynn, K. J. and Freeman, K. W. 2002. Influence of late season foliar nitrogen application on yield and grain nitrogen in winter wheat. *Agron. J.* 94, 429–434.
- Worrall, F., Spencer, E. and Burt, T.P. 2009. The effectiveness of nitrate vulnerable zones for limiting surface water nitrate concentrations. *J. Hydrol.* 30, 21-28.
- Yoder, B.J. and Pettigrew-Crosby, R.E. 1995. Predicting nitrogen and chlorophyll content and concentrations from reflectance spectra (400–2500 nm) at leaf and canopy scales. *Remote Sens. Environ.* 53, 199–211

Zillmann, E., Graeff, S., Link, J., Batchelor, W.D. and Claupein, W. 2006. Assessment of cereal nitrogen requirements derived by optical on-the-go sensors on heterogeneous soils. *Agron. J.* 98, 682–690

Cited Websites

www.faostat.org

www.eurostat.org

Chapter II

Understanding the effect of site-specific fertilization on yield and protein content in durum wheat: prodrome to site-specific harvest

2.1. Introduction

North Italy represents the northern limit for cultivation of durum wheat in Europe with variable results in terms of grain quality (e.g. protein content). Indeed, grain quality is strongly influenced by the interactions between cultivar, crop management and pedo-climatic conditions. Water stress during grain filling, for instance, negatively affects the crop yield but conversely increases the grain protein content (Flagella, 2006; Rharrabti et al., 2003). Furthermore, high relative water content could cause an increase on starch concentration, resulting in a decrease on protein content (Simmonds, 1989).

According to Delin (2004) within-field variations in protein content are due to differences in available soil nitrogen. Mulla (1992) and Fiez (1994) proved also that the interaction between water content and N availability could increase the protein content in fields with lower water capacity. Indeed variables associated with water retention, i.e. soil texture and organic carbon, are usually negatively correlated with the grain yield and positively with the protein content (Stewart et al., 2002).

Water stress during grain filling causes also a higher accumulation of glutenin subunits (GS) (Flagella, 2010), which are compounds responsible for the elasticity and strength of dough. Grain characterized by high glutenin GS content are preferred by the pasta industry, especially in case of the prevalence of high molecular weight gGSlutenins (LMW- GS) (Feillet et al., 1989; Pogna et al., 1988; Carrillo et al., 1990).

A N management aiming to optimize both grain quality and quantity should combine rate, timing, splitting and sources (Grant et al., 2001). High quality standard could be guaranteed with an increase in N input at rates often double than those required to maximize grain yield (Garrido-Lestache et al., 2005) but with risk for the environment (e.g.

nitrate pollution) (Ercoli et al., 2013). N foliar spray applications have been suggested as an alternative environmentally-sound technique to increase gluten protein content (Gooding and Davies, 1992). Foliar urea applications just before or after flowering significantly increased protein content in winter wheat (Woolfolk et al., 2002; Wuest and Cassman, 1992), but without effect on grain quantity yield (Varga and Svečnjak, 2006).

Recent advances in precision agriculture offer new potentialities to meet grain quality standards. On one hand, N variable rate application (VRA) could play a pivotal role in driving a quality-oriented fertilisation and, on the other hand, precision harvesting could be an alternative method to maximize the tonnage of higher quality grades.

When N amount in soil and factors driving N availability vary among the field, a precision N management approach can be applied (Pierce and Nowark, 1999) i.e. through the partitioning of the field in management zones (MZ) homogeneous for the edaphic factors (Fridgen et al., 2004). Meyer-Aurich et al. (2010b) have demonstrated that wheat gross margin can be maximized by the combination of site-specific fertilization with quality-specific criteria. Protein content is recognized to be essential in reaching the best economical results (Meyer-Aurich et al. 2010), especially for contracts that recognize a quality premium. Allowing to separate the grain according to its quality, precision harvesting could be useful to reach protein requirements established in this contracts. (Bongiovanni et al., 2007).

Within-field variability of protein content is often such significant to justify grain segregation during harvest (Skerrit et al., 2002). Grain segregation according to the quality requirements could be performed during the harvest (Maertens et al., 2004) or later at the farm by mean of specific sensors (Thylén & Rosenqvist, 2002). On the contrary, pre-harvest segregation requires a collection of previous information on grain quality and yield (Stewart et al., 2002; Martin et al., 2013), which could be drawn for growers applying VRA on the basis of the management zones (Tozer & Isbister, 2007). An additional approach for precision harvesting could be applied using NIR (Near Infrared Reflectance) sensors mounted on combine harvesters. Advances in technologies moves from online sensors, as a part of a recirculated system which remove the sample from the grain stream, analyse it and return it to the grain steam (Maertens et al., 2004), to in-line sensors, able to measure protein percentage directly on the grain stream (Long et al. 2008). Combine harvesters are

not currently designed to automatically segregate grain by protein concentration, but recent outcomes by Long et al (2013) are encouraging in adopting this strategy.

In Italy the Rural Development Programme (Piano di Sviluppo Rurale, PSR) implements the EU Regulation and establishes regional strategies and interventions in agriculture, agribusiness, forestry and rural development matters. The next Rural Development Programme (2014-2020) adopted by the Veneto Region (NE Italy) will put a great emphasis to the implementation of the PA principles, i.e. N-VRA as a tool to increase the N use efficiency reducing at the same the water and air pollution. In the present study, spatial distribution of yield and protein and their interactions with soil and N fertilizations were studied in an area located in the Venice Lagoon watershed and classified as vulnerable according to the Nitrate Directive. Using real-time sensors on a combine harvester, it was possible to investigate differences induced by N-VRA in terms of both agronomic and environmental indicators, and to verify the feasibility to implement precision harvesting.

2.2. Materials and methods

2.2.1 Study Site

The 2-yr experiment was carried out in a 13.6-ha field in Mira (NE Italy, 45°22' N; 12°08' E) along the Venice Lagoon margin, an area classified vulnerable according to the Nitrate Directive 91/676 (EEC, 1991) because of high potential nitrate leaching in ground and surface waters. The experimental field was rectangular in shape (about 520 m length x 256 m width) bordered by open ditches along the two longer sides. Soil texture varied greatly in the study area, ranging from sandy to silty-loam (Soil Survey Staff, 1999). The climate is sub-humid, with annual rainfall around 864 mm. In the median year, rainfall is highest in autumn (304 mm) and lowest in winter (182 mm). Temperatures increase from January (minimum average: -0.7 °C) to July (maximum average: 29.7 °C).

Durum wheat (*Triticum durum* Desf.) var. Biensur (Apsamenti, Voghera, Italy) was grown in 2010-2011 (seeding October 28th and harvest June 27th) and 2011-2012 (seeding October 24th and harvest July 4th). Daily weather data were collected by an automatic meteorological station located near the experimental field (ARPAV, Bureau of Meteorology of Veneto Region). The first crop season was characterized in the last part of

the crop cycle by high temperatures and low rainfall (112 mm from April to June, compared to average 251 mm), which caused water stress and accelerated grain maturity. In 2011-2012 rainfall was particularly low at the beginning of stem elongation (-89.24%), influencing early N uptake .

2.2.2 Identification of management zones and VR fertilization

A mixed-sampling scheme of the top soil layer (0–30 cm) was followed based on a regular grid (Morari et al., 2013): 40 samples were collected at the nodes of a 60-m grid and 80 additional points were collected at the nodes of 10 transects, resulting in a total of 120 samples. Transects were set in the north and east axis at 1, 5, 15, 30 m from 10 randomly chosen nodes of the grid. Soil texture was determined using the hydrometer method (Klute and Dirkens, 1986), soil bulk density was measured with the core method (Grossman and Reinsch, 2002) and soil pH and electric conductivity were measured with a pH/EC tester on a soil water extract. Organic carbon was measured using the Walkley–Black method (Walkley and Black, 1934) and the results converted to organic matter by multiplying the carbon percentage by 1.72. Total N was determined using Kjeldahl method and labile phosphorus was determined with the Olsen method. In addition, spatial soil electric conductivity (ECa) was measured with an EMI sensor (Geonics EM38DD) which determined conductivity in both horizontal and vertical orientations. This instrument provided a weighted depth reading to approximately 0.5 m in the horizontal orientation and 1.5 m in the vertical orientation.

Homogeneous zones were delineated according to Chiericati et al. (2007) by measured soil properties (sand, clay and organic matter) and the map of soil electrical resistivity obtained in the horizontal orientation. An overlay of all these data layers was performed using a Fuzzy C-means method (Fridgen et al., 2004).

Three MZs were delineated, high fertility zone (HFZ), medium fertility zone (MFZ) and low fertility zone (LFZ) (Tab.1). A fertilization of 130, 160 and 200 kg N ha⁻¹ y⁻¹ with ammonium nitrate was applied in HFZ, MFZ and LFZ, respectively. N doses were defined according to a 30-yr model simulation carried out in the three MZs with DSSAT model (Sartori, 2010). Criteria for selecting N doses aimed to balance the productivity with water quality goals (e.g. low N leaching).

At tillering stage a uniform N rate ($52 \text{ kg N ha}^{-1} \text{ y}^{-1}$) was supplied, while VR fertilization was managed during stem elongation. Due to the high N amount to distribute, in LFZ this latter N application was supplied in two application to avoid N losses. At flowering stage each zone was split into a control (0) and a treated test with UAN (urea-ammonium-nitrate) solution ($15 \text{ kg N ha}^{-1} \text{ y}^{-1}$) (Fig.1). Dates and amount of fertilizations for both the crop seasons are listed in table 2.

In both the crop seasons, management consisted in no-tillage and conventional fungicides and insecticides treatments.

Table 1. Main soil properties of the management zones and relative N input

MZs	sand		silt		clay		SOM		N input (kg ha^{-1})	
	%		%		%		%		base	flowering
HFZ	55.6	(2.34)	33.3	(1.85)	11.1	(0.53)	1.2	(0.05)	130	0
HFZ	55.2	(1.22)	33.7	(0.98)	11.1	(0.25)	1.2	(0.03)	130	15
MFZ	57.6	(0.63)	32.4	(0.5)	10	(0.19)	1.1	(0.02)	160	0
MFZ	60.7	(0.79)	30.5	(0.71)	8.8	(0.22)	1	(0.03)	160	15
LFZ	64.7	(1.26)	27	(0.93)	8.3	(0.33)	0.9	(0.04)	200	0
LFZ	70.6	(1.91)	22.6	(1.47)	6.8	(0.55)	0.9	(0.06)	200	15

Table 2. Dates and amount of N fertilization

	HFZ		MFZ		LFZ	
	130+0	130+15	160+0	160+15	200+0	200+15
2011						
24 Feb	52	52	52	52	52	52
7 Apr	78	78	108	108	100	100
19 Apr	0	0	0	0	48	48
9 May	0	7.5	0	7.5	0	7.5
17 May	0	7.5	0	7.5	0	7.5
Total	130	145	160	175	200	215
2012						
2 Mar	52	52	52	52	52	52
6 Apr	78	78	108	108	100	100
27 Apr	0	0	0	0	48	48
14 May	0	7.5	0	7.5	0	7.5
24 May	0	7.5	0	7.5	0	7.5
Total	130	145	160	175	200	215

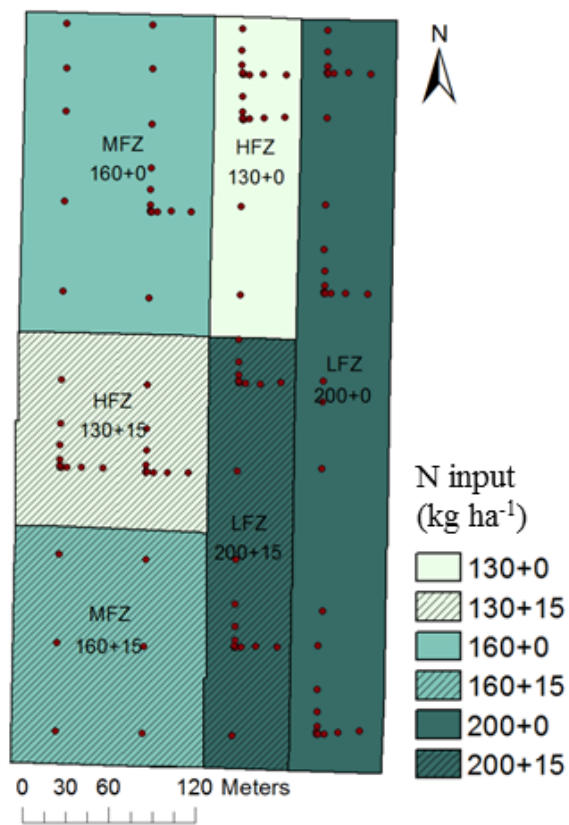


Figure 1. Map of management zones. Black dots identify the soil sampling locations

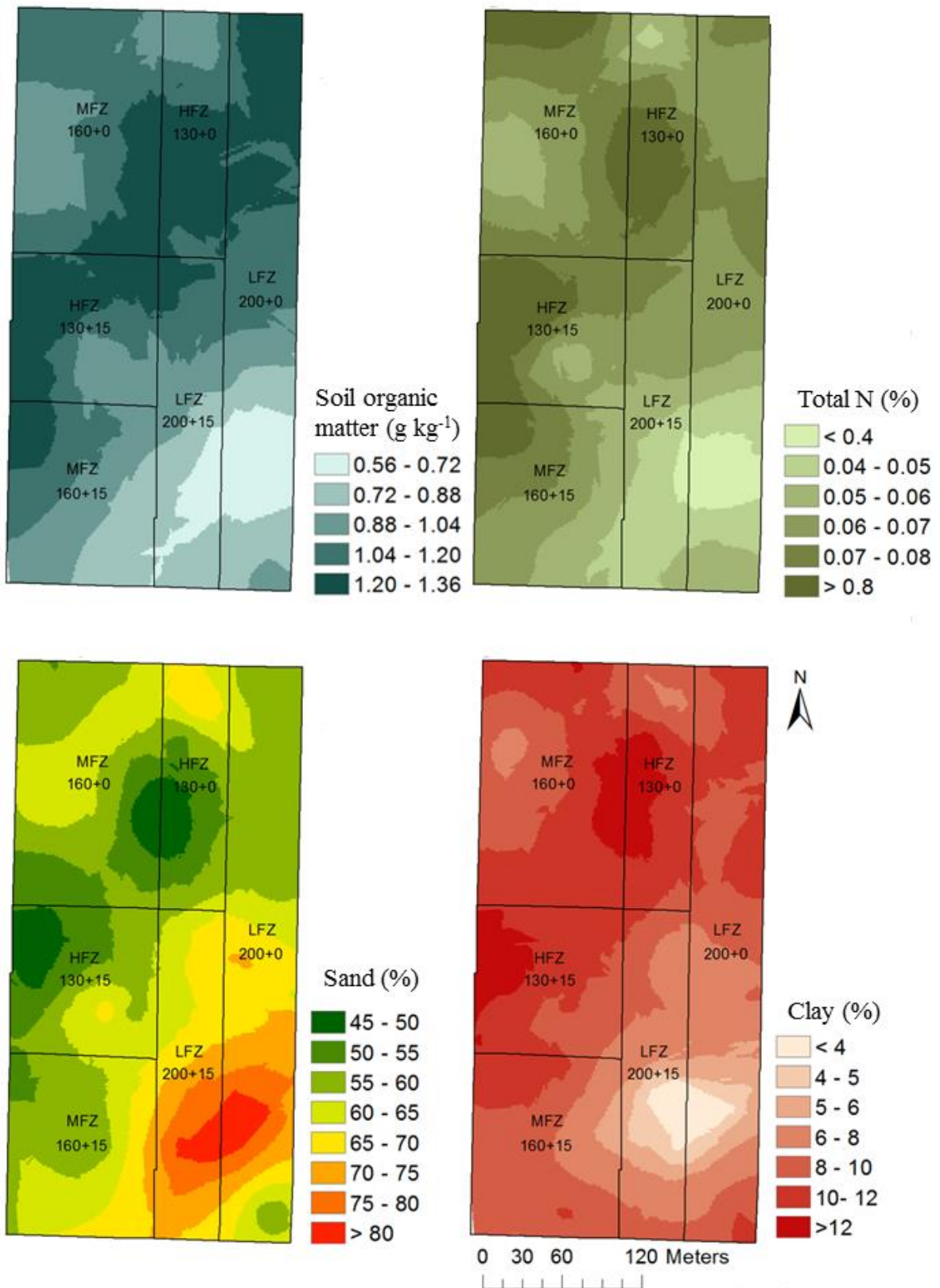


Figure 2. Soil properties.

2.2.3 Data collection

2.2.3.1 NDVI measurements

Spectral data was collected to detect differences in crop biomass during the crop cycle. An active spectrometer (Greenseeker, Ntech Industries, Ukiah, CA, USA), linked with a DGPS was used. This instrument measures canopy reflectance at 660 nm (VIS) and 770 nm (NIR). The normalized difference vegetation index (NDVI) was computed according to Rouse et al. (1973):

$$NDVI = \frac{NIR - VIS}{VIS + NIR}$$

Eq.1

Data collection was conducted three times per season at different crop stages: stem elongation (April 7th, 2011 and April 6th, 2012), flowering (May 17th, 2011 and May 24th, 2012) and milky dough maturity (June 8th, 2011 and June 20th, 2012). Measurements were taken holding the spectrometer 50 cm above the canopy, parallel to wheat rows on 15 m distant transects, with a 1 second time acquisition interval, for a total of 5400 points on average.

2.2.3.2 Grain harvest and post-harvest analysis

Grain yield was recorded by a yield mapping system (Agrocom CL021) mounted on a combine harvester (Claas Lexion 460). Yield data was then converted in dry biomass.

Similarly, protein content was measured with a NIR spectrometer that was interfaced to a GPS. The system was made of a 256 pixel diode array sensor (MMS1, Zeiss, Germany) covering the range of 400-1100 nm, a light source from a 20W halogen lamp and a reference using a neutral density filter with a transmission coefficient of 0.5% (OD 2.5). The pathlength of 12mm was created by the space between the lamp and the fiber optic probe bringing the light to the sensor. The NIR system was calibrated using the protein content measured both with spectroscopy and traditional Kjeldhal methods at 32 locations in the field, yielding a relative root mean square error of 0.3 %. Both yield and protein data

were collected using a 5 second time acquisition interval, covering an average of 2600 points.

In addition, in each of the 6 combinations of MZs and flowering fertilization, a composite sample of 100 kg was collected in order to evaluate possible modification due to N inputs in the gluten protein fractions. Sequential protein extraction on grain flour were performed on 6 sub-samples per MZ following the procedure of Singh et al. (1999); different gluten protein fractions, gliadins, high (HMW-GS) and low-molecular weight GS (LMW-GS) were quantified spectrophotometrically (Bradford, 1976).

2.2.4 Statistical analysis

Spatial data were subjected to ordinary kriging analysis through ArcGIS 10.1 (Redlands, CA, USA) to produce maps. Maps of N removal with harvest (N_{out}) and N fertilization (N_{in}) were processed with Map Algebra tool in ArcGIS to calculate the apparent N balance ($N_{in} - N_{out}$) and N efficiency maps ($N_{out}/N_{in} * 100$).

To compare the effect of fertilizations and soil properties on NDVI, quantity and quality of the final production datasets were standardized over a 10×10 m grid (1293 points). A mixed linear model was used, considering as discrete factors the base fertilization (130, 160, 200 kg N ha⁻¹) and the foliar fertilization (0, 15 kg N ha⁻¹), and the sand content as a continuous factor. The resultant residuals were interpolated through ordinary kriging and furthermore spatial correlations were modeled using REPEATED statement of PROC MIXED (SAS- Cary, NC, USA).

Glutein proteins data were subjected to factorial ANOVA (CoStat 6.4, CoHort Software, Monterey, CA, USA) to test the effect of base and flowering fertilization applying the Student-Newman-Keuls test for post-hoc comparison ($p < 0.05$).

2.3 Results

2.3.1 NDVI measurements

A negative correlation between sand content and NDVI was observed all along the crop cycle in 2011 and 2012 ($p < 0.05$). NDVI measured in 2011 at the beginning of stem

elongation showed higher values in the most fertile area located in the center of the field, while the bottom of both LFZ and MFZ 160+16 reported values < 0.40 (Fig.3). On average, HFZ showed slightly greater values than MFZ and LFZ (Tab. 3). Weather data in 2012 underlined a limited amount of precipitations in March, thus the map of NDVI and the average of the points measured on April 6 reflected the effect of the water stress, reporting values lower than 2011 in almost all the homogeneous zones. The most fertile area in the center of the field was the less impacted and showed few peaks >0.8 (Fig.4).

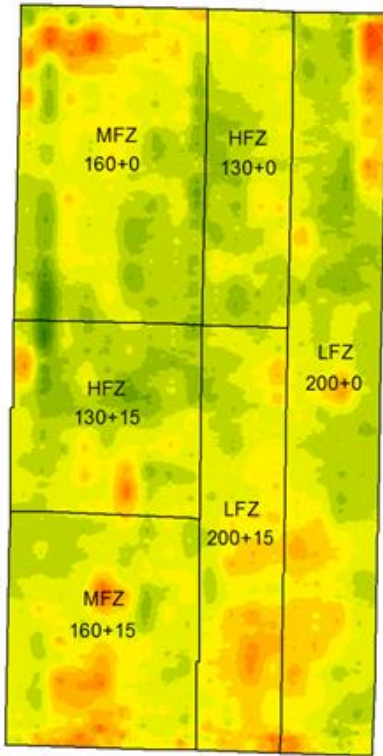
At this stage, differences in crop status were related only to soil fertility, because only a uniform N rate had been supplied at tillering. Conversely, at flowering, base fertilization was able to discriminate HFZ from LFZ both in 2011 and 2012 (+ 10.81% and 2.56%, respectively), while MFZ reported intermediate values. In 2011, map at flowering clearly shows low values in the southern part of LFZ 200+15 and LFZ 200+0, where soil had high sand content, in contrast with higher NDVI (> 0.65) in almost all the field (Fig.7). The average of the points confirmed the differences between LFZ (NDVI equal to 0.67) and the other two management zones. This NDVI survey was carried when higher water stress occurred, and reflected its impact in zones with sandier texture, where plants were not able to take advantage of the foliar fertilization. Map of NDVI at flowering in 2012 reflected a good wheat nutritional status, underlined by high NDVI values in all the MZs, with the exception of a restricted sandier area in LFZ 200+15 and 200+0. Consequently, NDVI variability, as shown in Tab. 3, was reduced.

The NDVI collection on June at the milky –dough maturity is a snapshot of plant senescence, with values < 0.55 in all the field. In 2011, senescence was accelerated in almost all LFZ (NDVI < 0.2) because of sandy texture and sandy soil, while it was more uniform in 2012. (Fig.4). Thanks to the favorable weather conditions the effect of foliar N fertilization on NDVI was significant only in 2012 (+4.29%, on average).

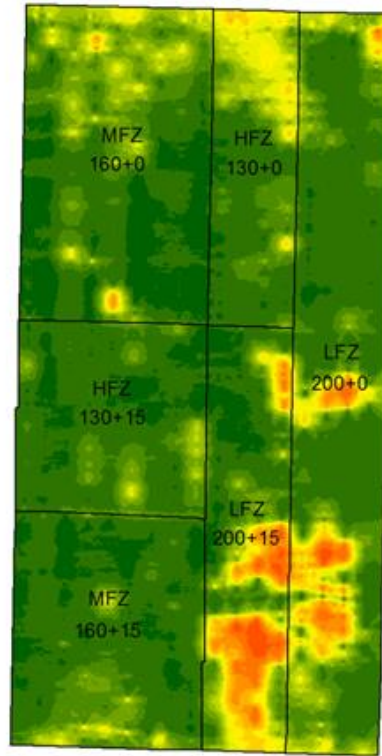
Table 3. NDVI average and standard deviation in different dates and MZs.

MZ	2011					
	Apr-07		May-17		Jun-08	
	Average	St.dev.	Average	St.dev.	Average	St.dev.
HFZ						
130+0	0.55	0.04	0.70	0.10	0.27	0.09
130+15	0.56	0.05	0.77	0.04	0.43	0.10
Total	0.55	0.05	0.74	0.08	0.36	0.12
MFZ						
160+0	0.53	0.06	0.74	0.07	0.37	0.09
160+15	0.50	0.05	0.77	0.05	0.39	0.09
Total	0.52	0.06	0.75	0.06	0.37	0.09
LFZ						
200+0	0.52	0.06	0.69	0.12	0.29	0.12
200+15	0.49	0.06	0.61	0.18	0.21	0.06
Total	0.51	0.05	0.66	0.15	0.26	0.11
MZ	2012					
	Apr-12		May-24		Jun-20	
	Average	St.Dev.	Average	St.Dev.	Average	St.Dev.
HFZ						
130+0	0.55	0.08	0.76	0.08	0.23	0.03
130+15	0.52	0.05	0.80	0.04	0.25	0.02
Total	0.53	0.06	0.78	0.06	0.24	0.03
MFZ						
160+0	0.46	0.06	0.78	0.03	0.25	0.03
160+15	0.46	0.04	0.78	0.03	0.26	0.04
Total	0.46	0.05	0.78	0.09	0.26	0.04
LFZ						
200+0	0.49	0.06	0.78	0.05	0.29	0.06
200+15	0.49	0.07	0.72	0.09	0.24	0.03
Total	0.49	0.06	0.76	0.07	0.27	0.06

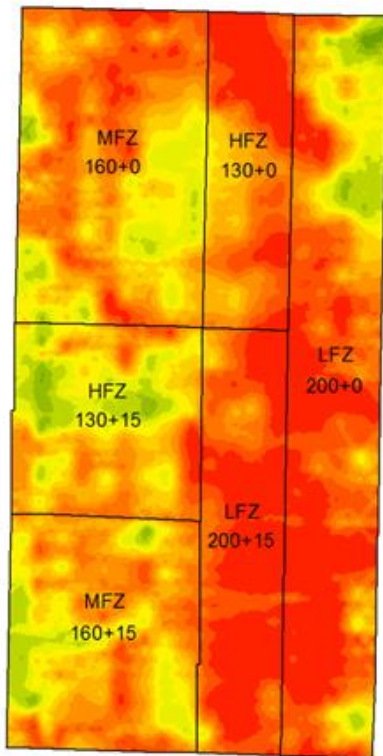
April 7th, 2011- stem elongation



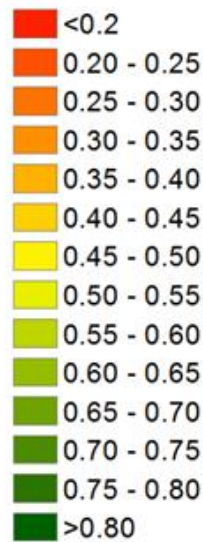
May 17th, 2011- flowering



June 8th, 2011- Milky-dough maturity



NDVI

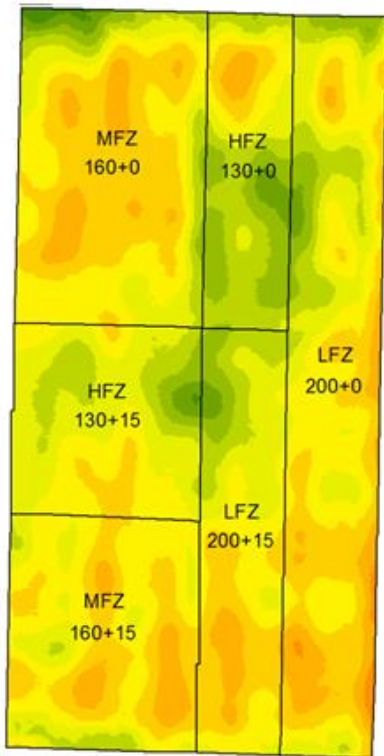


0 30 60 120 Meters

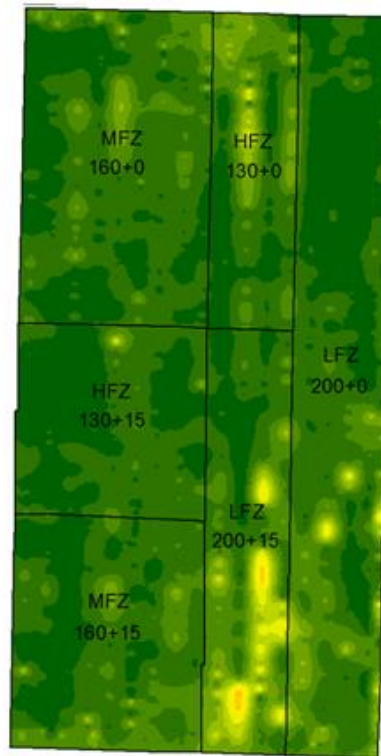


Figure 3. NDVI maps of 2011.

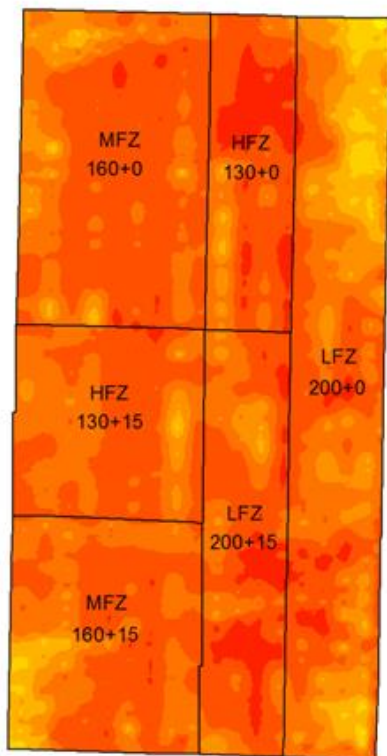
April 6th, 2012- stem elongation



May 24th, 2012- flowering



June 20th, 2012- Milky-dough maturity



NDVI

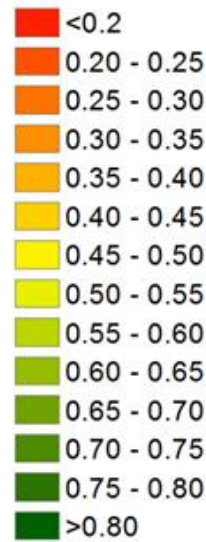


Figure 4. NDVI maps of 2012

2.3.2 Yield and protein content

The 2011 yield map showed high variability along the field with values ranging from less than 3 t ha⁻¹ to more than 7 t ha⁻¹ (Fig. 5). The pattern followed the soil properties spatial distribution being the low productive areas associated with low soil organic matter and high sand contents while the higher productive areas matched with the finer texture zones (Fig. 2). Statistical analysis confirmed the significance of the soil texture on crop yield, resulting the sand content negatively correlated to the final production. N fertilization differentiated the crop yield only when applied during stem elongation ($p < 0.05$), conversely foliar N application did not have any effect (Fig.6). MFZ receiving a base fertilization of 160 kg N ha⁻¹ was the most productive, with a yield of 6.1 t ha⁻¹, while LFZ (4.7 t ha⁻¹) did not differ from HFZ (5.7 t ha⁻¹).

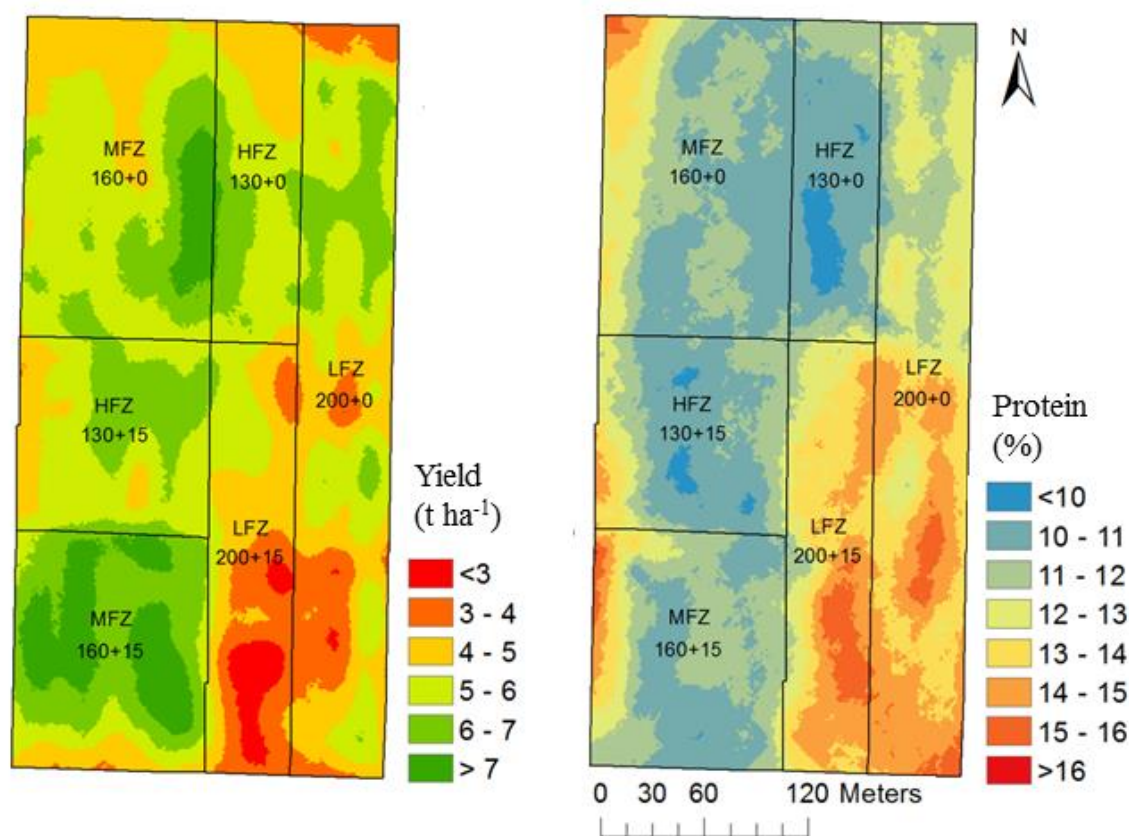


Figure 5. Maps of yield (left) and protein content (right) of 2011.

Protein map (Fig.5) showed a protein content ranging from less than 10% to more than 16%. Zones with higher protein content matched with the ones characterized by low soil fertility and subsequently less productivity. Similarly, sand content and base fertilization positively impacted protein content ($p < 0.05$); however, on the contrary to expectations, N foliar fertilization did not show any effect (Fig. 6). LFZ reported the higher protein percentage (13.45%) while no differences were observed between HFZ and MFZ, characterized by an average of 10.46% and 11.46%, respectively.

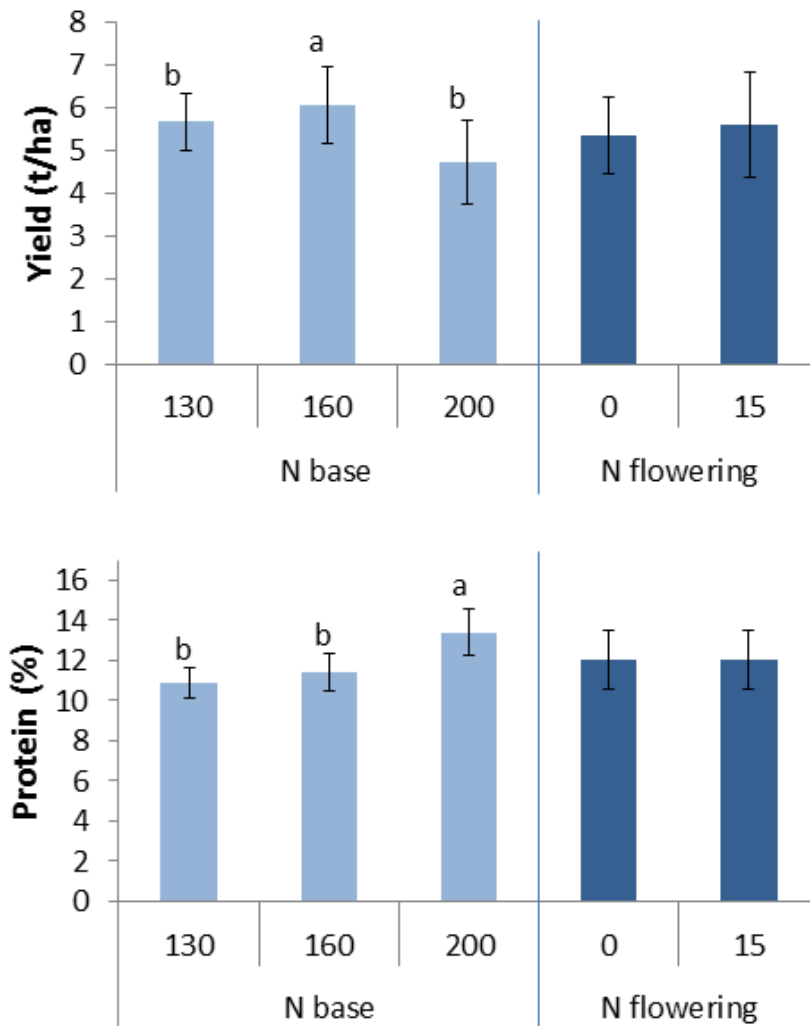


Figure 6. Effects of base and flowering fertilization on yield (above) and protein content (below) in 2011. Different letters identify significant difference ($p < 0.05$). Vertical bars: standard deviation.

Lesser spatial variability was observed on final production in 2012 with respect to 2011 (Fig. 7). In almost all the MZs, yield ranged from 5 to 7 t ha⁻¹ and only limited regions showed a production lower than 5 t ha⁻¹ or greater than 7 t ha⁻¹. The highest productivity (6-7 t ha⁻¹) was observed in the central part of the field, identified by low sand content and high organic matter.

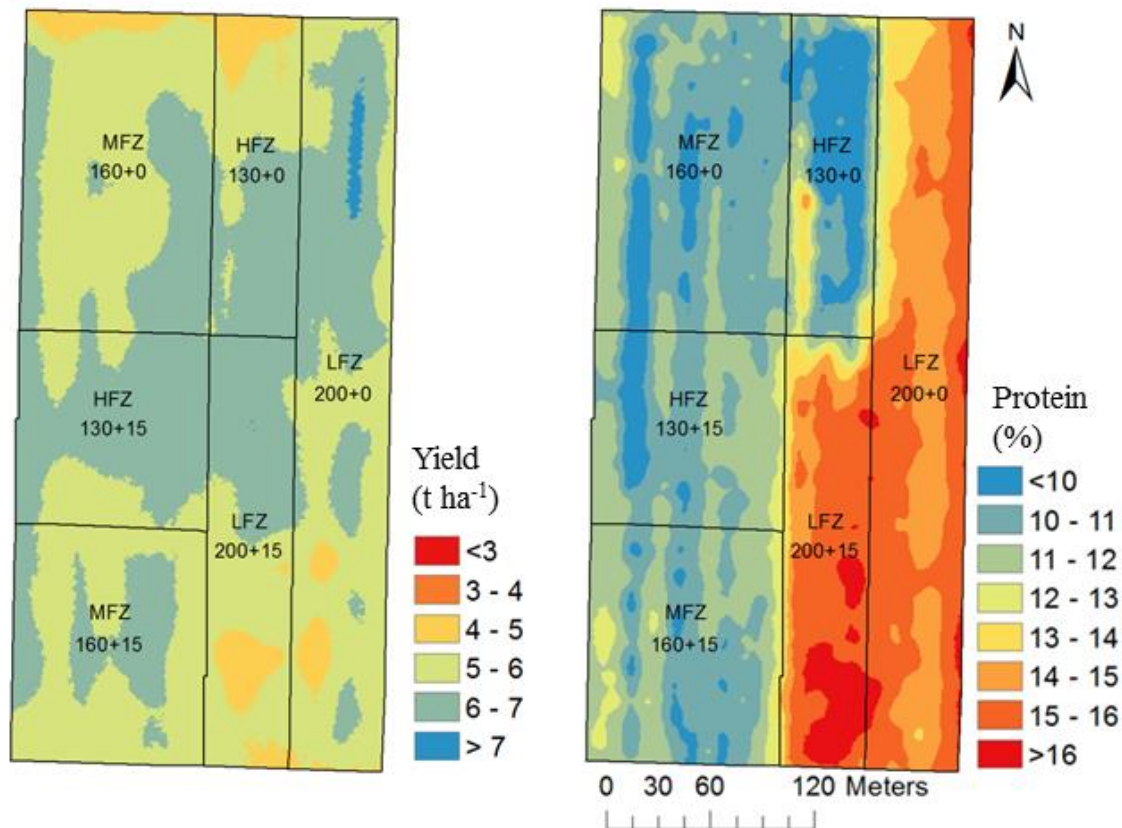


Figure 7. Maps of yield (left) and protein content (right) of 2012.

Base fertilization was able to discriminate LFZ from HFZ ($p < 0.05$) while MFZ had intermediate value (Fig. 7). Moreover, both foliar N application and sand content had a significant effect on yield. Zones receiving 15 kg N ha⁻¹ at flowering slightly increase grain yield (Fig. 8); it was confirmed the negative dependency between wheat yield and sand. Protein map (Fig.7) showed sharp borders between LFZ and the other MZs. Both LFZ

200+0 and 200+15 reached a protein content higher than 14% with peaks > 16% in 200+15, whereas in MFZ and HFZ values were < 12%.

Statistical analysis allowed disentangling the effects of fertilizations and soil texture on the grain protein (Fig. 8). Specifically, LFZ reached values higher than HFZ and MFZ, while foliar fertilization contributed on the one hand to increase the crop production and on the other hand to slightly reduce the protein content (-1.13%). Sand was positively related to the yield.

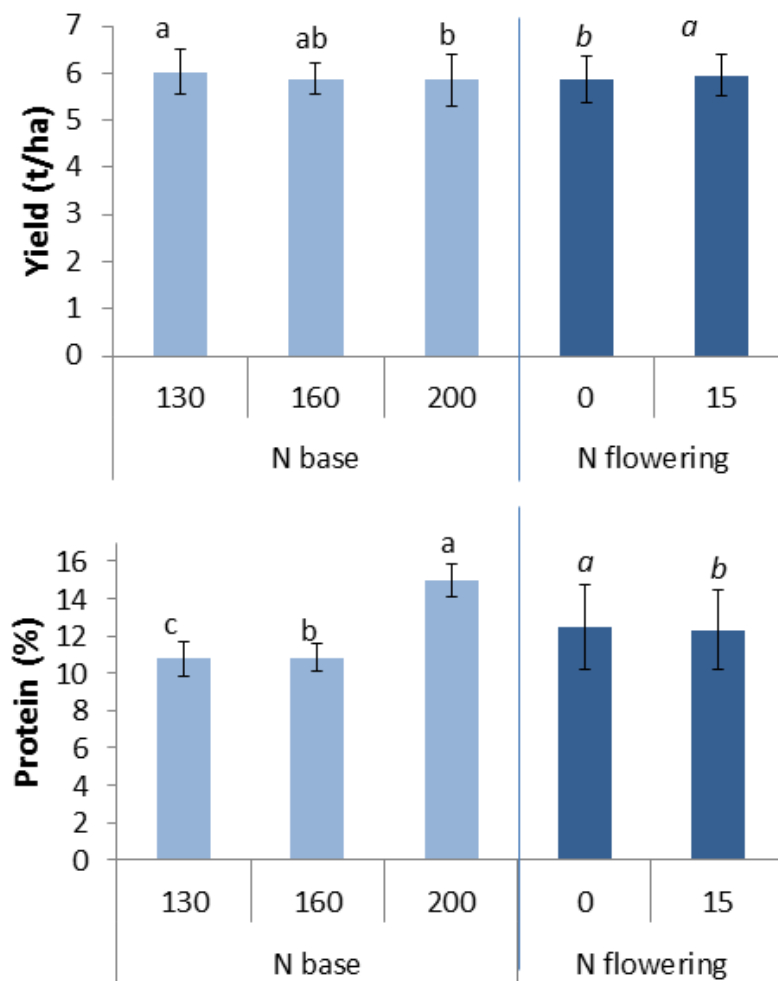


Figure 8. Effects of base and flowering fertilization on yield (above) and protein content (below) in 2011. Different letters identify significant difference ($p < 0.05$). Vertical bars: standard deviation.

2.3.4 Grain quality

The average protein of the entire field was roughly 12% in both the years, clearly below the premium quality threshold of 13.5% recognized by the Italian cereal market. Only LFZ 200+ 15 in 2011 and LFZ 200+0 and 200+15 in 2012 were eligible for this premium, reaching an average protein content >13.5%, with peaks > 15%.

In both 2011 and 2012, gluten protein quantity and ratio between GS/gliadin and HMW-GS/LMW-GS were discriminated by the base fertilization ($p < 0.05$) (Fig. 11). LFZ resulted in higher total gluten proteins ($22.17 \text{ mg/g} \pm 0.41$ in 2011 and $23.65 \text{ mg/g} \pm 0.92$ in 2012) than MFZ and HFZ.

In 2011, HFZ and MFZ reported similar GS/gliadin ratio (mean 0.46), lower than LFZ (+18.94%), whereas in 2012 the ratio was still lower in MFZ than HFZ and LFZ (-28.21% and -62.65%, respectively). Only in MFZ flowering fertilization had a significant effect, contributing to reduce the GS/gliadin ratio (0.43 ± 0.02 in MFZ +0 vs 0.26 ± 0.01 in MFZ 160 +15).

HMW-GS/ LMW-GS ratio discriminated LFZ and MFZ from HFZ, the latter characterized by higher values in both the years, +27.79% and + 21.25% in 2011 and 2012, respectively (Fig.9).

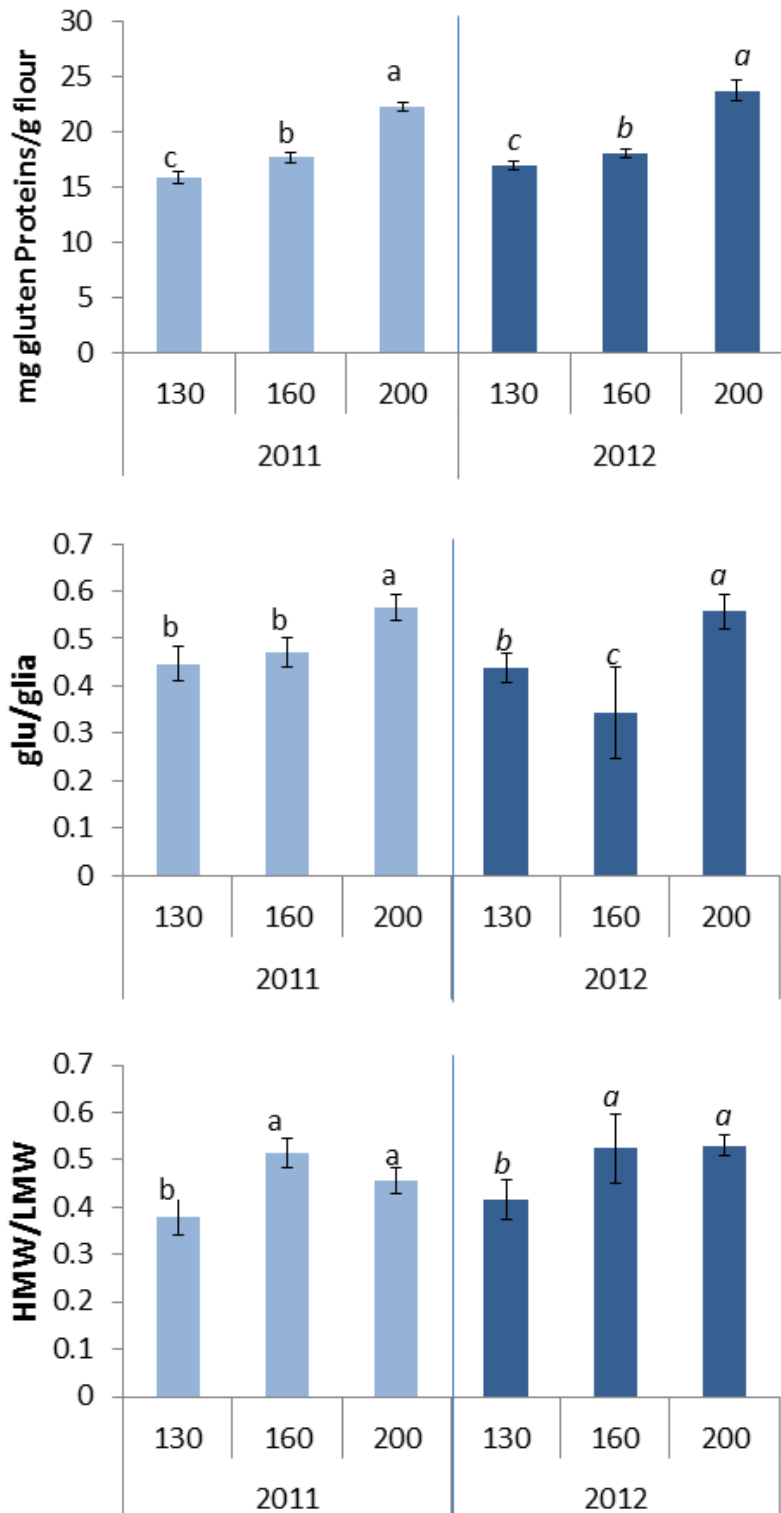


Figure 9. Data on gluten extraction in different MZs in 2011 and 2012: total gluten content (above); ratio between glutenin and gliadin (in the middle); ratio between HMW-GS/LMW-GS (below). Different letters identify significant difference ($p < 0.05$). Vertical bars: standard deviation.

2.3.5 N balance and N efficiency

As a result of the unexpected low productivity, apparent N balance (N input-N output) in 2011 was largely positive in almost all the field (Fig. 10). Indeed the water stress in the last part of the cycle hindered the crop growth leaving part of the N unexploited. As a consequence, apparent N surplus exceeded 75 kg ha⁻¹ in LFZ with peaks > 140 kg ha⁻¹ in the sandy areas. In HFZ, thanks to the higher yield and the lowest N rates, N surplus was lower. Consequently, N use efficiency was even < 30% in LFZ, while HFZ and MFZ ranged from 60 to 90%.

In 2012 (Fig.11), N surplus was similar to 2011 in HFZ, whereas the favorable weather conditions improved N uptake in LFZ, causing a N surplus > 110 kg ha⁻¹ only in restricted areas. Therefore, N efficiency was more uniform all along the field, ranging mostly from 60 to 90%.

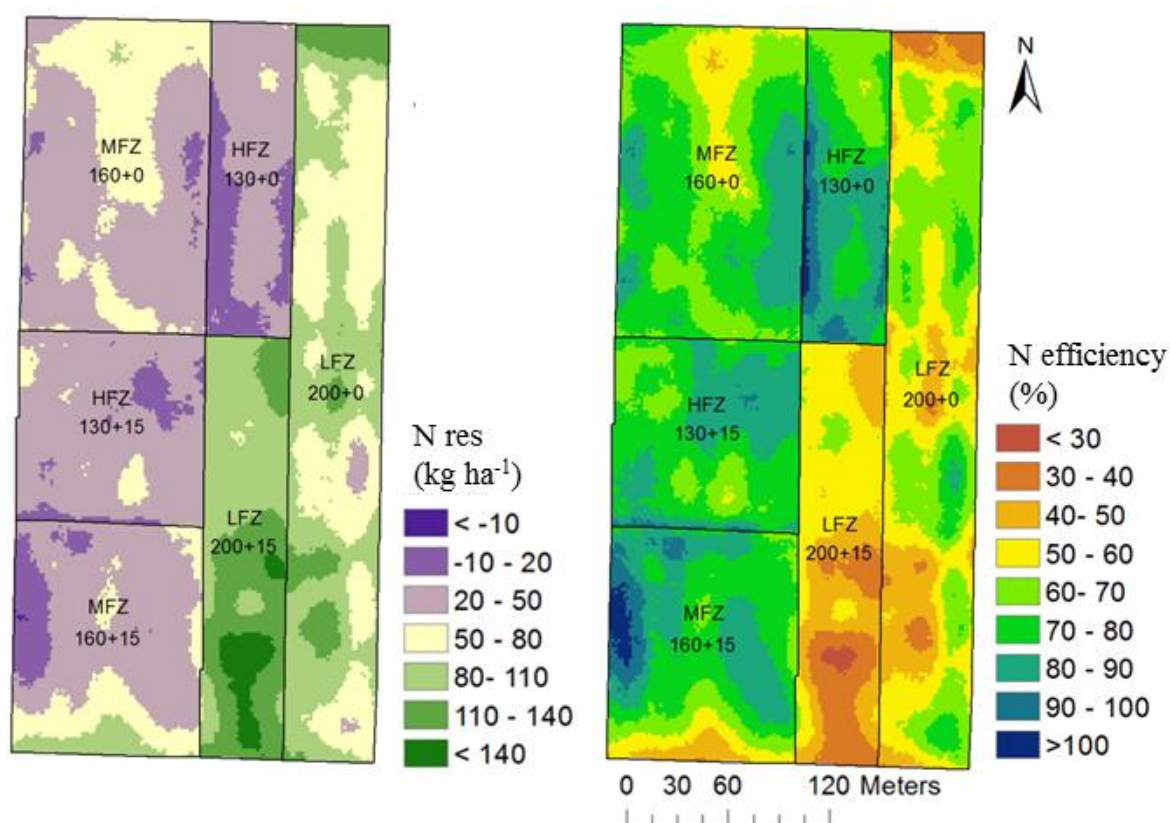


Figure 10. Maps of N apparent balance (left) and N efficiency (right) of 2011.

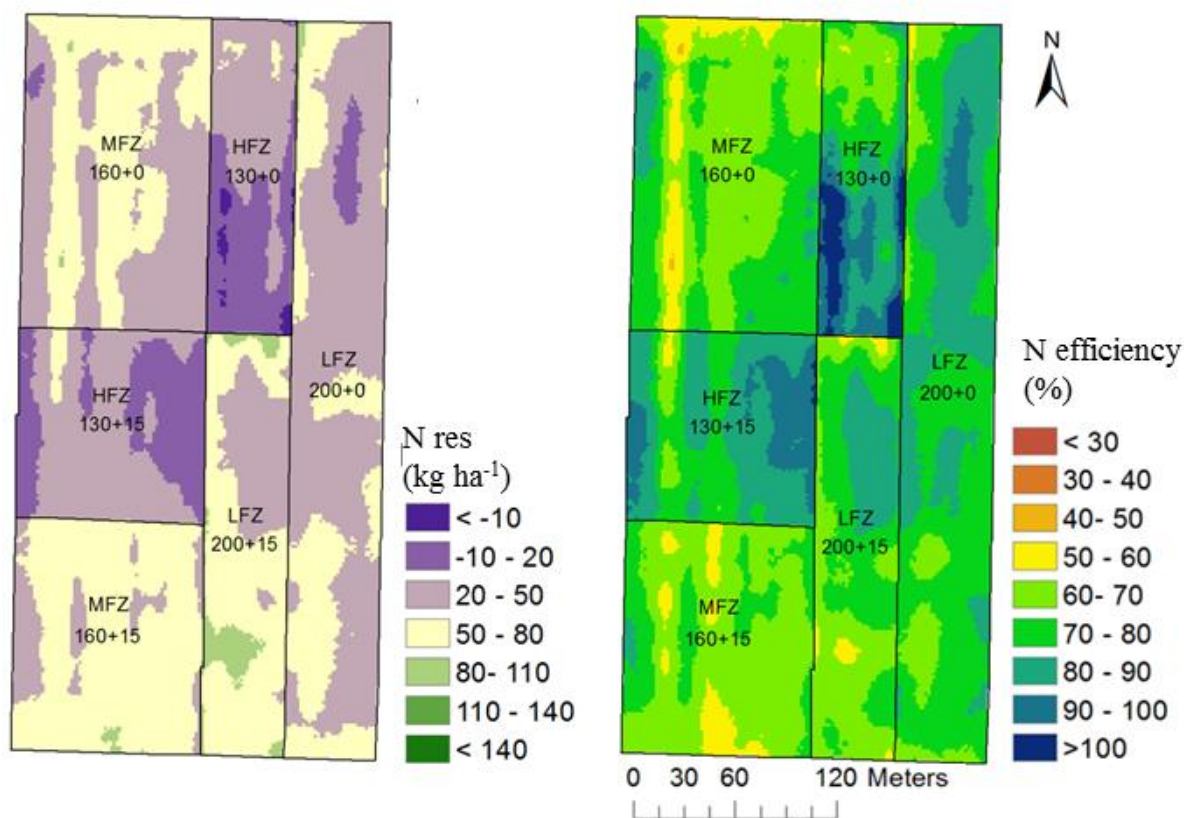


Figure 11. Maps of N apparent balance (left) and N efficiency (right) of 2012.

2.4. Discussion and conclusions

Spatial variability of yield and protein content was mainly driven by soil texture and base fertilization in both the years, confirming also the well-known negative relation between grain yield and protein content (Simmonds, 1995). Even though variable rate fertilization based on management zones have been suggested as a strategy to increase the nitrogen use efficiency (Koshla et al., 2002; Hornung et al., 2003), this method could fail when N uptake is subjected to adverse factors (e.g. water stress). Indeed, VRA allowed to mitigate the weather impact only partially, modulating N input according to soil fertility. However, the unpredictable weather conditions in 2011 resulted in low N use efficiency, with risks for the environment. NUE values were close to the ones estimated by Raun and Johnson (1999) for worldwide cereal crops (39%). On the contrary, in 2012 favorable weather conditions allowed the crop to better exploit its yield potential.

Foliar fertilization failed in increasing grain protein content in both 2011 and 2012. This is probably due not only to the adverse weather condition that limited N uptake, but also to the low N input. Foliar N application at flowering was successful in winter wheat at doses of 30 kg N ha⁻¹ (Woolkolf et al., 2002; Blandino et al., 2009) or when base fertilization was sub-optimal (Varga and Svečnjak, 2006). In this experiment, only half of the dose recommended by the Authors was spread, moreover fertilization was sufficient to meet crop needs because of the water-limited crop production.

Grain quality parameters were sensitive to VRA management and weather conditions, recommending their use as an alternative criterion to set a quality premium. It is well known that the abundance and the relative content of specific gluten protein fractions are both important parameters for the wheat quality (El-Khayat et al., 2006) and that these components are subjected by variation according not only to fertilization techniques but also to changes in environmental conditions during grain filling. In particular, Flagella et al. (2010) stated that water deficit during grain filling can cause a higher aggregation level of GS subunits, increasing flour technological quality.

Within-field variability of protein content was such significant to justify grain segregation during harvest (Skerrit et al., 2002). In spite of the number of technical solutions (e.g. Martin et al., 2013), so far only zone harvesting could be a feasible method to perform precision harvesting in our environment. The key factors when deciding to adopt this strategy are the costs of harvesting by zone and the return for each zone. In this experiment LFZ not only showed higher total protein content, but also reported higher technological gluten protein quality. Conversely, the average protein content of the entire field (12.48% and 12.12% in 2011 and 2012, respectively) did not report the quality standard necessary to be eligible for the quality premium.

A prior knowledge of the spatial variability of proteins and the potential yield is essential to evaluate the convenience of zone harvesting, considering the costs of harvesting by zones and the economic return from each MZ (Tozer and Isbister, 2007). The variability of crop behavior in response to climate and management could be monitored by NDVI collection, which could address in-season N fertilization at different scales. NDVI measurements were able to detect N fertilization effects among the management zones in

different crop stages. Thanks to the well-known relation between NDVI, plant biomass and N uptake, this index is still a good indicator of crop nutritional status (Ma et al., 1996).

A drawback in applying VRA arises from the difficulties to predict precisely final crop yield at the time of fertilizing (Heege, 2013). Indeed, uncertainties in the weather-forecasting beyond a few days do not allow a precise prediction of the expected final yield. Such uncertainties affect also the temporal stability of the management zones, whose boundaries are strongly affected by the response of crop to the weather conditions as well as observed in our experiments either for the crop yield or protein content. Only the very sandy zones (sand content >60%) of the field, resulted stable over the two years in terms of both quantity and quality indicators. Using weather forecasts, crop growth and development could be predicted and this information could be used to manage an in-season N application able to minimize N losses and maximize the economic return (Vermeulen et al., 2002).

The application of high N input confirmed to be on one hand a leverage to reach high quality standards, but on the other hand a cause of high positive N balance in the soil. This poses a dilemma to the farmer in order to select the best strategy, aiming to satisfy both quality and environmental standards. The marked spatial variability on grain quality in term of total protein and gluten protein content, and ratio between GS/gliadin and HMW-GS/LMW-GS suggested the implementation of zone- harvesting as a strategy to exploit the positive interaction between grain quality and soil fertility.

2.5. References

- Blandino, M., Pilati, A. and Reyneri, A. 2009. Effect of foliar treatments to durum wheat on flag leaf senescence, grain yield, quality and DON contamination in North Italy. *Field Crop Res.* 114, 214-222.
- Bradford, M. 1976. A rapid and sensitive method for the quantitation of microgram quantities of protein utilizing the principle of protein-dye binding" *Anal. Biochem.* 72, 248-254
- Bongiovanni, R.G. Robledo, C.W. and Lambert, D.M. 2007. Economics of site-specific nitrogen management for protein content in wheat. *Comp. Electron Agric.* 58, 13-24.
- Carrillo, J.M., Vazquez, J.F. and Orkellana, J. 1990. Relationship between gluten strength and glutenin proteins in durum wheat cultivars. *Plant Breeding* 104, 325–333.
- Chiericati, M., F. Morari, L. Sartori, B. Ortiz, C. Perry, and G. Vellidis. 2007. Delineating management zones to apply site-specific irrigation in the Venice lagoon watershed. In: Stafford, J.V. (Ed.), *Precision Agriculture '07 –Proceedings of the Sixth European Conference on Precision Agriculture (6ECPA)*, Skiathos, Greece, pp. 599-605.
- Delin, S. 2004. Within-field variations in grain protein content—relationships to yield and soil nitrogen and consistency in maps between years. *Precis. Agric.* 5, 565-577.
- EC-Council Directive, 1991. Council Directive 91/676/EEC Concerning the Protection of Waters Against Pollution Caused by Nitrates from Agricultural Sources.
- El-Khayat, G.H., Samaan, J., Manthey, F.A., Fuller, M.P. and Brennan, C.S. 2006. Durum wheat quality I: Correlations between physical and chemical characteristics of Syrian durum wheat cultivars. *Int. J. Food Sci.Technol.* 41, 22-29.
- Ercoli, L., Masoni, A., Pampana, S., Mariotti, M. and Arduini., I. 2013. As durum wheat productivity is affected by nitrogen fertilisation management in Central Italy. *Eur. J. Agron.* 44, 38-45.
- Feillet, P., Ait- Mouh, O., Kobrehel, K. and Autran, J. C. 1989 The role of low molecular weight glutenin proteins in the determination of cooking quality of pasta products: an overview. *Cereal Chem.* 66 (1), 26 – 30.
- Fiez, T. E., Miller, B. C. and Pan, W. L. 1994. Winter Wheat Yield and Grain Protein across Varied Landscape Positions. *Agron. J.* 86 ,1026–1032.

- Flagella, Z. 2006. Qualità nutrizionale e tecnologica del frumento duro. *Rivista Italiana di Agronomia* 1, 203-239.
- Flagella, Z., Giuliani, M.M., Giuzio, L., Volpi, C. and Masci, S. 2010. Influence of water deficit on durum wheat storage protein composition and technological quality. *Eur. J. Agron.* 33, 197-207.
- Fridgen, J.J., Kitchen, N.R., Sudduth, K.A., Drummond, S.T., Wiebold, W.J. and Fraisse, C.W. 2004. Management zone analyst (MZA): software for subfield management zone delineation. *Agron. J.* 96, 100-108.
- Garrido-Lestache, E., Lopez-Bellido, R. and Lopez-Bellido, L. 2005. Durum wheat quality under Mediterranean conditions as affected by N rate, timing and splitting, N form and S fertilisation. *Eur. J. Agron.* 23, 265-278.
- Gooding, M.J. and Davies, W.P. 1992. Foliar urea fertilization of cereals: a review. *Nutr Cycl Agroecosyst* 2, 209-222.
- Grant, C.A., Brown, K.R., Racz, G.J. and Bailey, L.D. 2001. Influence of source, timing and placement of nitrogen on grain yield and nitrogen removal of durum wheat under reduced and conventional tillage management. *Can. J. Plant Sci.* 81, 17–27.
- Grossman, R.B. and Reinsch, T.G. 2002. Bulk Density and Linear Extensibility. In: Dane, J.H. and Topp, G.C., Eds., *Methods of Soil Analysis: Physical Methods, Part 4*, Soil Science Society of America, Madison, 201-228.
- Hornung, A., Khosla, R., Reich R. and Westfall, D.G.. 2003. Evaluation of site-specific management zones: Grain yield and nitrogen use efficiency. In: J. Stafford and A. Werner, editors, *Precision agriculture*. Wageningen Academic Publ., Wageningen, the Netherlands. 297–302.
- Khosla, R., Fleming, K., Delgado, J. A., Shaver, T. M. and Westfall, D. G. 2002. Use of site-specific management zones to improve nitrogen management for precision agriculture. *J Soil Water Conserv.* 57, 513-518.
- Klute, A. and Dirksen, C., 1986. Hydraulic conductivity and diffusivity: laboratory methods. In: Klute, A. (Ed.), *Methods of Soil Analysis. Part 1. Physical and Mineralogical Methods*, 2nd ed. Agron. Monogr. 9. ASA, Madison, WI, pp. 687–734.
- Long, D.S., Engel, R.E. and Carlson, G.R. 2000. Method for precision nitrogen management in spring wheat: II. Implementation. *Precis. Agric.* 2, 25–38.

- Long, D.S., Engel, R.E. and Siemens, M.C. 2008. Measuring grain protein concentration with in-line near infrared reflectance spectroscopy. *Agron. J.* 100, 247-252
- Long, D.S., McCallum, J.D. and Scharf, P.A. 2013. Optical-mechanical system for on-combine segregation of wheat by grain protein concentration. *Agron. J.* 105, 1529-1535.
- Ma, B.L., Morrison, M.J. and Dwyer, L.M. 1996. Canopy light reflectance and field greenness to assess nitrogen fertilization and yield of corn. *Agron. J.* 88:915-920.
- Maertens, K., Reyns, P. and De Baerdemaeker, J. 2004. On-line measurement of grain quality with NR technology. *Trans. ASAE* 47, 1135-1140.
- Martin, C.T., McCallum, J.D. and Long, D.S. 2013. A Web-Based Calculator for Estimating the Profit Potential of Grain Segregation by Protein Concentration. *Agron. J.* 105, 721-726.
- Meyer-Aurich, A. Griffin, T.W., Herbst, R., Giebel, A. and Muhammad, N. 2010. Spatial econometric analysis of a field-scale site-specific nitrogen fertilizer experiment on wheat (*Triticum aestivum* L.) yield and quality. *Comput. Electron. Agric.* 74, 73-79.
- Meyer-Aurich, A., Weersink, A., Gandorfer, M. and Wagner, P. 2010. Optimal site-specific fertilization and harvesting strategies with respect to crop yield and quality response to nitrogen. *Agric. Syst.* 103, 478-485.
- Morari, F., Loddo, S., Berzaghi, P., Ferlito, J.C., Berti, A., Sartori, L., Visioli, G., Marmiroli, N., Piragnolo, D. and Mosca, G. 2013. Understanding the effects of site-specific fertilization on yield and protein content in durum wheat In: Stafford, J.V. (Ed.), *Precision Agriculture '13 – Proceedings of the Nineth European Conference on Precision Agriculture (9ECPA)*, Leida, Spain, pp. 321-327.
- Mulla, D.J., Bhatti, A.U., Hammond, M.W. and Benson, J.A. 1992. A comparison of winter wheat yield and quality under uniform versus spatially variable fertiliser management. *Agr. Ecosyst Environ* 38, 301–311.
- Pierce, F.J. and P. Nowak. 1999. Aspects of precision agriculture. *Adv. in Agron.* 67, 1-85.
- Pogna, N.E., Lafiandra, D., Feillet, P. and Autran, J. C. 1990. Evidence for a direct casual effect of low molecular weight subunits of glutenins on gluten viscoelasticity in durum wheat. *J. Cereal Sci.* 7, 211-214.

- Raun, W.E. and Johnson, G.V. 1999. Improving nitrogen use efficiency for cereal production. *Agron. J.* 91, 357-367.
- Rouse, J.W., Haas, R.H., Schell, J.A. and Deering, D.W., 1974. Monitoring vegetation systems in the Great Plains with ERTS. In: Third ERTS symposium. NASA SP-3 51: 309–317.
- Rharrabti, Y., Royo C., Villegas, D., Aparicio, N., Garcí'a del Moral, L.F. 2003. Durum wheat quality in Mediterranean environments I. Quality expression under different zones, latitudes and water regimes across Spain. *Field Crop Res.* 80, 123-131.
- Rural Development Programme for Veneto region.
- Sartori, L. 2010. III SOTTOPROGETTO: Agricoltura di precisione e conservativa. Azione 1: agricoltura di precisione. In: Veneto agricoltura (Ed.).Messa a punto di modelli produttivi innovativi nelle colture estensive per una gestione ecocompatibile nell'ambito del Bacino Scolante in Laguna di Venezia: 2007-2009 : sintesi dei risultati Progetto Ecobasco. pp. 67-76.
- Skerritt, J.H., Adams, M.L., Cook, S.E. and Naglis, G. 2002. Within-field variation in wheat quality: implication for precision agricultural management. *Aust. J. Ag. Res.* 53, 1229-1242.
- Simmonds, D.H. 1989. Wheat and Wheat Quality in Australia. CSIRO, William Brooks Queensland.
- Singh, N.K., Shepherd, K.W. and Cornish, G.B. 1991. A simplified SDS-PAGE procedure for separating LMW subunits of glutenin. *J. Cereal Sci.*14, 203-208.
- Soil Survey Staff, 1996. Keys to Soil Taxonomy, 7th edn. U.S.D.A Soil Conservation Service, Blacksburg.
- Stewart, C.M., McBratney, A. and Skerrit J.H. 2002. Site-specific durum wheat quality and its relationship to soil properties in a single field in Northern New South Wales. *Precis. Agric.* 3, 155-168.
- Thylén, L. and Rosenqvist, H. 2002. Economical Aspects of sorting grain into different fractions. In: Robert, P.C. (Ed.) Precision Agriculture. Proceedings of the Sixth International Conference on Precision Agriculture (Conference CD). ASA, CSSA and SSSA, Madison.

- Tozer, P.R. and Isbister, B.J. 2007. Is it economically feasible to harvest by management zone? *Precis. Agric.* 8, 151-159.
- Varga, B. and Svečnjak, Z. 2006. The effect of late-season urea spraying on grain yield and quality of winter wheat cultivars under low and high basal nitrogen fertilization. *Field Crop. Res.* 96, 125–132.
- Vermeulen, S.J., Aggarwal, P.K., Ainslie, A., Angelone, C., Campbell, B.M., Challinor, A.J., Hansen, J.W., Ingram, J.S.I., Jarvis, A., Kristjanson, P., Lau, C., Nelson, G.C., Thornton, P.K. and Wollenberg, E. 2012. Options for support to agriculture and food security under climate change. *Environ. Sci. Policy* 15 (1), 136-144.
- Walkley, A. and Black, I.A. 1934. An examination of Degtjareff method for determining soil organic matter, and proposed modification of the chromic acid titration method. *Soil Sci.* 37,29-38.
- Wuest, S.B., and K.G. Cassman. 1992. Fertilizer-nitrogen use efficiency of irrigated wheat: I. Uptake efficiency of preplant vs. late season application. *Agron. J.* 84, 682–688.
- Woolfolk, C.W., Raun, W.R., Johnson, G.V., Thomason, W.E., Mullen, R.W., Wynn, K.J. and Freeman, K.W. 2002. Influence of late-season foliar nitrogen applications on yield and grain nitrogen in winter wheat. *Agron. J.* 94, 429–434.

Chapter III

Coupling proximal sensing, medium weather forecasts and crop modelling to optimize nitrogen variable rate application in durum wheat

3.1 Introduction

Traditionally, N fertilization has been set based on yield goals, without taking into account temporal and spatial variability of the yield potential, which made this approach rarely be correct (Johnson and Raun, 2003; Sharf et al., 2005; Girma et al., 2007).

Real time spectral data collection has been proposed since the 90s as a method to overcome this drawback (Stone et al., 1996; Heege and Reish, 1996), indeed optical measurements not only are correlated to potential yield (Raun et al., 2001), but they are also able to detect differences among the crop at different spatial resolution (Solie et al., 1996). These differences could be subsequently translated into site-specific N rates through algorithms relating optical measures and potential yield.

Lukina et al (2001) confirmed the results obtained by Raun et al (2001), proving that NDVI could be a good predictor of N uptake and allowed to estimate in-season the final yield in winter wheat. They suggested a fertilization optimization algorithm to take into account the amount of N in the wheat plant at the time of sensing and adjust N rate accordingly to the in-season the final yield, replacing previously algorithms based only on yield goals.

An additional aspect when applying N equation is the prediction of the response of N fertilization and its magnitude. The response index (i.e. ratio between the highest yield obtained with N treatment and yield obtained with no N applications) developed by Raun et al. (2002) alone didn't allow in-season adjustment of N fertilization (Mullen et al., 2003). In-season response index, measured through NDVI could overcome this issue, measuring the ration between NDVI of a N rich strip, in which N is not a plant limiting

factor, and NDVI measured in a parallel strip, representative of N availability across the field (Raun, 2002).

The algorithm proposed by Raun et al., in 2002 for winter wheat, and improved in 2005, took into account spatial variation of potential yield, early season N uptake and responsiveness to crop N input. Top-dress N required in order to achieve the potential yield was calculated as the difference in grain N between potential yield with added fertilizer and early season N uptake corrected by a fertilization efficiency factor.

A different approach was suggested by Holland and Shepers (2010) for corn, based on a N fertilizer response function (sensor index vs. N rate) and the relationship between N rate and in-season crop vegetation index data, without considering the yield potential. A sufficiency index is calculated as the ratio between a given vegetation index (e.g. NDVI) of the crop locally sensed and its 95 percentile or the vegetation index measured in a non limiting N situation (Holland and Shepers, 2013).

Despite the fact that these optical-oriented approaches have been proved to result in higher wheat yield and N use efficiency, and reduce N losses in the environment, (Raun et al., 2002; Solari et al., 2008; Chung et al., 2010;), they are based on previous weather conditions, and crop response after sensing is not taken into account (Holland, 2013).

The combination of seasonal weather forecasts and crop growth simulation models could allow to adjust N fertilization, reducing over-fertilization in case of low-yielding seasons, or under-fertilization, in case of high yielding years, and consequently increase farmers' profitability (Vermeulen et al., 2002).

Crop growth simulation models are proved to be feasible to be fed with measured weather data in a specific location up to a point, as the moment of fertilization, and then with weather forecasts up to harvest (Marletto et al., 2007; Lawless and Semenov, 2005). Studies carried out by Dailey et al. (2006) in England and Wales with different crops evaluated the potential of medium term forecasts to improve the accuracy of N recommendations, using in-season weather forecast at fertilization time. Even if a decreasing in N denitrification and leaching, and an increasing in crop N offtake were observed, no great advantages derived from the use a perfect weather forecast were reported. Higher benefits could be achieved using a more accurate 3 weeks weather

forecasts, and could be obtained with any recommendation system which explicitly uses post-application weather.

Hasseng et al. (2012) used seasonal rainfall prediction for N fertilizer decision making for wheat grown in Australia, proving that the knowledge of weather prediction could increase farmers' gross margin and N use efficiency, especially if combined with other system information (e.g. initial soil water content).

The importance to predict early final production could be particularly relevant for a crop as durum wheat grown in the Mediterranean basin, where weather variability, irregular rainfall and high temperatures could unexpectedly influence both grain quantity and quality (Diacono et al., 2012; Dalla Marta et al., 2015) and the interfere with the effects of fertilization.

This study aimed to integrate proximal sensing data, medium weather forecast and crop modelling to manage site-specific N fertilization on durum wheat in an area classified as vulnerable according to the Nitrate Directive. A N-variable rate approach based on economic criteria was applied in a 13-ha field, in function of the crop response to predicted weather conditions, and subsequent correction driven by proximal sensing information. The viability of the site-specific method was evaluated in terms of both agronomic (e.g. final yield and protein content) and environmental indicators (N surplus and potential N₂O emissions).

3.2 *Materials and methods*

3.2.1 Study Site description and management

This study was managed in the same field of the experiment reported in Chapter III, where 3 management zones (MZ) were delineated according to the on soil fertility i.e. high fertility zone (HFZ), medium fertility zone (MFZ) and low fertility zone (LFZ) (Tab.1). Details on the procedure followed to identify the MZs are reported in Chapter III.

The high variability observed in 2010-11 and 2011-12 within the LFZ (i.e. the southern part was always lesser productive than the northern one) suggested to split the zone in two sub-zones, LFZb (top) and LFZ (bottom) (Fig.1; Tab. 1) .

Durum wheat var. Biensur (Apsov Sementi, Voghera, Italy) was cultivated in 2012-2013 (seeding October 18th and harvest June 25th), implementing sod seeding and conventional fungicides and insecticides treatments, as well as reported in Chapter III .

Table 1. Main soil properties of MZs.

MZ	Sand (%)		Silt (%)		Clay (%)		SOM. (%)	
	Average	St.dev.	Average	St.dev.	Average	St.dev.	Average	St.dev.
HFZ	59.19	9.85	30.37	7.77	10.45	2.71	1.11	0.31
MFZ	56.63	7.19	32.88	5.81	10.49	2.63	1.11	0.27
LFZ	70.33	9.58	22.73	7.12	6.94	2.88	0.91	0.29
LFZb	58.07	4.73	32.06	3.56	9.87	1.77	1.23	0.24

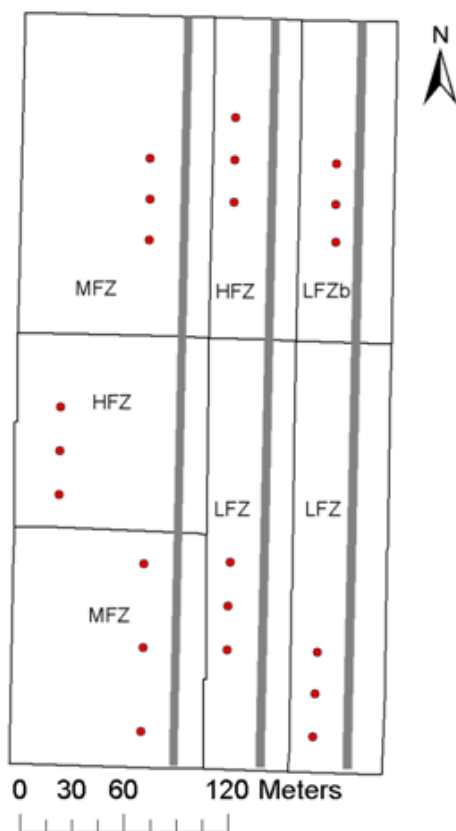


Figure 1. Experimental field: management zones, N rich strip (gray trips)and NDVI sampling point (red dots).

3.2.2 Site- specific fertilization

In the present study, an original mixed VRA approach integrating proximal sensing data, medium weather forecast and crop modelling was applied according to the following steps: 1) Definition of the optimal N rate on the MZs; 2) estimation of the N uptake using proximal sensing technology; 3) development of an algorithm for variable rate N application; 4) implementation of the N-VRA.

1) Definition of the optimal N rate on the MZs

The crop simulation model

The optimal N rate was identified according to an approach coupling crop simulation model and weather forecast. For the simulation of durum wheat phenology and yield, the model SiriusQuality2 (SQ2) was adopted. SQ2 is the latest version of a process-based wheat simulation model that is able to reproduce crop development and growth in response to weather and crop management. The model simulates crop phenology based on the phyllochron and the final leaf number as estimated from daylength and vernalization requirements. Crop growth is calculated on a daily time step from intercepted solar radiation and radiation use efficiency. The potential growth is then limited depending on water and nitrogen availability. Simple partitioning rules determine the accumulation of biomass and nitrogen into the grain after anthesis. The model allows users to specify soil properties, cultivar-specific parameters and crop management options. For an in-depth description of the model, the reader is referred to Martre et al. (2006).

SiriusQuality has been extensively used to simulate wheat phenology and yield in several environments and climates (Martre et al. 2007, Asseng et al. 2013). The model was calibrated for simulating phenology and yield of a medium cycle durum wheat variety using data from a field experiment conducted in Central Italy (Ferrise et al. 2010). The ability of the model in reproducing observed durum wheat yields at local and regional scale across the Mediterranean basin was tested against independent data, showing good agreement between simulated and observed yields in the diverse environments (Ferrise et al. 2011).

In this study, SQ2 was calibrated for reproducing the phenology and yield of the durum wheat cultivar BIENSUR. (. The model crop parameters were estimated from data collected during the growing season 2010-2011 in an experimental farm at Legnaro (45°20' N; 11°56' E).

For testing the ability of the model in reproducing observed phenology and yield, SQ2 was applied for simulating crop development and growth, during the first two crop seasons (2010 and 2011), in the four MZs identified at Mira. The outputs of the model were compared with observed data.

The empirical forecasting model

Climate variability, from monthly to quarterly timescales, is often captured by relevant spatio-temporal low-frequency features, such as empirical orthogonal functions (Barnston & Livezey 1987). Accordingly, global circulation atmospheric and oceanic indices can be used as predictors to build up seasonal forecasting statistical models (Kim et al. 2007, Kim & Kim 2010, Magno et al. 2014).

In this study, a multi-regressive approach based on a linear combination of atmospheric and oceanic observed indices (predictors) was used to forecast monthly temperature and precipitation anomalies (predictands) with respect to the baseline. This latter consisted of daily weather data from 1992 to 2012 recorded by a weather station close to the experimental fields (ARPAV, Bureau of Meteorology of Veneto Region, 45° 26' 7.0794" N, 12° 7' 3.6834" E) . The empirical model adopted is in the form:

$$a_k(s, t) = \beta_1(s, t) Pred_1 + \beta_2(s, t) Pred_2 + \dots \dots \dots + \beta_n(s, t) Pred_n$$

Eq. 1

where a is the monthly anomaly of temperature or precipitation for the k^{th} month after the prediction date (t) at a specific site (s); β is the coefficient of the predictor ($Pred$) computed for the specific site (s) and prediction date (t).

Creating input meteorological data for yield predictions

To simulate crop development and growth, SiriusQuality2 needs weather inputs for the whole growing season. To allow the model to provide estimates of yield during the growing season (i.e. with incomplete meteorological inputs) on a specific prediction date, sets of mixed observed/forecast daily weather data were generated. The first part of these data coincides with the observed values, while the remaining part represents the possible continuation for the site.

In this study, to create an ensemble of synthetic site-specific weather scenarios representing samples of possible future outcomes, the procedure indicated in Lawless and Semenov (2005) was adopted using the weather generator LARS-WG (Semenov and Barrow 1997, Semenov et al. 1998). This is a tool capable of creating synthetic time-series of meteorological variables with statistical properties similar to the observed climate at a site. The procedure for generating the data includes, firstly, a calibration phase. During calibration, LARS-WG analyses observed daily weather data of a specific site, thus providing a statistical characterization of the observed time-series. This implies the calculation of a set of parameters describing the probability distributions of atmospheric variables and the relevant correlations between them. Once calibrated, LARS-WG was forced with monthly anomalies forecast by the empirical model to generate synthetic series of daily weather data deviating from the reference climatology, as predicted by the empirical model.

To compute crop yield estimates accurately, LARS-WG was used to generate probabilistic ensembles of 100 years of possible future meteorological series. Thus, SQ2 was run for each year in the ensemble and the average yield was calculated and used as an estimator of the expected yield (Semenov and Doblas-Reyes 2007).

Model simulations

At the end of March 2013, the calibrated crop simulation model was run separately in each MZ to estimate crop response curves, for yield and protein content, to nitrogen fertilization. The model was set up for simulating the effect of increasing doses of N fertilization ranging from 70 to 250 kg N ha⁻¹. The distribution of N fertilization was simulated to be supplied on March, 26th (52 kg N ha⁻¹) and on April, 13th (the remaining

part, from 18 to 198 kg N ha⁻¹). The model was fed with an ensemble of mixed observed/forecast daily weather data. The final yield and protein content were calculated as the average of the model outputs produced with such ensemble. The crop response curves were used to produce a prescription map for VR fertilization, which was subsequently corrected based on NDVI readings.

2) Estimation of the N uptake within the field using proximal sensing technology

Definition of the relationships between NDVI and N uptake

In 2010-2011 and 2011-2012, eighteen (18) 1-m² areas (6 areas per MZ) were selected to measure NDVI, biomass and total N concentration (fig. 1). An active spectrometer (Greenseeker, Ntech Industries, Ukiah, CA, USA) was used to measure reflectance at 660 nm (VIS) and 770 nm (NIR). The normalized difference vegetation index was then computed using the equation provided by Rouse et al. (1974), as follows:

$$NDVI = \frac{NIR - VIS}{VIS + NIR}$$

Eq.2

Measurements (10 per second) were collected on five dates per season from tillering to milky-dough maturity (tillering: 131 DAS in 2011 and 140 in 2012; stem elongation: 158 and 161 DAS in 2011 and 165 in 2012; flag leaf swollen: 173 DAS in 2011 and 186 in 2012; booting: 187 DAS in 2011 and 203 in 2012; flowering: 201 DAS in 2011 and 213 DAS in 2012). Plants growing in the same areas were sampled to measure total dry biomass (biomass was dried at 60 °C in a forced draft oven for 24h) and Total N (Kjeldahl method; AACC 46-11.02).

Creation of the N-uptake map

At stem elongation (April, 8th), two days before the VRA, NDVI measurements were taken holding the spectrometer linked with a DGPS, 50 cm above the canopy, parallel to wheat rows on 5-m distant transects, with a 1 second time acquisition interval, for a total of 7573 points.

An NDVI map was built using kriging analysis (grid 1x1 m) and for each raster the corresponding N uptake (act Nup) was computed according to the relationship developed between N-uptake and NDVI.

3) Development of the algorithm for variable rate N application

Identification of the optimum N rate

An economic criterion was chosen to identify the optimum N rate, defined as the rate able to level off the gross revenue and the price of the N units applied. Prices at the moment of VR N fertilization were derived from Bologna cereal market (www.agerborsamerici.it), and they were quantified in 1 € kg⁻¹ of N and 0.27 € kg⁻¹ of grain. In addition, since the Italian cereal market recognizes the well known role of grain protein in increasing technological quality for pasta industry (Dexter and Matsuo, 1980; Troccoli et al., 2000), repaying grain with high quality, a premium for grain stocks with a protein content >13.5 %, was considered (+ 0.015 € kg⁻¹). The model was run for each of the MZs applying 10 kg-increasing N rate , ranging from 70 to 250 kg N ha⁻¹, and the optimum N rate was then selected.

Identification of the VRA

Once selected the optimum N rate and defined the corresponding yield and protein content, final N uptake (opt Nup) and fertilization efficiency coefficient (Kc) , i.e. the ratio between N uptake and N applied, were computed.

N rate to supply was calculated as the difference between actual and optimum N uptake, corrected by the N fertilization efficiency:

$$N \text{ rate} = \frac{\text{opt Nup} - \text{act Nup}}{Kc}$$

Eq.3

The prescription map was built considering the spatial resolution of the fertilizer spreader, averaging N rate over a 15 x 30 m- grid.

4) Implementation of the N-VRA

In 2013 a undifferentiated fertilization (52 kg N ha^{-1}) was supplied at tillering stage (March, 26th), while the side-dress site-specific N application based on the combination of simulation modeling and spectral data was applied on April, 13th.

VR urea application was managed through a weight controlled spreader (Bogballe M2W plus; Bogballe S/A, Uldum, Denmark), equipped with a double-disk centrifugal distribution system and a control unit (Calibrator Zurf, Bogballe S/A, Uldum, Denmark). Prescription maps were uploaded to an integrated display (Fmx, Trimble, Sunnyvale, C, USA), with a SBAS correction (30 cm accuracy). A RS-232 serial system was used for data communication to the control unit.

Furthermore, at the moment of VR N application, three N rich strips were created, cutting all the MZs (fig. 1). In order to compare the results of site-specific fertilization with a non limited N situation, a massive N amount (250 kg ha^{-1}) was supplied, splitting N rate in two applications (weekly interval) in order to avoid nitrogen losses and foliar burns.

3.2.3 Yield and protein content data

In all the seasons yield data was recorded by a yield mapping system (Agrocom CL021) mounted on a combine harvester (Claas Lexion 460). Yield data was then converted in dry biomass.

Similarly, protein content data was collected with a NIR spectrometer, linked to a GPS. The system was made of a 256 pixel diode array sensor (MMS1, Zeiss, Germany) covering the range of 400-1100 nm, a light source from a 20W halogen lamp and a reference using a neutral density filter with a transmission coefficient of 0.5% (OD 2.5). The pathlength of 12mm was created by the space between the lamp and the fiber optic probe bringing the light to the sensor. The NIR system was calibrated using the protein content measured both with spectroscopy and traditional Kjeldhal methods at 32 locations in the field, yielding a relative root mean square error of 0.3 %.

Both yield and protein data were collected using a 5 second time acquisition interval, covering an average of 1875 points.

3.2.3 Data processing and statistical analysis

To evaluate the environmental benefit derived from N-VRA, nitrous oxide (N₂O) were computed multiplying total N input by 0.06 %.

In order to compare N-VRA and uniform fertilization with high N rate in term of economic convenience, the gross margin was computed (gross revenue – N cost).

Spatial data was subjected to ordinary Kriging through ArcGIS 10.1 (Redlands, CA, USA) in order to produce maps. Yield, protein content and prescription maps were elaborated through Map Algebra tool in ArcGIS to compute N balance (N out – N in) and efficiency map(N out/N in *100).

To test the effect of N-VRT and soil texture, yield and protein content datasets were standardized over a 15×30 m grid (N-VRA grid). A mixed linear model was used, considering total N input (N-VRA + uniform application) and the sand content as a continuous factors. The resultant residuals were interpolated through ordinary kriging and furthermore spatial correlations were modeled using REPEATED statement of PROC MIXED (SAS- Cary, NC, USA).

The accuracy of the model was evaluated using the pearson's correlation coefficient (r), the normalized Mean Bias Error (nMBE) (Eq 4) and the normalized Root Mean Square Error (nRMSE). (Eq. 5).

The normalized root mean squared error (nRMSE) of simulations (*Sim*) from measurements (*Ref*) ($n=8$ observations) was calculated as:

$$nRMSE = \frac{100}{Ref} \sqrt{\frac{1}{n} \sum_{i=1}^n (Sim_i - Ref_i)^2}$$

Eq.4

This is a measure of the relative difference (as a percentage of the reference average) of simulated versus reference data. The lower the value of nRMSE, the higher the ability of the model in capturing the variability of observed data.

The normalized mean bias error (nMBE) is the deviation between simulated and observed means. It can be used as an indicator of the overall model under- or over-estimation of the observed values. It was calculated as:

$$nRBE = \frac{100}{Ref} \left(\frac{1}{n} \sum_{i=1}^n (Sim_i - Ref_i) \right)$$

Eq.5

where n is the number of estimate-observation pair, Sim are simulated values and Ref are the observed ones.

3.3 Results

3.3.1 Model calibration

The outputs of SQ2, in terms of phenology, yield and protein content, during the 2010-2011 and 2011-2012 crop seasons, were compared with measured values for testing the model. In both years, no differences were observed in the phenological development of the crop among the four MZs. Coherently, SQ2 did not show any difference in the occurrence of the phenological stages among the MZs. As shown in table 2, the model was able to correctly reproduce the development of the crop. The model matched the anthesis date in 2010-2011 and simulated only 2 days of delay in following year, while the harvest dates were simulated with 2 and 5 days of difference in 2010-2011 and in 2011-2012, respectively.

As concerning yield, the model reproduced with great accuracy the measured values. (Fig. 2). In particular, the Pearson's correlation coefficient between the observed and simulated values turned out to be very high ($r = 0.98$, $df=7$, $p<0.01$), with a nMBE of -1.5% and nRMSE of 4.3%.

The simulation of the protein content resulted poorer ($r=0.64$, $df= 7$, $p>0.05$; nMBE of 7.4% and nRMSE=16.4%), mainly due to the overestimation occurred in LFZ and LFZb in 2010-2011 (Fig. 2).

Table 2. Observed and simulated phenological stages (Day of the Year).

Crop Season	Anthesis		Harvest	
	Observed	Simulated	Observed	Simulated
2010-2011	136	136	178	180
2011-2012	135	133	184	179

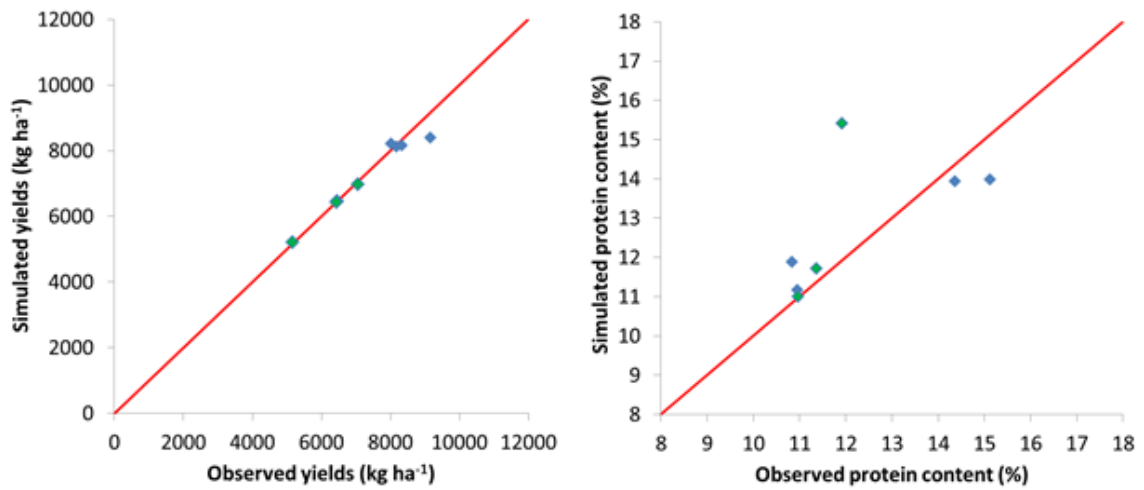


Figure 2. Comparison between observed and simulated yields (left) and protein content(right) Green dots are referred to the 2010-2011 crop season, while blue dots are from 2011-2012. The red line is the line of perfect correspondence

3.3.2 Medium term weather forecast and crop response to N fertilization

Observed temperatures in the period April-June were similar to the average recorded in the previous 20 years (T min +0.34°C, T max -0.9°C), while greater was the increasing in rainfall amount (+46 mm). Even though LARS- WG was able to simulate this trends, rainfall was underestimated (+20 mm in respect to historical data); while temperatures were overestimated (T min +0.79°C and T max +0.1°C, in respect to historical data) (tab. 3).

SQ2 simulated a positive response of grain yield to increasing N fertilization (Fig. 4). Wheat grain yield increased as N fertilization increased, although at N rates >190 kg ha⁻¹, a saturation effect was observed and grain yield tended to reach a plateau. This effect was less evident in LFZb, where yield resulted always lower than in the other MZs. Compared to the lowest level of N fertilization (70 kg N ha⁻¹), at the highest N supply yield increased by 15% in HFZ, 18% in MFZ and in LFZ and by 25% in LFZb, Protein content was simulated to increase up to 77% in response to N supply, ranging, on average, from 9.1% to 16.1% in HFZ, MFZ and LFZ. In LFZb, although showing similar increases (75%), the total content of proteins resulted lower than in the other MZs, ranging from 8.3% to 14.5% (Fig. 3).

3.3.3 Identification of the optimum N rate

Optimum N rate ranged from 170 kg ha⁻¹ in HFZ to 200 kg ha⁻¹ in LFZ, with a weighted average of 183 kg N ha⁻¹. Predicted yield resulted greater than 8000 kg ha⁻¹ in all the homogenous zones, while the protein content, even if high, identified only MFZ as potentially eligible for the quality premium. Optimum rates were able to optimize both yield and protein content, in disagreement with the negative correlation between grain quantity and quality found by Simmonds (1989).

Kc was around 1 in all the MZs, meaning that N losses (e.g. N leaching) were reduced and /or the crop was able to exploit the natural fertility of the soil. Optimum N rates, relative yield, protein content; N uptake and N fertilization efficiency coefficient are reported in table 4.

Table 3. Comparison between historical, observed and predicted rainfall and temperatures (T).

	Hist. Average	Observed	Predicted
Rainfall (mm)	245	291	265
T min (°C)	11.8	12.14	12.59
T max (°C)	22.7	21.8	22.88

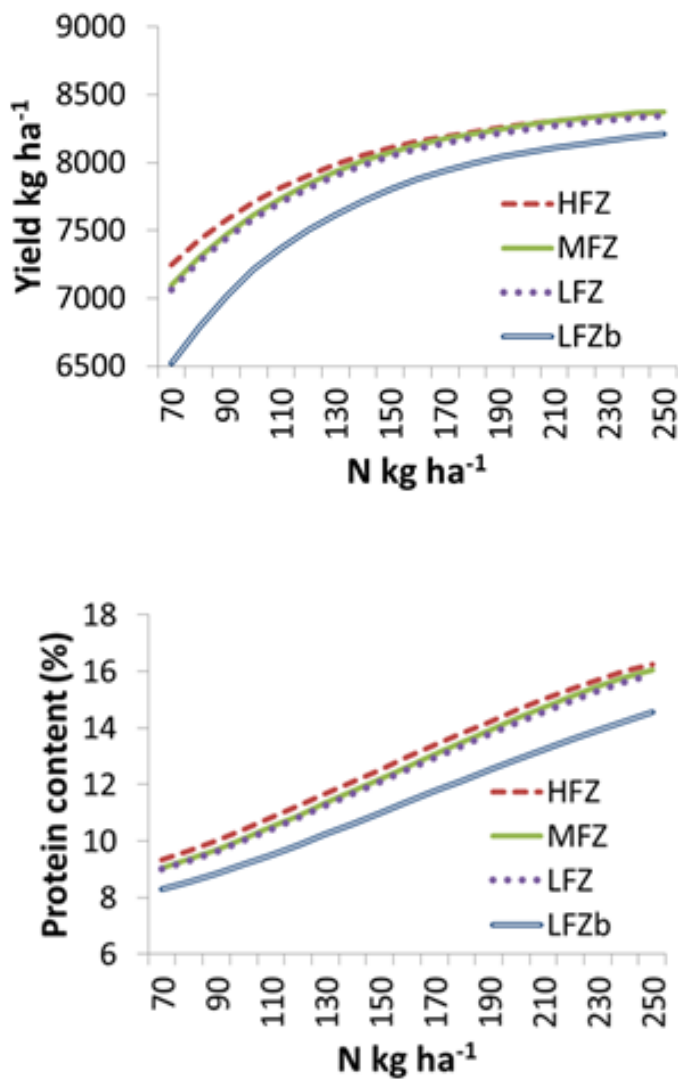


Figure 3. Yield (above) and protein (below) response curves to N fertilization as simulated with SQ2 in the four MZs

Table 4. Optimum N rates and relative yield, protein content, N uptake and N fertilization efficiency

MZ	Optimum N rate (Kg N ha⁻¹)	Yield (Kg ha⁻¹)	Protein content (% ss)	N uptake (Kg N/ha)	Kc
HFZ	170	8193.08	13.38	192.37	1.13
MFZ	180	8213.84	13.49	194.36	1.08
LFZ	200	8076.96	12.88	182.45	0.91
LFZb	180	8182.12	13.36	191.73	1.07

3.3.3 NDVI – N uptake relation and NDVI measurements across the field

N uptake measured in 2010-2011 and 2011-2012 reported the same response to increase in NDVI values (fig. 4) An exponential relationship was found between NDVI and N uptake confirming the results obtained by Morges et al., (2004), Stone et al. (1996) and Li et al. (2008) on winter wheat. NDVI appeared to be a good predictor of total N uptake, with a determination coefficient (R^2) equal to 0.91. NDVI values were close to the saturation during the boot and flowering phases when the crop canopy was fully developed (Sembring et al., 2000). This could lead to an underestimation of biomass and subsequently of N uptake, due to a decreasing in NDVI sensitivity at high leaf area index (Hatfield et al., 1985; Sellers, 1985).

NDVI measured across the field ranged from 0.37 to 0.79. The central area of the field, characterized by sandier soil texture and higher fertility (fig. 5) resulted in greater NDVI (> 0.75), confirming the negative correlation between NDVI and sand content found by Basso et al (2009) on durum wheat. On average, MZs reported NDVI values proportional to their fertility, ranging from 0.66 in HFZ to 0.56 in LFZ, with a low standard deviation in all the homogeneous zones (Tab. 5).

In the more fertile regions of the field NDVI was close to saturation. However, the majority of the field showed NDVI values beyond this threshold, providing accurate estimations of N uptake.

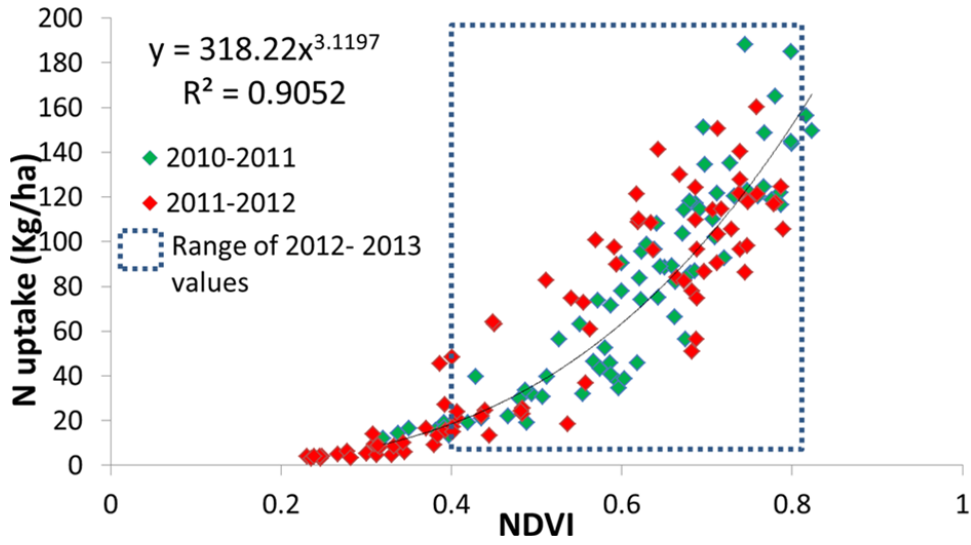


Figure 4. NDVI – N uptake relationship.

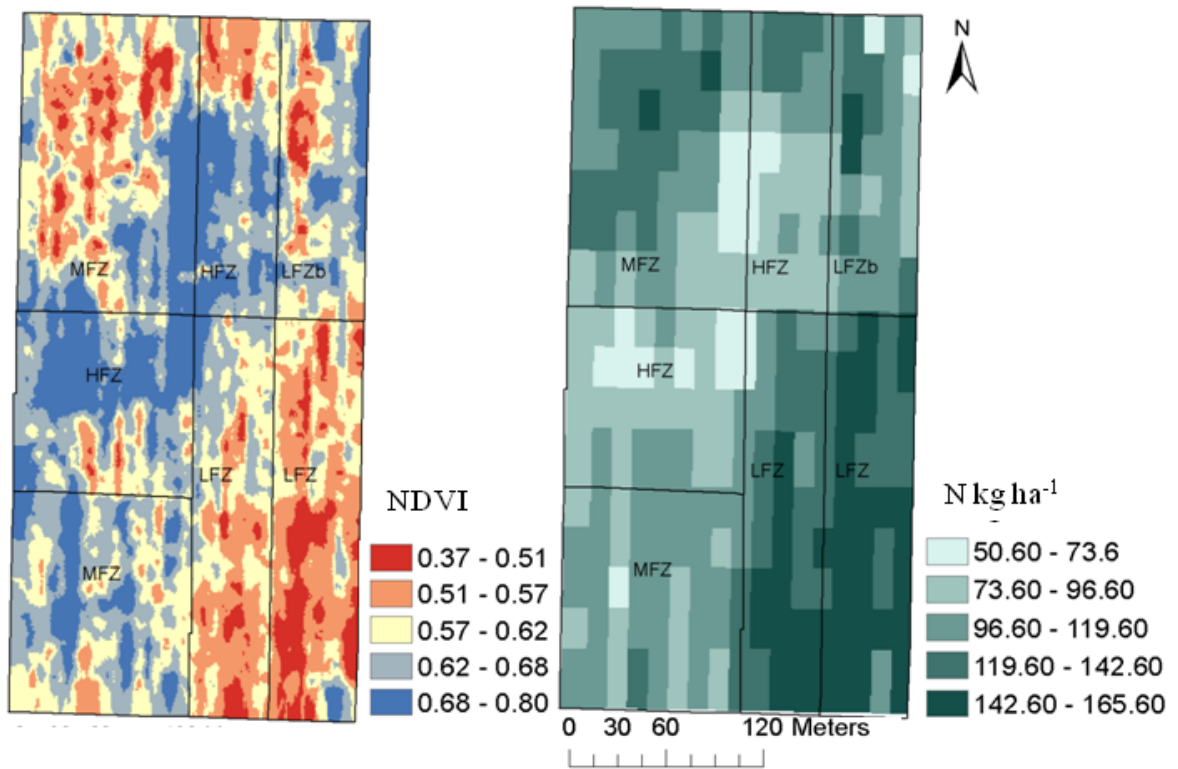


Figure 5. Maps of NDVI (left) and N-VRA prescription

Table 5. NDVI, N variable rate, yield and protein content in the different MZs.

MZ	NDVI		N rate (kg ha ⁻¹)		Yield (kg ha ⁻¹)		Protein content (% ss)	
	Average	St.dev.	Average	St.dev.	Average	St.dev.	Average	St.dev.
HFZ	0.66	0.07	93.95	18.89	3840.27	428.55	14.81	0.52
MFZ	0.62	0.07	107.25	20.87	3730.35	459.36	14.72	0.53
LFZ	0.56	0.06	136.31	16.51	3671.83	567.56	14.49	0.55
LFZb	0.61	0.07	111.55	19.31	3976.05	567.79	15.09	0.82

3.3.4 Prescription map

Prescribed N rates ranged from 50.6 to 165.6 kg N ha⁻¹ coherently matching with the spatial pattern of NDVI (fig. 5). Indeed, higher N amount was found in polygons located in the North-Western and South-Eastern corners of the field, where higher sand content and lesser soil organic carbon were observed.

HFZ confirmed to require lower N input (average of 94 kg N ha⁻¹) than MFZ and LFZ (107 kg N ha⁻¹ and 136 kg N ha⁻¹, respectively), while LFZb reported intermediate values (111 kg N ha⁻¹) due to its inner intermediate soil fertility. It is worth to underline the large variability observed within the MZs, especially in MFZ and LFZb where the prescribed doses ranged from 50 kg N ha⁻¹ to > 140 kg N ha⁻¹.

On average, simulated N rate according to NDVI resulted in a reduction of N amount in all the MZs with respect to the simulated optimal doses (-14.2% in HFZ, -6.3 % in MFZ, -5.8% in LFZ; -9.1% in LFZb). Total N supplied was equal to 164 kg N ha⁻¹, well below the limit set out by the Regional Action Plan of the European Nitrate Directive for durum wheat in the vulnerable zones (190 kg N ha⁻¹).

3.3.4 Yield and protein content maps

Yield (fig. 6) showed a reduced spatial variability ranging between 3.5 and 4.5 t ha⁻¹ in almost all the field with the exception of restricted portions of the field showing values <3000 t ha⁻¹. On average, yield was around 4 t ha⁻¹ in all the MZs (Tab 5). In respect to

2012, and particularly 2011 (Fig. 7 and Fig. 5, Chapter II) the spatial variability driven by the soil fertility was less marked, resulting in a narrow difference between the fertile central zone and the rest of the field. A similar low-variability was observed also in the protein content (fig. 6) with values ranging from 14% to 16%, on average eligible for the quality premium (tab.5).

Statistical analysis underlined a significant effect of soil texture and N fertilization both on yield and protein content ($p < 0.005$). N application positively influenced grain quantity and quality. Conversely, sand content had a negative impact on yield and on the contrary to the expectation also on protein content.

With respect to model performances, a discrepancy was observed between mean predicted and measured yield and protein content. Model simulation overestimated the yield (+ 53.13% in HFZ; + 54.58% in MFZ; +54.54% in LFZ; +51.41% in LFZb) while on the contrary protein content was under-predicted (-19.95% in HFZ; -18.02% in HFZ; - 27.74 % in LF; -26.64% in LFZb).

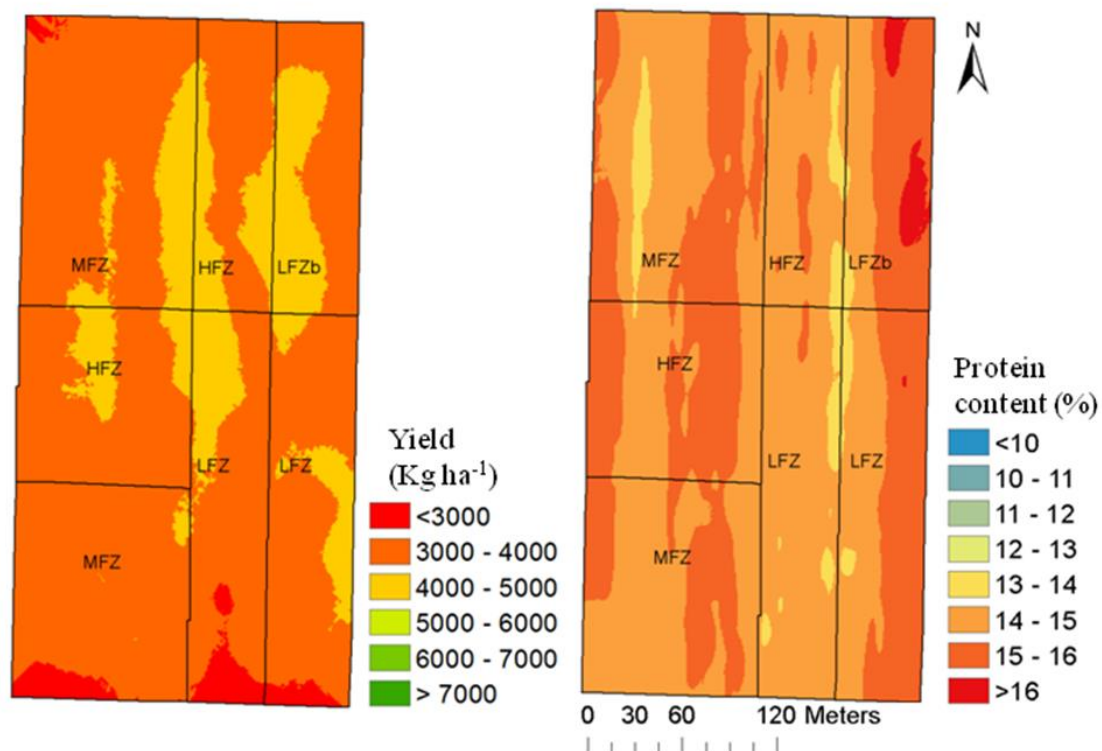


Figure 6. Yield and protein maps of 2013.

3.3.5 Environmental and economic indicators

The inaccuracy in yield prediction resulted in an unexpected high N surplus, especially in the poorer zones (Fig. 7). N surplus matched with the soil fertility pattern, i.e. LFZ and the top of MFZ reported higher values, with peaks $>100 \text{ kg N ha}^{-1}$. Soil N balance was even negative in some spots located in the central area of the field, characterized by finer-textured soil (fig.7) On average, HFZ reported lower N surplus ($46.2 \text{ kg N ha}^{-1}$), while MFZ and LFZb showed similar values ($62.9 \text{ kg N ha}^{-1}$ and $58.3 \text{ kg N ha}^{-1}$), higher than LFZ. The high N surplus resulted in a specular low N efficiency, even lower than 46%, but with picks $> 100\%$, in the finer zones (e.g. HFZ) (Fig. 7; Tab. 7).

N_2O emissions were proportional to N rates received: values ranged from $0.88 \text{ kg N ha}^{-1}$, in HFZ, to $1.13 \text{ kg N ha}^{-1}$, in LFZ, with an average of $0.99 \text{ kg N ha}^{-1}$ (Tab.7).

The economic margin was similar in all the MZs; N VR fertilization showed the lowest economic convenience in LFZ (846.04 € ha^{-1}), while a 100 € ha^{-1} higher income was reported in LFZb. Intermediate values were recorded in the others MZs.

3.3.6 N rich strips

Table 6 reported average and standard deviation of yield and protein content recorded in N rich strips cutting the different homogenous zones. Even if N was not a limiting factor for the crop, yield was lower than expected ($43252.63 \text{ kg ha}^{-1}$, average); on the contrary, protein content reached high levels ($>15.92\%$). As a consequence, N surplus in the soil was largely positive and close to 120 kg ha^{-1} in all the MZS, while N efficiency resulted ca. 50%, with lower values in the coarser zones.

The massive N rate supplied resulted in high nitrous oxide emission ($1.50 \text{ kg N ha}^{-1}$). The gross margin was $> 1000 \text{ € ha}^{-1}$ in HFZ and MFZ, while lower values were reported in LFZ and LFZb (883.02 € ha^{-1} and 995.03 € ha^{-1} , respectively).

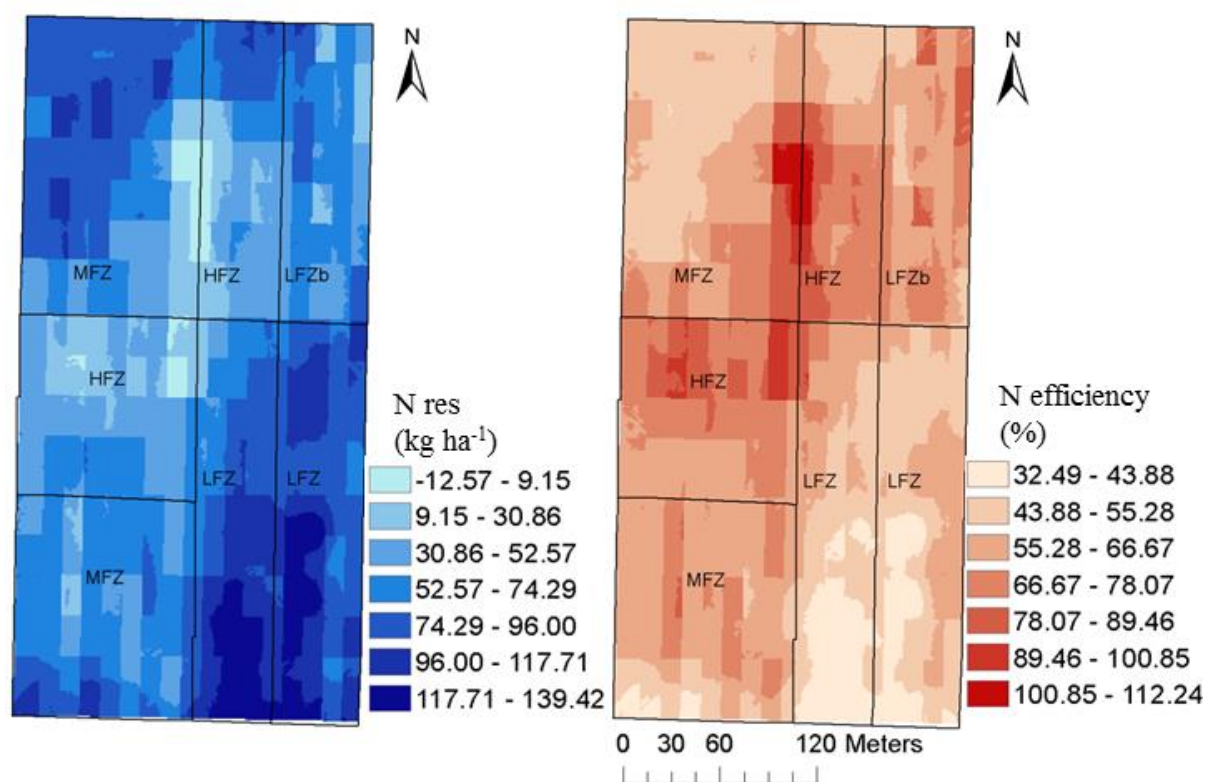


Figure 7. Maps of nitrogen balance (left) and N efficiency (right).

Table 6. Yield and protein content recorded in N rich strips.

MZ	Yield (kg ha ⁻¹)		Protein content (%)	
	Average	St.dev.	Average	St.dev.
HFZ	4.66	0.20	16.05	0.39
MFZ	4.63	0.52	15.92	0.35
LFZ	4.09	0.62	16.45	0.57
LFZb	4.02	0.44	16.92	0.35

Table 7. Environmental and economic indicators of VR fertilization and N rich strips

	N surplus Kg ha⁻¹	N efficiency %	N₂O emissions Kg ha⁻¹	Income € ha⁻¹
VR fertilization				
HFZ	46.20	68.35	0.88	935.86
MFZ	62.94	60.48	0.96	891.59
LFZ	94.95	49.58	1.13	846.04
LFZb	58.29	64.36	0.98	956.50
Total	67.42	59.71	0.99	896.33
N Rich strips				
HFZ	118.74	52.50	1.50	1062.94
MFZ	120.75	51.70	1.50	1053.82
LFZ	132.05	47.18	1.50	901.46
LFZb	130.64	47.74	1.50	883.02
Total	124.50	50.20	1.50	995.03

3.4 Discussions and conclusions

The common approach to apply N-VRA relies on the delineation of management zones (MZs), generally classified by the combination of temporally stable soil properties (Heege, 2013). In 2010-11 and 2011-12, the durum wheat was managed according to a MZs approach, applying at stem elongation 130, 160 and 200 kg N ha⁻¹ y⁻¹ in HFZ, MFZ and LFZ, respectively. In spite of the efficient fuzzy C-means method (Fridgen et al., 2004) used to delineate the homogeneous zones (Chiericati et al., 2007), yield and protein content, which showed a significant variability not only among the MZs (i.e. inter variability) but also within the MZs (intra variability) driven by soil texture. These outcomes were confirmed by other Authors (e.g.. Raun, 1998; Solie et al., 1999; Crain et al., 2013) who demonstrated that the spatial variability in winter wheat yield can be large even at the short-range, in areas < 1 m².

Moreover, the temporal stability of the management zones either for the crop yield or protein content in terms was strongly affected by the response of crop to the weather conditions. Even though VRA based on management zones has been suggested as a strategy to increase the nitrogen use efficiency (Koshla et al., 2002; Hornung et al., 2003), this method could fail when N uptake is subjected to adverse factors (e.g. water stress).

The new method allowed to capture and practically manage the soil variability on a 15m x30m grid, partially matching with the suggestion provided by Crain et al. (2013), who reported that a 15 m grid should be course to sufficiently account for spatial variability, and Wibawa et al. (2003), who proved that a grid of the same dimensions provided adequate information to explain spatial variability. Furthermore, Franzen and Peck (1993) reported that a grid of 30 m is the maximum allowance for site-specific fertilization. N_VRA resulted in a reduction of spatial variability in yield and protein content, allowing to reach similar productive levels in all the MZs. However, yield forecasts resulted highly overestimated with respect to those actually measured at harvest leading to a subsequent overestimation of optimum N rates. Monitoring crop nutritional status through NDVI permitted only a partial reduction of N optimum rate (-10.11 % on average), but this was not sufficient to avoid heavy N loss in the sandier zone of the field.

By one hand, the discrepancy between yield forecasts produced with SQ2 and actual measured yield can be due to the abundant precipitations really occurred since the sowing date (620 mm) as well as those forecast for the remaining part of the season (on average 287 mm). This in turn caused the model to not simulate water as a limiting factor. Indeed, the simulated crop evapotranspiration was on average 422 mm, well below the cumulated precipitation (907 mm).

On the other hand, the model likely under-estimated the N leaching. This latter was simulated to increase in response to increasing N fertilization. On average, simulated N leaching ranged from 19 kg N ha⁻¹ at lowest N supplies, up to a maximum of 45 kg N ha⁻¹ simulated in LFZb (Fig. 8). As a result, N availability in the soil from fertilizer was simulated to range from 50 (i.e. 70 kg N ha⁻¹ from fertilizer – 20 kg N ha⁻¹ of N leaching) to 205 kg N ha⁻¹. Therefore, the simulated high N availability in addition to the great water availability may explain the high level of yield simulated by the model.

Therefore, the model showed to be able to produce accurate estimations of final production in seasons with average precipitations (2012), or water stress (2011), but it was not able to correctly translate the abundant precipitations occurred into the 2013 season into good yield predictions, resulting in overestimation of the optimum N rate. Minimizing the environmental impact of fertilization both in term of water and air pollution is now a main goal of European agriculture (ECC 2011; COM(2013) 918). For this reason, a compromise

between yield maximization, nitrate leaching and N₂O emission should be considered when applying N-VRA.

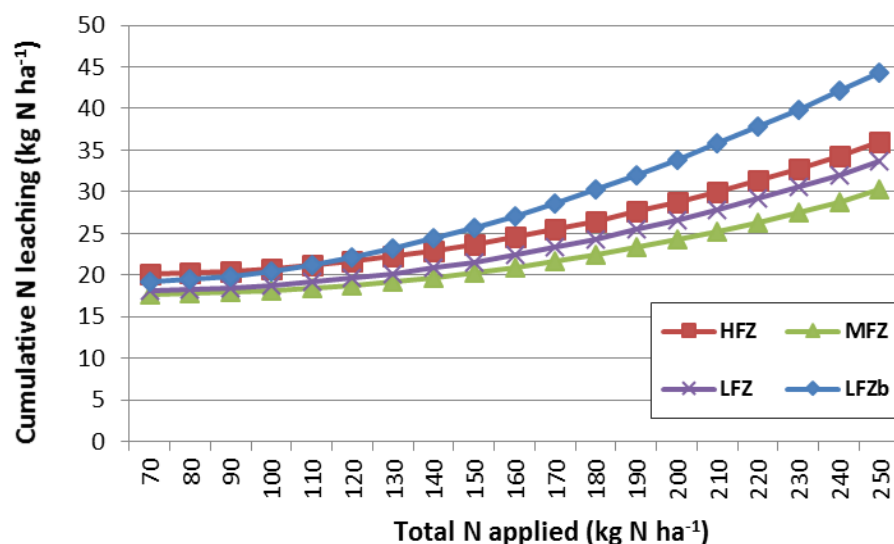


Figure 8. N leaching in response to N fertilization in the four MZs as simulated by SQ2. Data are the average of the outputs produced with the ensemble of 100 mixed observed/synthetic years.

Even if N was not a limiting factor, N rich strips reached a productive level lower than expected, probably due to leaching phenomena that reduced N availability. The average yield was 653 kg ha⁻¹ higher than the N-VRA, allowing the farmer to increase the gross margin revenue (gross revenue- N cost) by almost 100 € ha⁻¹. However, the slight economic convenience derived from a massive N fertilization was not paired with environmental benefit. In fact, it must be remembered that N dose distributed in the rich-strip was 60 kg N ha⁻¹ over the limit set out by the Action Plan (DGR 1150/2011) within the context of the Nitrate Directive.

In absence of direct measurements, N surplus in the soil can be considered as an indicator of water nitrate pollution due to N leaching (Sieling and Kage, 2006) and it can be particularly relevant for fields located in nitrate vulnerable zones. In this experiment, the over-estimation of the yield negatively impacted N surplus, especially in the coarser zones of the field, which reached values close to 100 kg ha⁻¹ N. With the exception of LFZ,

N-rich strips reported a N surplus almost double in all the MZs, and an average value 46% higher.

Another issues to consider when environmental sound fertilization is adopted regard the emissions of climate-altering gases (Robertson and Goffman, 2007) such as the nitrous oxide (N₂O). It was estimated that high N input boosted N₂O emissions by ca. 34% with respect to N-VRA (tab. 7).

Eventually, even if the discrepancy between predicted and measured yield lead to a N surplus higher than expected, N-VRA based on the integration of proximal sensing, weather forecast and crop modelling, still confirmed to be a more environmental sustainable practice than the uniform N application with high doses.

Even if the high N leaching caused by high precipitation amount occurred was not correctly predicted by the model, the algorithm developed is a promising approach for N-VRA, because it takes into account, along with spatial variation of crop nutritional status at NDVI sensing time and early N uptake, also crop response to weather conditions after sensing.

3.5 References

- Barnston, A.G. and Livezey, R.E. 1987. Classification, seasonality and persistence of low-frequency atmospheric circulation patterns. *Mon. Weather Rev.* 115, 1083–1126.
- Basso, B., Cammarano, D., Chen, D., Cafiero, G., Amato, M., Bitella, G., Rossi, R and Basso, F. 2009. Landscape position and precipitation effects on spatial variability of wheat yield and grain protein in Southern Italy. *J. Agron. Crop Sci.* 195(4), 301-312.
- Chung, B., Gurma, K., Raun, W.R. and Solie, J.B. 2010. Changes in response indices as a function of time in winter wheat. *J. Plant Nutr.* 33, 796-808.

- Crain, J.A., Waldschmidt, K.M. and Raun, W.R. 2013. Small-scale spatial variability in winter wheat production. *Commun. Soil Sci. Plant Anal.* 44 (19), 2830-2838.
- Dailey, A.G., Smith, J.U. and Whitmore, A.P. 2006. How far might medium-term weather forecasts improve nitrogen fertiliser use and benefit arable farming in the England and Wales? *Agric. Ecosyst. Environ.* 117 (1): 22-28.
- Dalla Marta, A., Orlandi F., Mancini, M., Guasconi, F., Motha, R., Qu, J. and Orlandini, S. 2015. A simplified index for an early estimation of durum wheat yield in Tuscany (Central Italy). *Field Crop Res.* 170, 1-6.
- Dampney, P.M.R., Goodlas, G., Froment, M.A. and Stafford, J.V. Environmental and production effects from variable rate nitrogen fertilizer to winter wheat in England. *Proceedings 4th International Conference on Precision Agriculture*. Robert, P. C., Rust, R. H. and Larson, W.E. ed. pp. 697–708. ASA, CSSA, SSSA, Madison, USA.
- Dexter, J.E. and Matsuo, R.R. 1980. Relationship between durum wheat protein properties and pasta dough rheology and spaghetti cooking quality. *J. Agric. Food Chem.* 28 (5), 899–902.
- DGR 1150/2011 Programma d'azione per le zone vulnerabili ai nitrati del Veneto.
- Diacono, M., Castrignanò, A., Troccoli, A., De Benedetto, D., Basso, B. and Rubino, P. 2012. Spatial and temporal variability of wheat grain yield and quality in a Mediterranean environment: a multivariate geostatistical approach. *Field Crop Res.* 131, 49-62.
- EC-Council Directive, 1991. Council Directive 91/676/EEC Concerning the Protection of Waters Against Pollution Caused by Nitrates from Agricultural Sources.
- EC- Communication from the Commission to the European Parliament, the Council, the European Economic and Social Committee and the Committee of the Regions. COM (2013) 918.
- Franzen, D.W. and Peck, T.R.. 1993. Soil sampling for variable rate fertilization. In *Proceeding of Illinois Fertilizer Conference* , ed. R. G. Hoefl, 81–91. Springfield, University of Illinois.
- Girma, K., Holtz, S.L., Arnall, D.B., Fultz, L.M., Hanks, T.L., Lawles, K.D., Mack, C.M., Owe, K.W. Reed, S.D., Dantillano, J., Walsh, O. White, M.J. and Raun, W.R. 2007. Weather, fertilizer, previous year grain yield and fertilizer response level affect

- ensuing year grain yield and fertilizer response of winter wheat. *Agron. J.* 99, 1607–1614.
- Hatfield, J.L., Kanemasu, E.T., Asrar, G., Jackson, R.D., Pinter, P.J., Reginato, R.J. and Idso, S.B. 1986. Leaf-area estimates from spectral measurements over various planting dates of wheat. *Int. J. Remote Sens.* 6, 167–175.
- Heege, H.J. and Reusch, S. 1996. Sensor for on-the-go control of site specific nitrogen top dressing. Paper No. 961018 ASAE, St Joseph, MI, USA
- Heege, H.J. 2013. Precision in Crop Farming. Site specific concepts and sensing methods: application and results. Hernan J. Heege editor.
- Holland, K.H. and Schepers, J. S. 2010. Derivation of a variable rate nitrogen application model for inseason fertilization of corn. *Agron. J.* 102, 1415–1424.
- Holland, K.H. and Schepers, J.S. 2013. Use of a virtual-reference concept to interpret active crop canopy sensor data. *Precis. Agric.* 14, 71–85.
- Johnson, G.V. and Raun, W.R. 2003. Nitrogen response index as a guide to fertilizer management. *J. Plant Nutr.* 26, 249–262.
- Kim, M.K. and Kim, Y.H. 2010. Seasonal prediction of monthly precipitation in China using large-scale climate indices. *Adv. Atmos. Sci.* 27, 47–59.
- Kim, M.K., Kim, Y.H. and Lee, W.S. 2007. Seasonal prediction of Korean regional climate from preceding large-scale climate indices. *Int. J. Climatol.* 27, 925–934.
- Lawless, C. and Semenov, M.A. 2005. Assessing lead-time for predicting wheat growth using a crop simulation model. *Agric. For. Meteorol.* 135 (1-4), 302-313.
- Li, F., Gnyp, M.L., Jia, L., Miao, Y., Yu, Z., Koppe, W., Bareth, G., Chen, Y. and Zhang, F. 2008. Estimating N status of winter wheat using a handheld spectrometer in the North China Plain. *Field Crop Res.* 106 (1), 77–85.
- Lukina, E.V., Freeman, K.W., Wynn, K.J., Thomason, W.E., Mullen, R.W, Klatt, A.R., Johnson, G.V., Elliott, R.L., Stone, M.L., Solie, J.B .and Raun. W.R. 2001. Nitrogen fertilization optimization algorithm based on in-season estimates of yield and plant nitrogen uptake. *J. Plant Nutr.* 24, 885–898.
- Magno, R., Angeli, L., Chiesi, M. and Pasqui, M. 2014 Prototype of a drought monitoring and forecasting system for the Tuscany region. *Adv. Sci. Res.* 11, 7–10.

- Marletto, V., Ventura, F., Fontana, G. and Tomei, F. 2007. Wheat growth simulation and yield prediction with seasonal forecasts and a numerical model. *Agric. For. Meteorol.* 174 (1-2), 71-19.
- Moges, S.M., Raun, W. R., Mullen, R.W., Freeman, K.W., Johnson, G.V. and Solie, J.B. 2004. evaluation of green, red, and near infrared bands for predicting winter wheat biomass, nitrogen uptake, and final grain yield. *J. Plant Nutr.* 27 (8), 1431–1441.
- Mullen, R.W., Freeman, K.W., Raun, W.R., Johnson, G.V., Stone, M.L. and Solie, J.B. 2003. Identifying an In-Season Response Index and the Potential to Increase Wheat Yield with Nitrogen. *Agron. J.* 95, 347–35
- Raun, W.R. and Johnson, G.V. 1999. Improving nitrogen use efficiency for cereal production. *Agron. J.* 91, 357–363
- Raun, W.R., Johnson, G.V., Stone, M.L., Solie, J.B., Lukina, E.V., Thomason, W.E. and J.S. Schepers. 2001. In-season prediction of potential grain yield in winter wheat using canopy reflectance. *Agron. J.* 93, 131–138.
- Raun, W.R., Johnson, G.V., Lees, H.L., Sembiring, H., Phillips, S.B., Solie, J.B., Stone, M.L. and Whitney, R.W. 1998. Microvariability in soil test, plant nutrient, and yield parameters in bermudagrass. *Soil Sci. Soc. Am. J.* 68 (3), 683-690.
- Raun, W.E., Solie, J.B., Gordon, V.J., Stone, M.L., Mullen, R.W., Freeman, K.W., Thomason, W.E. and Lukina, E.V. 2002. Improving nitrogen use efficiency in cereal grain production with optical sensing and variable rate application. *Agron. J.* 94, 815–820.
- Raun, W. R., Solie, J. B., Stone, M. L., Martin, K. L., Freeman, K. W., Mullen, R. W., Zhang, H., Schepers, J.S. and Johnson, G.V. 2005. Optical sensor-based algorithm for crop nitrogen fertilization. *Commun. Soil Sci. Plant Anal.* 36, 2759–2781.
- Robertson, G.P., Goffman, P., 2007. Nitrogen transformations. In: *Soil Microbiology Ecology, and Biochemistry*, third ed. Paul, E.A. (Ed.), Academic/Elsevier, New York, pp. 341–364.
- Sellers, P.J. 1885. Canopy reflectance, photosynthesis and transpiration. *Int. J. Remote Sens.* 6, 135–1372.
- Sembiring, H., Lees, H.L., Raun, W.R., Johnson, G.V., Solie, J.B., Stone, M.L., DeLeon, M.J., Lukina, E.V., Cossey, D.A., LaRuffa, J.M., Woolfolk, C.W., Phillips, S.B. and

- Thomason, W.E. 2000. Effect of growth stage and variety on spectral radiance in winter wheat. *J. Plant Nutr.* 23 (1), 141-149.
- Semenov, M.A. and Barrow, E.M. 1997. Use of a stochastic weather generator in the development of climate change scenarios. *Clim. Change* 35, 397–414
- Semenov, M.A. and Doblas-Reyes, F.J. 2007. Utility of dynamical seasonal forecasts in predicting crop yield. *Clim. Res.* 34, 7-81.
- Semenov, M.A., Brooks, R.J., Barrow, E.M. and Richardson, C.W. 1998. Comparison of the WGEN and LARS-WG stochastic weather generators for diverse climates. *Clim. Res.* 10, 95–107.
- Scharf, P.C., Kitchen, N.R., Sudduth, K.A., Davis, J.G., Hubbard, V.C. and Lory, J. 2005. field-scale variability in optimal nitrogen fertilizer rate for corn. *Agron. J.* 97, 452–461.
- Sieling K. and Kage, H. 2006. N balance as an indicator of N leaching in an oilseed rape – winter wheat – winter barley rotation. *Agr. Ecosyst. Environ.* 115, 261–269.
- Simmonds, D.H. 1989. *Wheat and wheat quality in Australia*. CSIRO, William Brooks Queensland.
- Solari, F., Shanahan, J., Ferguson, R., Schepers, J. and Gitelson, A. 2008. Active sensor reflectance measurements of corn nitrogen status and yield potential. *Agron. J* 100, 571–579.
- Solie, J. B., Raun, W. R. and Stone, M. L. 1999. Submeter spatial variability of selected soil and bermudagrass production variables. *Soil Sci. Soc. Am. J.* 63, 1724–173.
- Stewart, C.M., McBratney, A. and Skerrit, J.H. 2002. Site-specific durum wheat quality and its relationship to soil properties in a single field in Northern New South Wales. *Precis. Agric.* 3, 155-168.
- Stone, M.L., Solie, J.B., Raun, W.R., Whimey, R.W., Taylor, S.L. and Ringa, J.D. 1996. Use of spectral radiance for correcting in-season fertilizer nitrogen deficiencies in winter wheat. *Transactions ASAE* 39, 1623-1631.
- Teal, R.K., Tubana, B., Girma, K., Freeman, K.W., Arnall, D.B., Walsh, O. and Raun, W.R. 2006. In-season prediction of corn grain yield potential using normalized difference vegetation index. *Agron. J.* 98, 1488–1494.

- Thiessen, E. 2001. Experiences with sensor-controlled nitrogen-application. *Landtechnik* 56, 278-279.
- Thomason, W.E., Raun, W.R., Johnson, G.V., Freeman, K.W., Wynn, K.J. and Mullen, R.W. 2002. Production system techniques to increase nitrogen use efficiency in winter wheat. *J. Plant Nutr.* 10, 2261-2283.
- Troccoli, A., Borrelli, G.M., De Vita, P., Fares, C. and Di Fonzo, N. 2000. Mini review: durum wheat quality: a multidisciplinary concept. *J. Cereal Sci.* 13 (2), 99-113.
- Vermeulen, S.J., Aggarwal, P.K., Ainslie, A., Angelone, C., Campbell, B.M., Challinor, A.J., Hansen, J.W., Ingram, J.S.I., Jarvis, A., Kristjanson, P., Lau, C., Nelson, G.C., Thornton, P.K. and Wollenberg, E. 2012. Options for support to agriculture and food security under climate change. *Environ. Sci. Policy* 15 (1), 136-144.
- Wibawa, W.D., Dlodlu, D.L., Svenson, L.J., Hopkins, D.G. and Dahke, W.C. 2013. variable fertilizer application based on yield goal, soil fertility, and soil map unit. *J. Prod. Agric.* 6 (2), 255-261.

Cited Website

www.agerborsamerici.it

Chapter IV

Combining proximal sensing and simulation modelling to assess within-field corn N stress

4.1. *Introduction*

It has been demonstrated that site-specific application of N fertilizer provides economic and environmental benefits, such as higher quality and quantity of production (Mulla et al., 1992), higher nitrogen use efficiency (NUE) (Raun et al., 2002), as well as better groundwater quality (Hong et al., 2006). This management strategy suggests changing within-field N rate and it can be implemented by assessing crop canopy status with the use of active light sensors.

Remote sensing and lately proximal sensing data have been used to develop N recommendation, based on algorithms that relate spectral data with yield potential (Raun et al., 2005; Ortiz-Monasterio & Raun, 2007; Solie et al., 2012). A collection of NDVI data during the most affected growth stages is required to develop these algorithms. Martin et al. (2007) identified this critical period for corn at V8 stage (8 leaves stage) while Teal et al. (2006) recommended a time window between V7 and V9. Identify a proper relationship between NDVI and nutrient plant status can be challenging since NDVI sensors can get saturated in coincidence of the rapid biomass accumulation of corn after V6, when $LAI > 3$ (Viña et al., 2011).

In spite of its positive applications, the use of active light sensors has some drawbacks. Crop sensing provides an estimation of the nutrient status but it is not able to predict the nutrient requirements from the sensing time to the harvest (Heege, 2008). As a consequence, it could result in under- or over- fertilization according to the real weather conditions and/or other adverse factors (e.g. pathogen attack). Furthermore, the development of the algorithms relating NDVI to N doses is based on multiple-years and multi locations data which requires time and resources to be collected (Raun, 2004).

Therefore a complementary method assessing N-status might increase N-rate determination accuracy. Crop simulation models can be used to improve estimation of N-status and optimum N-rate because they can simulate crop growth and yield as a response of soil, climate and management information. The Decision Support System for Agrotechnology Transfer (DSSAT) Cropping System Model (Jones et al., 2003) is a package that includes different crop growing models, such as the CERES-Maize model (Jones and Kiniri, 1986). This computes daily corn growth and development in response to soil, environmental and management conditions. It has been used for long time to assess maize response to stress conditions (Castrignanò et al., 1994), evaluate management options to mitigate climate risks (Persson et al., 2009) and predict final yield, its variability and the impact of different agronomic practices (Tojo Soler et al., 2007; Hodges et al., 1987).

A big limitation when incorporating crop simulation modeling with precision agriculture applications it has been running the models across spatial scales. Even though DSSAT is a point-based model, which simulates crop growth on a single point or on a homogeneous area unit, it can be used on precision agriculture studies, which require to simulate the variability of crop behavior spatially across the fields. Basso et al (2001) divided a priori the field in homogenous zones in which they run DSSAT; a similar approach was used by Miao et al (2006), who evaluated management zones optimal N rate using CERES-Maize and 15 years of simulations. Paz et al. (1999) applied the same model to determine variable rate N prescriptions in grids across field and to test ability of the model to predict yield variability and crop response to N.

To avoid the tediousness of running, calibrating and validating DSSAT separately for each management zone, Thorp et al. (2006) developed APOLLO, a decision support system able to manage input data by zones, and automate the processes of model calibration and validation for each zone. It has been used to study the impact climate on corn yield and nitrogen response (Thorp et al., 2006). This study evaluated the potential for using variable nitrogen management in order to achieve corn production goals and reduce N losses in the system. DeJonge et al. (2006) used the same application for evaluation of the potential of variable rate irrigation.

Optimization of the initial values of model parameters to reduce the error between the measured and the simulated data, is another issue in model calibration and it gets more complex when the optimization involves a large data set. The geospatial simulation (GeoSim) plug-in of Quantum GIS is a tool for managing geographic data, conducting spatial model simulation and optimizing model parameters on the spatial scale of the study area (Thorp and Bronson, 2013). GeoSim also allows simulations to be performed over different management units/polygons within a field which facilitate assessment of spatial variability of a specific parameter. The limitation of this type spatial simulation is that each polygon is considered independent from the neighboring polygons. Another function of GeoSim is model optimization which is based on a simulated annealing algorithm. As with model simulation, GeoSim does not take into account the spatial autocorrelation between locations when running the spatial model optimization.

Thorp and Bronson (2013) tested GeoSim applicability both with Aquacrop (Raes, 2009; Steduto, 2009) and DSSAT models, proving its usefulness for precision agriculture studies. The incorporation of remote sensing data into cropping system models can improve model calibration, especially if spatial simulations are conducted. Remote sensing data have been integrated into crop models to assess and predict crop yield (Seidl et al., 2000), monitor crop growth (Launay and Guerif, 2005), driving crop model simulations (Thorp et al., 2010), reducing within-field data collection and re-calculate missing data (Batchelor et al., 2002), and guide the decision making process for precision agriculture applications (Jones and Barnes, 2000).

Different methods have been evaluated to merge remote sensing data into different models. The forcing method is based on the direct replacement of state variables with observed data, losing the information provided by model. This data insertion assumes that the remote sensed data are free of errors, or that the propagation of the observed error into the model is acceptable (Maas, 1987). The optimization method aims to re-initialize or re-parametrize the model by adjusting initial conditions or model parameters to reduce the error between measured (i.e. remotely sensed biophysical data) and predicted data. Some studies have shown that the accuracy of the yield prediction was improved using remote sensed LAI to minimize the error between measured and predicted LAI (Fang et al., 2011). Dente et al. (2008) also mapped with an accuracy of 420 kg ha⁻¹ wheat yield after having

optimized sowing dates, soil wilting point and field capacity using remotely retrieved LAI. A limitation of this method is the large amount of time required by the optimization procedures.

A third method is based on the continuous update of the state variables in the model (Dorigo, 2008) by means of several algorithms such as the Kalman filter (Ma et al., 2013; Ines et al., 2013).

Despite the increasing interest of farmers on sensor-optimized N fertilization, its application in real field conditions is still limited because of the lack of a robust methodology able to convert the canopy sensor readings into N rates. The aims of this study were: 1) develop a methodology for combining remote sensor data (NDVI) with CERES-Maize simulations to assess within-field variability of corn N stress and improve estimation of in-season N rates; 2) demonstrate the utility of GeoSim for managing large geospatial dataset, optimizing initial model parameters, and conducting spatial crop simulations.

4.2. *Materials and methods*

4.2.1 Study Site

The data used for this study were collected from a precision agriculture project, carried out at Giare di Mira in Italy (45° 20 '52.8" N, 12° 10' 12.0", E) during the 2007-2009 seasons. This area is classified as nitrate vulnerable zone according to the European Nitrate Directive (91/676/CEE).

The climate of the experimental site is sub-humid, with annual rainfall around 96 mm. In an average year, rainfall is highest in autumn (440 mm) and lowest in winter (88 mm). Temperatures increase from January (minimum average: 1.12 °C) to July (maximum average: 29.6 °C). The soil, classified as Aquic Haplusteps, coarse-loamy, mixed, mesic, is alluvial in origin, with a moderate alkaline reaction (Tab. 1).

The field experiment compared three crop rotations - continuous corn, corn-wheat, corn-wheat-soybean - subject to two management systems or treatments. The first treatment consisted of conventional tillage and high N fertilization rates (High Input – HI) while the second treatment consisted of minimum tillage, cover crops, lower N fertilization

rates (low input – LI). Experimental fields were rectangular in shape (about 400 m length x 30 m width) with an average size of 1.2 ha. The two longer sides were bordered by 1.4 m depth, 30 m spaced open ditches. Each field was divided into four large plots (0.3 ha size each) where the two management systems with two replications were implemented (Fig. 1). Tillage and fertilization practices for both the management systems implemented on corn fields are listed in tables 2 and 3. Corn hybrid Pioneer 33T56 was sowed on April 29, 2008 in fields A, B and F, and on May 7, 2009 in fields A, C and E, with a plant density of 8 plants m⁻². This early maturity hybrid requires 113 days to reach physiological maturity and 130 growing degree units (GDUs) to reach silking.

Corn was harvested with a combine harvester equipped with a yield monitor (GreenStar, John Deer, Moline, Illinois, USA, in 2008; Cebis, Claas, Harsewinkel, Germany, in 2009) on October 1st, 2008 (fields A, B and F) and on September 3rd, 2009 (fields C and E). Grain yield data was corrected to dry biomass.

Table 1. Soil average properties

Depth (cm)	Sand (%)	Silt (%)	Clay (%)	pH	EC 1:2,5 (mS/m)	SOM g/kg ⁻¹	N _{tot} (%)	C/N	P Olsen (mg kg ⁻¹)	CEC (cmol kg ⁻¹)
0-20	64.64	26.96	8.40	7.49	25	8.62	0.06	7.88	13.79	13.78
20-40	62.45	27.87	9.68	7.53	27	8.82	0.06	8.43	13.61	15.48
40-60	66.30	24.46	9.24	7.58	24	6.26	0.05	7.84	12.07	14.48
60-80	66.58	23.97	9.45	7.61	22	6.01	0.04	7.65	8.11	15.36

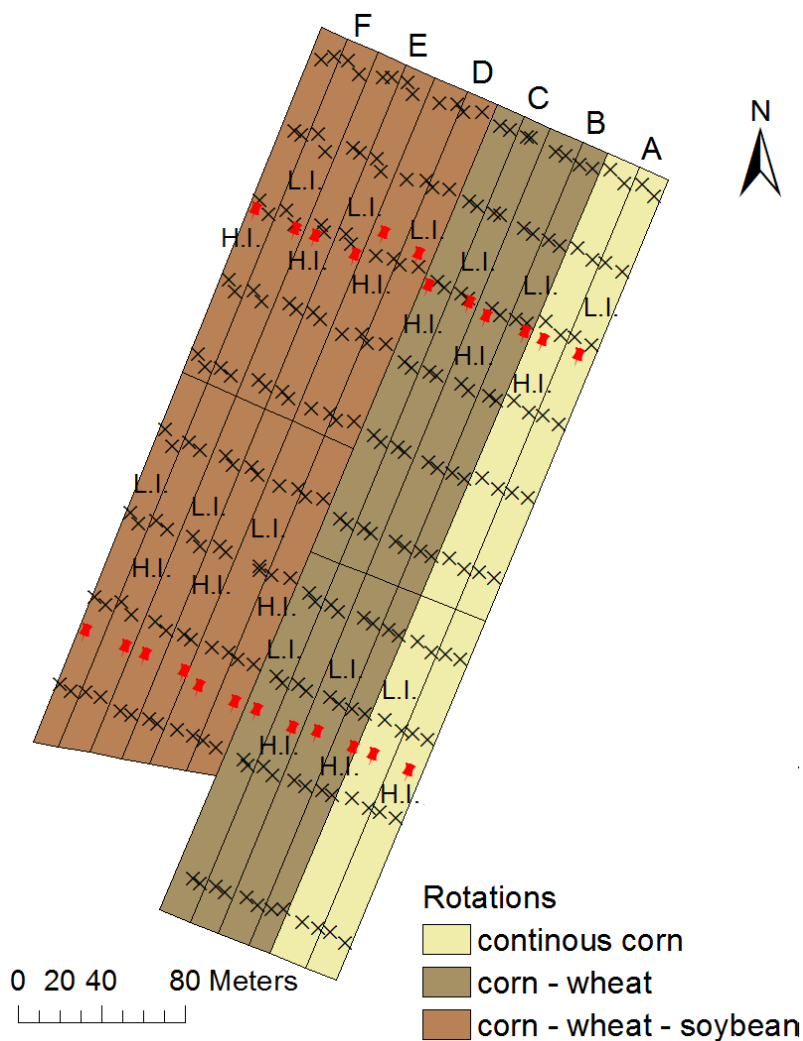
EC: electrical conductivity; SOM: soil organic matter; CEC: cation exchange capacity.

Table 2. Tillage practices implemented in the two treatments.

Year	LI		HI	
	Date	Tillage	Date	Tillage
2008	28 Apr.	Disk (10 cm deep)	1 Apr.	Moaldboard plow (30 cm deep)
	4 Jun.	Rod weeder (3 cm deep)	1 Apr.	Disk (10 cm deep)
			1 Apr.	Cultivator (10 cm deep)
			4 Jun.	Rod weeder (3 cm deep)
2009	22 Apr.	Disk (10 cm deep)	22 Apr.	Moaldboard plow (30 cm deep)
	18 Jun.	Rod weeder (3 cm deep)	22 Apr.	Disk (10 cm deep)
			22 Apr.	Cultivator (10 cm deep)
			18 Jun.	Rod weeder (3 cm deep)

Table 3. Fertilizations for the two treatments.

Year	Date	L.I.			H.I.			
		N kg ha ⁻¹	P kg ha ⁻¹	K kg ha ⁻¹	Date	N kg ha ⁻¹	P kg ha ⁻¹	K kg ha ⁻¹
2008	1 Apr.	16	20	17	1 Apr.(organic)	50	11	58
	1 Apr.	126			2 Apr.			30
	29 Apr.		5		29 Apr.	36	40	
	15 May	98			4 Jun.	115		
					10 Jun.	115		
	Total	240	25	17	Total	316	51	88
2009	22 Apr.	16	20	17	19 Mar.			10
	7 May		5		19 Apr.(organic)	50	11	58
	20 May	98			16 Apr.			25
	3 Jun.	126			7 May	36	40	
					10 Jun.	115		
					18 Jun.	115		
	Total	240	25	17	Total	316	51	93



4.2.2 Weather data and soil sampling

Weather data was provided by a weather station located in Mira, which is 15 km far from the experimental site ($45^{\circ} 26' 7.0794''$ N, $12^{\circ} 7' 3.6834''$ E).

At the beginning of the experiment, an apparent soil electrical conductivity (soil EC_a) survey was carried out over the study fields using a EM38DD sensor (Geonics Limited, Ontario, Canada). This sensor collects data in horizontal (up to 75 cm sensing depth) and vertical dipole orientation mode (up to 150 cm sensing depth) which allows collection of soil EC_a at two soil depths. The sensor was linked to a stand-alone DGPS in

order to georeference the sensor readings (1 reading per second). An average of 416 readings per field were collected on a transect of 5.5- 7.5 m in length along each field.

Along with the soil EC_a data, soil samples for physico-chemical analyses were collected at several locations within each field. At the center of each plot (4 locations), soil cores extracted to a 80 cm depth were divided into samples every 20 cm depth . In addition, soil analyses were conducted on samples collected in the 0-30 cm profile at additional 32 (fields A, B, C) or 36 locations (fields E, F) per field following a regular grid (fig. 1).

4.2.3 NDVI collection

Changes in corn biomass and N leaf levels were assessed by collecting spectral data with a handheld active spectrometer, linked to a GPS unit. The APS1-CropCircle (Holland Scientific, Lincoln, NE, USA) measures canopy reflectance at 590 nm (Visible-VIS) and 880 nm (Near Infrared-NIR). An average of 1705 points per field was covered, holding the sensor 0.8 m above the canopy, parallel to the corn rows. The data collected were processed to calculate NDVI (Normalized Difference Vegetation Index), according to the equation provided by Rouse et al. (1973):

$$NDVI = \frac{NIR - VIS}{VIS + NIR}$$

Eq.1

The data collection was conducted once per season, after side-dress N application, at 73 days after sowing (DAS) in 2008 and 63 DAS in 2009 .

An average of 1705 points per field was covered, holding the sensor 0.8 m above the canopy, parallel to corn rows, with a 1 second acquisition interval..

4.2.4 LAI measurements

Indirect LAI (Leaf Area Index) estimations were obtained using a Sunfleck Ceptometer (Delta-T devices LTD, Cambridge, England). This instrument measures PAR (Photosynthetic Active Radiation) above (incoming radiation) and under the canopy (transmitted radiation), through a probe equipped with 80 light sensors. Twelve

observations in a 5 m –radius area from the center of each plot were collected at 73 DAS in 2008, LAI values were derived from PAR values according to the Norman- Jarvis modified model (Norman and Jarvis, 1975).

4.2.5. Data processing

Even though one of the objectives of this study was to simulate the spatial variability of yield and N stress, the data available restricted the scale and the size of the smallest area at which the model was run. Every field was split in polygons of 0.03 ha size each because this is the scale at which soil texture data were available. A shapefile delineating every polygon was created as base layer for the subsequent 32 to 36 site-specific simulations, keeping as the center of each polygon the location where soil samples were collected. Average NDVI and yield data were calculated for every polygon. Due to the scarcity of NDVI data in some zones of the fields, polygons with less than 15 measurements point were excluded from the simulation.

Although soil texture data at multiple soil depths is required for running the CERES-Maize, the initial soil data from this study was available up to 80-cm depth only for four locations per field and the other locations had only soil texture estimated at 30-cm depth. Therefore, for all soil sampling locations, soil texture up to 180-cm depth on 30-cm depth intervals was estimated by conducting a regression kriging analysis that combined the soil EC_a data (readings at 0-75 cm and 0-150cm soil depth) and the soil texture data available (Goovaerts, 1997).

An ordinary kriging analysis was conducted to estimate soil EC_a data at the locations with soil texture data. Subsequently, a regression kriging analysis (Goovaerts, 2000) was run to predict the local mean of soil texture as a function of depth, horizontal EC_a , vertical EC_a , and the log of the ratio of vertical EC_a and horizontal EC_a . Eventually, SGeMS (Stanford Geostatistical Modeling Software) was used to interpolate the regression residuals in 3D and then to regression estimate. Results of spatial interpolations of the upper layer (0-30 cm) are shown in figure 2.

4.2.6 Model calibration

Cultivar coefficients

The calibration of the cultivar coefficients was conducted using the Generalized Likelihood Uncertainty Estimation (GLUE) method available as a tool in DSSAT. GLUE uses a Bayesian Monte Carlo parameter estimation technique that measure the closeness-of-fit of modeled and observed data. GLUE was used to estimate cultivar coefficients related to phenology and growth parameters (He et al., 2010). . Cultivar coefficients of a hybrid with the same relative maturity, Pioneer 31G98, were chosen as a basis for this calibration (Tojo-Soler et al., 2007). Because the calibration has to be conducted in absence of crop limiting conditions, the cultivar coefficients were calibrated using 2008 data only from the high yielding polygons (yield > 6500 kg ha⁻¹) of the H.I. treatments (37 polygons). Data from the 2009 season was excluded because of the low amount of precipitation recorded early in the season (May) and during the grain filling period (July) (fig. 3). After running 10000 simulations, GLUE estimated the best combination of parameters that minimize the error between the observed and simulated harvested yield and silking and physiological maturity dates (tab. 4).

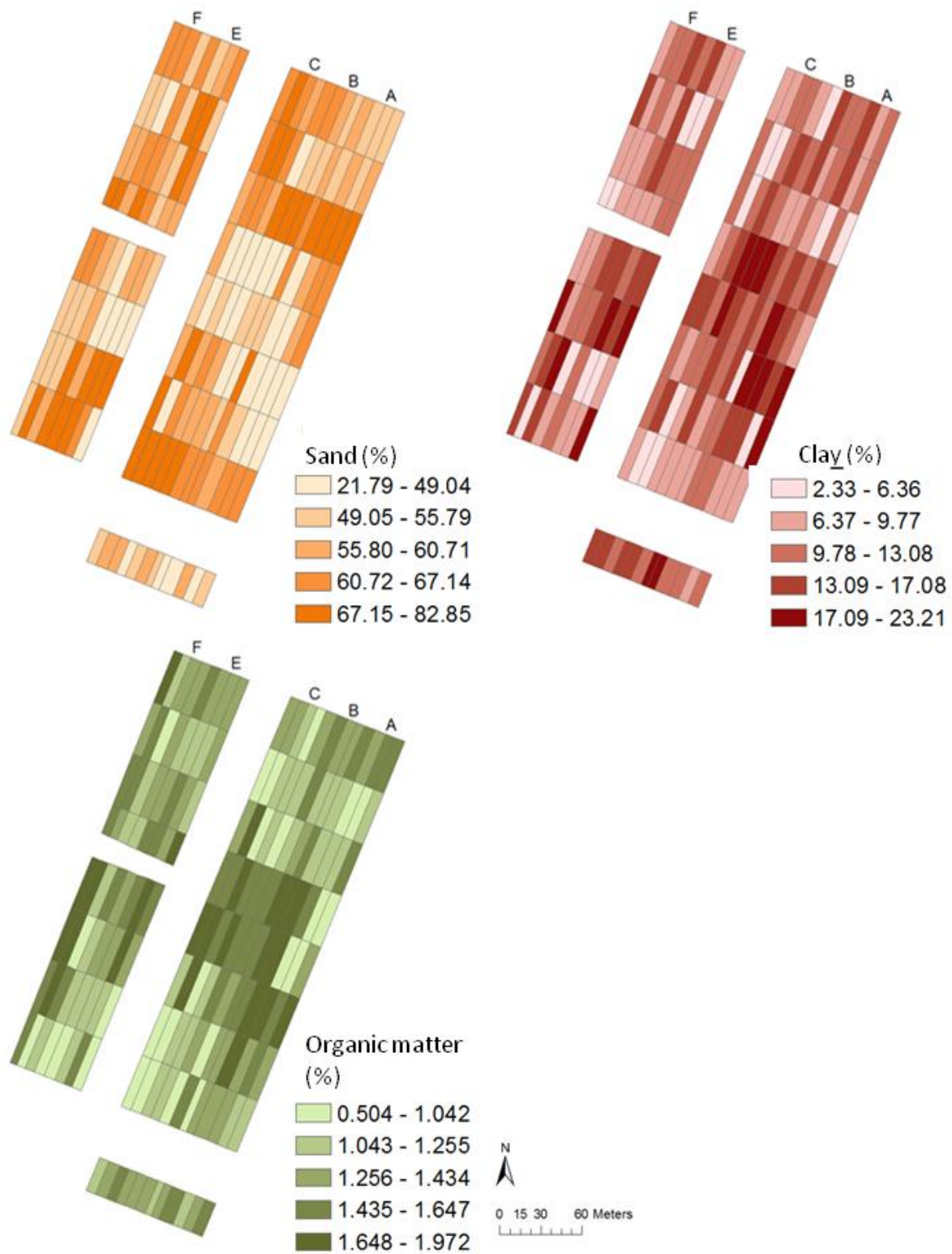


Figure 2. Main soil properties of the upper layer (0-20 cm) of the polygons, derived from regression kriging.

Tab. 4. Cultivar coefficients.

P1 (°C day)	P2 (days)	P5 (°C day)	G2 (Nr)	G3 (mg day ⁻¹)	PHINT (°C day)
215.5	0.452	884.4	838.6	8.93	48.00

P1: thermal time from seedling emergence to the end of the juvenile phase (expressed in degree days above a base temperature of 8 °C) during which the plant is not responsive to changes in photoperiod. P2: extent to which development (expressed as days) is delayed for each hour increase in photoperiod above the longest photoperiod at which development proceeds at a maximum rate (which is considered to be 12.5 hours). P5: thermal time from silking to physiological maturity (expressed in degree days above a base temperature of 8 °C). G2: maximum possible number of kernels per plant. G3: kernel filling rate during the linear grain filling stage and under optimum conditions (mg/day). PHINT: phyllochron interval; the interval in thermal time (degree days) between successive leaf tip appearances. (Hoogenboom et al., 2012).

Spatial model optimization using Geosim

GeoSim allows the optimization of model initial parameters to minimize the error between measured and simulated data through a simulation annealing algorithm. The optimization was conducted for each polygon and consisted of the identification of model parameters that reduced the error between observed and simulated values. Model calibration was a two-step process, the model was first calibrated for yield and subsequently LAI was calibrated.

1) Model optimization for yield

The model was firstly optimized to reduce the error between the predicted and the observed yield. This calibration aimed to capture the spatial variability of measured yield and involved soil water balance parameters such as initial soil water content, drained upper limit (DUL) and lower limit (LL). The range of initial values used to run de optimization was 10 to 30 % for initial soil water content, 0.16 to 0.38 for DUL, and 0.03 to 0.15 for LL (Tab. 5).

Tab.5: Initial maximum and minimum values for optimization-

Parameter	Max	Min
Initial water content	0.30%	0.13%
DUL	0.38%	0.16%
LL	0.15%	0.03%
PHINT	60	45

2) Use of proximal sensing to improve model calibration and simulation

The next step in model calibration involved incorporation of NDVI data to adjust LAI predicted values and therefore improve the estimation of crop N stress spatial distribution. Several studies have shown a relationship between LAI, NDVI and crop N status (Carlston & Ripley, 1997; Ma et al., 1996). For this reason, the model was calibrated to simulate LAI by reducing the deviation between measured and simulated spatial distribution of LAI. Because LAI was not directly measured at the experimental fields, a non-linear relationship was developed first to estimate LAI from NDVI data, using PAR-derived LAI. LAI values were related to the NDVI average values per experimental unit, using the modified Beer's law (2) (Choudhury et al., 1994):

$$NDVI = NDVI_{max} - (NDVI_{max} - NDVI_{min}) \exp(-k'GLAI)$$

Eq.2

where $NDVI_{max}$ is the index value when LAI is maximum (dense vegetation); $NDVI_{min}$ represents the value for bare soil and $GLAI$ stands for green leaf area index. Because NDVI data were collected before leaves senescence, LAI was considered as $GLAI$. According to Gitelson et al. (2003), a value of 0.9 was used as $NDVI_{max}$ while $NDVI_{min}$ was set to 0.1 because of the sandy-loam texture of the experimental site. The vegetation extinction coefficient k was estimated with a non-linear curve fitting procedure based on the Lavenberg-Marquardt algorithm implemented in Statistica (Statsoft, USA).

The comparison between the LAI estimated with equation 2 as a function of NDVI, henceforth called sensed LAI, and the LAI predicted by DSSAT, suggested the need of a second model calibration which involved data from both seasons 2008 and 2009. A preliminary sensitivity analysis suggested that the phyllochron interval (PHINT)

coefficient was the only sensitive parameter able to describe the spatial variability of LAI. Indeed this parameter controls the interval time between successive leaf tips appearance. By a physiological point of view PHINT depends on the genotype and it is not expected to vary within the fields. PHINT was used as a calibrated lumped parameter -losing in this way its physiological significance- in order to describe processes occurring at the small scale and not properly described by DSSAT. Furthermore, the PHINT value has some uncertainty even among the same cultivar, because it was not measured, but it was derived from the calibration of the cultivar coefficients. PHINT was adjusted ranging from 45 to 60 GDD. Similarly, spatial optimization of physiological cultivar coefficients was conducted by Thorp et al. (2014) in order to explain cotton yield variability at field level.

4.2.6 Model validation and statistical methods for performance assessment

The model performance was evaluated by linear regression and Root Mean Square (RMSE), computed as follows:

$$RMSE = \sqrt{\frac{\sum_{i=1}^n (Y_i - \hat{Y}_i)^2}{n}}$$

Eq.3

where Y_i is the observed value; \hat{Y}_i is the predicted value and n is the number of observed values.

The closer the RMSE is to 0, the closer the modeled values are to the measured ones.

4.2.7 Identification of the optimum N rate

Once the model was calibrated to simulate yield, LAI and subsequently crop N status, simulations were run to determine in-season site specific N rates that will reduce simulated crop N stress. Through GeoSim, different N rate scenarios can be run for each polygon, and resulting predicted yield and N stress on specific growth stages can be compared in order to find the optimum agronomical and/or economical N rate. A side-dress N

application was simulated to be applied on the same day of NDVI sensing (73 DAS in 2008 and 65 DAS in 2009), this in addition to all the previous uniformly N applications.

Four different criteria were used to set the optimum N rate: the minimization of N stress, the maximization of crop yield, the maximization of gross margin, and the minimization of the N surplus.

Studies carried out by Ciampitti and Vynn (2011) proved the importance of providing the adequate N supply in the post silking period in order to reach a high yield, especially for recent corn hybrids, which uptake an higher amount of N during the reproductive stage than older ones (Ciampitti and Vynn, 2013). For this reason the identification of the optimal N rates was based on the in-season N rates which minimized the simulated N stress (NSTD) at the beginning of the grain filling (83 DAS in 2008 and 82 DAS in 2009). The model was firstly run to predict N stress (NSTD73 and NSTD65 in the first and in the second crop season, respectively) and its variability on the same day of NDVI measurements. The optimum NSTD83 and NSTD82 were calculated as 50% of NSTD73 and NSTD65, respectively. Nitrogen rates were considered optimal when they allowed to reach a N stress level at grain filling equal to 50% of NST at NDVI measurement dates.

The maximization of crop yield was identified by running the model in each polygon with increasing N rates from 0 to 150 kg ha⁻¹ of N, while the optimum economical N rate was considered as the rate which allowed to level off the price of the N unit and the marginal gross margin.

Eventually, N surplus criterion was based on Veneto Region Action Plan Program of Nitrate Directive (DGR 1150/2011). Variable rate N input (N input) was calculated as follows:

$$N_{input} = N_{up} - (N_o * K_o + N_m * K_m)$$

Eq. 4

where N_{up} is the N uptake of the corn at the end of the season, N_o is the N rate uniformly applied by organic fertilization and K_o is its efficiency, N_m is the N rate uniformly applied by chemical fertilization and K_m is its efficiency. According to Veneto Region Action Plan

(DGR 1150/2011), N uptake is capped to 210 kg ha^{-1} , Ko is set 0.4 for solid manure distributed in and Nm is 1 for mineral fertilizers

4.3. Results and discussions

4.3.1 Calibration of the model to simulate yield

First simulations were run for each polygon using soil hydraulic properties estimated by geostatistics analyses. Since soil water content at the beginning of the experiment was not directly measured, it was set equal to 0.2 all along the experimental site.

Initial yield simulations did not represent the variability in soil properties, mainly texture, measured on the fields which influenced plant growth and final yield. On average for all the study fields, simulated yield ($7828.08 \text{ kg ha}^{-1}$) was close to the measured ($7692.62 \text{ kg ha}^{-1}$) one in 2008 while it was strongly underestimated in 2009 ($2601.94 \text{ kg ha}^{-1}$ -simulated Vs $7828.08 \text{ kg ha}^{-1}$ -observed). In both the years, total RMSE was particularly high being 1832 kg ha^{-1} in 2008 and 5501 kg ha^{-1} in 2009. RMSE was high even if calculated from a single field (tab. 6).

Since initial soil water content was considered a parameter influencing seed germination, plant health resulting in final yield variability, it calibrated in order to better simulated within-field yield changes. After calibration, initial soil water ranged from 0.13 % to 0.30 % in both 2008 and 2009. Although RMSE for yield slightly improved in both the crop seasons, yield results were still unsatisfactory, especially in 2009 when RMSE was the highest (Tab. 6)

A further model optimization was then required. Following the approach of Ruiz Nogueira et al. (2001) initial soil water content, DUL and LL were adjusted at the same time. After optimization, DUL and LL ranged from 0.16 to 0.37 and from 0.03 to 0.15, respectively. Final yield was predicted with good accuracy, and RMSE values were 298.55 and 269.41 in 2008 and 2009, respectively (Table 6, Fig. 4). Spatial yield variability was thus properly modeled in both the crop seasons and for both treatments, as shown in figure 5, with a standard deviation ranging from 612 kg ha^{-1} (field E, year 2009) to 1895 kg ha^{-1} (field C, year 2009) (tab. 7).

In 2008 the plots receiving the highest N rate were also the more productive fields, specially on fields A and F, while in field B LI plots reported higher yield HI. in. In 2009 a

higher productivity was observed from the or HI treated plots, particularly on field C where the interaction between meteorological, soil type and management resulted on higher crop productivity of ca. 2 t ha⁻¹ with respect to LI (Tab. 7).

4.3.2 NDVI variability

NDVI measurements were collected late in the season (73 and 63 DAS in 2008 and 2009, respectively), which results on NDVI average values of 0.74 and 0.72 for the seasons 2008 and 2009, respectively). In 2008 similar NDVI values were observed among the treatments in each field, as reported in table 8. In field A both the treatments had the same NDVI average (0.75), in field B slightly higher values were observed in HI plots while the opposite was noticed in field F. As a result, spatial variability was low in the fields, with low coefficient of variation (CV) and a standard deviation ranging from 0.02 to 0.04, and it was mainly driven by the fertilization factor. A similar behavior was observed in 2009 with high NDVI values (mean 0.73) and low standard deviation (0.03). On average, in field C, NDVI was higher in HI (0.76) than LI (0.74) while the opposite was observed in field F, with values slightly higher in LI than HI (0.72 vs 0.71) (tab.8).

Table 6. Impact of model calibration strategies on simulated yield: Average values and RMSE (root mean square error).

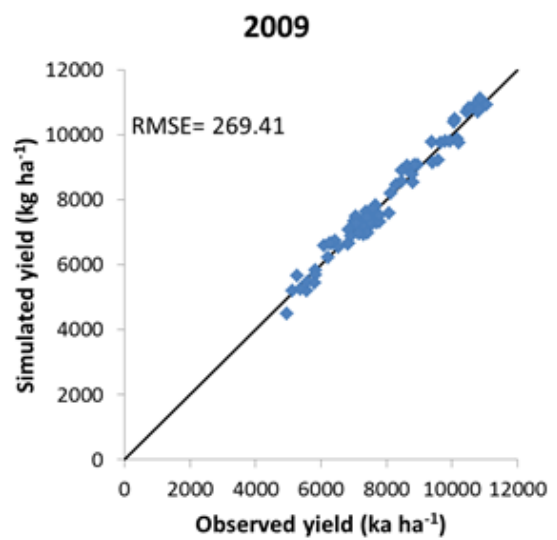
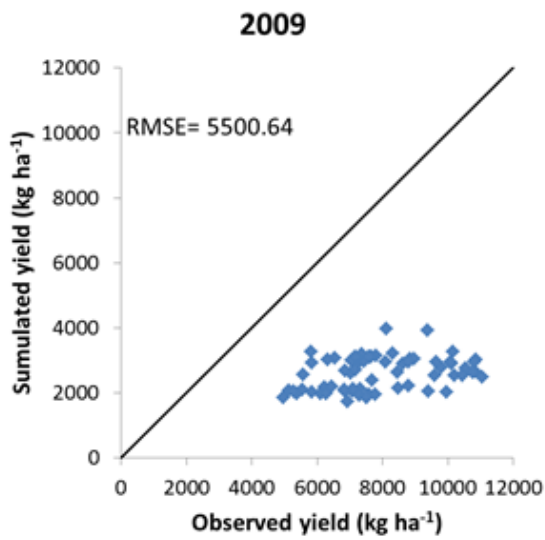
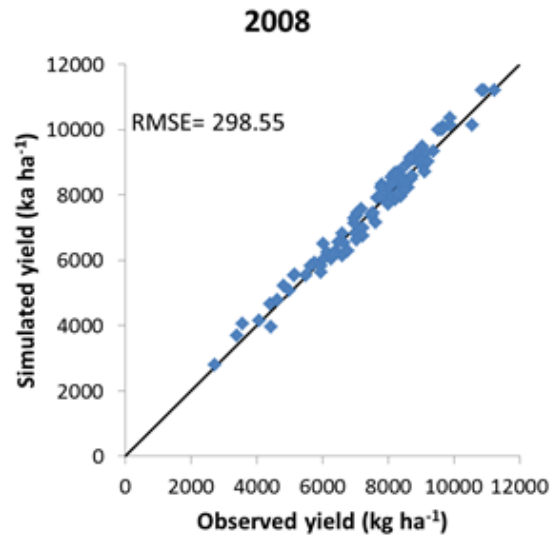
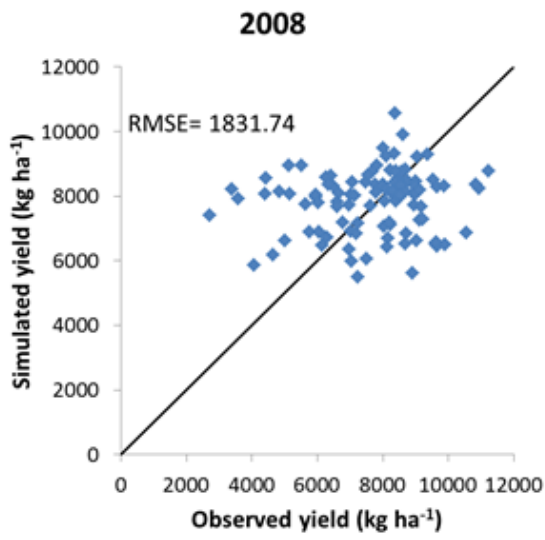
Field	Measured	Without calibration		Calibration Initial soil water content		Calibration Initial soil water content, DUL, and LL	
	Average (kg ha ⁻¹)	Average (kg ha ⁻¹)	RMSE	Average (kg ha ⁻¹)	RMSE	Average (kg ha ⁻¹)	RMSE
2008							
A	7345.22	8578.44	1832.12	8183.33	1545.66	7345.86	275.50
B	7368.23	7529.80	1518.09	7401.06	1469.73	7486.63	289.90
F	8376.40	7376.00	2287.59	7339.97	2065.18	8458.19	353.23
2009							
C	8686.86	2538.66	6246.45	2935.25	5959.40	8726.78	251.23
E	6986.68	2665.22	4516.74	2710.59	4683.66	6962.31	288.50

Table 7. Average, standard deviation (St.dev) and coefficient of variation (C.V.) of simulated yield and LAI for different fields and treatments

Field	Yield			LAI		
	Average	St.dev.	C.V.	Average	St.dev.	C.V.
2008						
A						
HI	6947.06	1718.79	0.25	3.02	0.26	0.09
LI	7744.67	1066.15	0.14	2.94	0.16	0.05
Tot	7345.86	1466.50	0.20	2.97	0.21	0.07
B						
HI	7385.18	1477.79	0.20	2.95	0.18	0.06
LI	7582.44	1518.21	0.20	2.97	0.25	0.08
Total	7486.63	1479.93	0.20	2.96	0.21	0.07
F						
HI	8555.75	2360.80	0.28	2.99	0.19	0.06
LI	8360.63	1671.12	0.20	3.16	0.24	0.08
Total	8458.19	2014.42	0.24	3.07	0.23	0.07
2009						
C						
HI	9694.11	1472.96	0.15	3.29	0.18	0.06
LI	7759.44	1800.54	0.23	2.94	0.25	0.09
Total	8726.78	1894.98	0.22	3.11	0.28	0.09
E						
HI	7062.44	677.85	0.10	2.90	0.06	0.02
LI	6862.19	541.97	0.08	2.62	0.11	0.04
Total	6962.31	612.21	0.09	2.76	0.16	0.06

Table 8. NDVI average and variability for different fields and treatment

Field	Average	St.dev.	C.V.
2008			
A			
HI	0.75	0.02	0.03
LI	0.75	0.01	0.01
Total	0.75	0.02	0.02
B			
HI	0.75	0.01	0.02
LI	0.74	0.01	0.02
Total	0.74	0.02	0.02
F			
HI	0.74	0.03	0.04
LI	0.75	0.02	0.02
Total	0.74	0.03	0.04
2009			
C			
HI	0.76	0.02	0.02
LI	0.74	0.03	0.04
Total	0.75	0.03	0.04
E			
HI	0.71	0.03	0.04
LI	0.72	0.02	0.03
Total	0.72	0.02	0.03



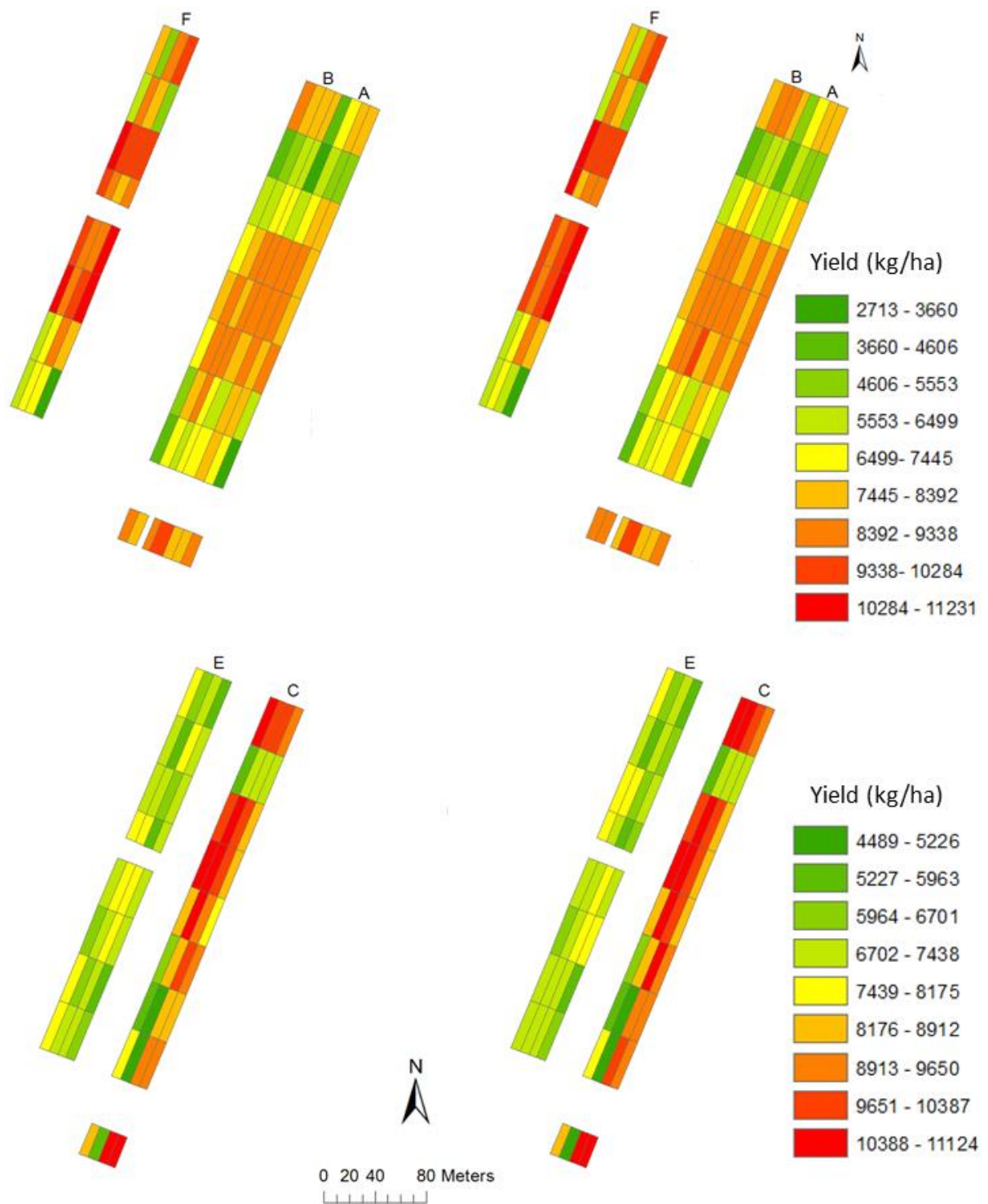


Figure 5. Observed yield (left) vs. simulated yield (right) in 2008 and 2009.

4.3.3 Calibration of the model to simulate LAI variability

Simulation of LAI using the third set of adjusted parameters (i.e. soil water content, DUL and LL) produced high errors with a total RMSEs of 0.68 in 2008 and 1.37 in 2009. Even when model performances were considered in each single field (Tab. 9), REMSs were still high.

An additional model optimization was thus necessary to simulate LAI spatial variability. According to Thorp et al., (2014), LAI variability could be explained by a variation in cultivar parameters. After a preliminary sensitivity analysis, it was optimized the phyllochron, which governs the thermal time between the sequential formation of leaves. For the simulated hybrid, the initial value was 48 GDD, while the values resulted from the optimization ranged between 36.1 and 56.9 in 2008, and 38.5 and 59.9 in 2009.

The adjustment of the phyllochron led to a decrease in the RMSE in both the years, 0.39 in 2008 and 0.22 in 2009. The higher value in 2008 was caused by the large discrepancy between measured and simulated LAI (error >0.8) in six polygons where low yield values were observed (< 4000 kg ha⁻¹). Lower yield was simulated by GeoSim operating a drastical reduction of the water field capacity in the polygons, which caused severe water stress and, accordingly, led to simulated LAI <2.4. However, field surveys in those polygons, highlighted that measured LAI was higher than the simulated ones. Indeed, it was weed competition and not water stress the factor limiting the crop yield in the polygons. Excluding these from the LAI simulation, led to a reduction to 0.22 of the total RMSEs (Fig.6). Final RMSEs for each field are reported in Tab. 7.

Simulated LAI shown the same behavior of NDVI since a low variability was observed in both the crop seasons, with a LAI standard deviation of 0.39 in 2008 and 0.29 the following year. No relevant differences were observed among the treatments of the same field (Tab. 7).

Because the applicability of the model is based on its capability to accurately predict the final productions, the model performance on yield simulation after this latter optimization was evaluated, running the model with the adjusted PHINT, DUL, LL and initial soil water content.

Both the years reported higher errors than the ones resulted after the optimization of the soil hydraulic parameters only, but the RMSEs are still acceptable (520.05 in 2008; 620. 96

in 2009). This means that the optimization of the phyllochron influenced mainly biomass accumulation and slightly affected the yield, proving that the applicability of the model is not limited by this adjustment. However, simulating correctly the LAI distribution within the field guarantees to represent properly also crop N status because of the close relationship existing between the two parameters. This provides potential advantages in order to manage in season site-specific fertilization based on the combination of model simulation and proximal sensing.

Table 9. average of sensed LAI and RMSEs and average of LAI simulations without any calibration and after PHINT optimization. Polygons with for which soil hydraulic characteristics were not the yield limiting factor were removed from this analysis.

Field	Sensed Average	Not optimized Average	RMSE	PHINT optimization Average	RMSE
2008					
A	3.12	3.21	0.61	2.95	0.22
B	3.08	3.395	0.57	2.96	0.23
F	3.07	3.45	0.879	3.07	0.22
2009					
C	3.15	2.50	0.72	3.11	0.14
E	2.79	3.45	0.3	2.794	0.28

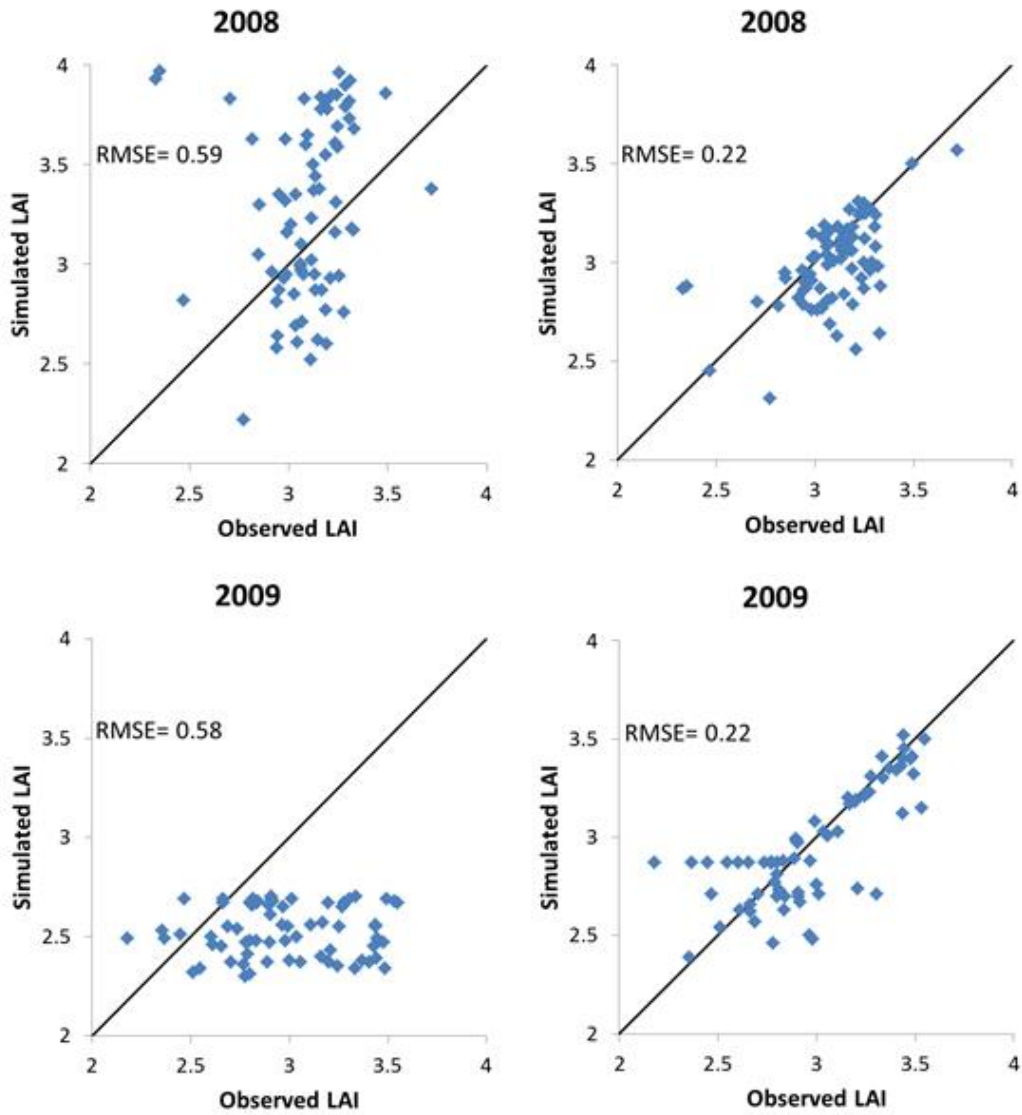


Figure 6. Simulated versus observed LAI in 2008 and 2009 without model calibration on the left, and after PHINT optimization, on the right.

4.3.4 Nitrogen stress simulation

In order to evaluate DSSAT sensitivity to represent nitrogen stress at spatial level, nitrogen stress maps were simulated on the same dates in which NDVI measurements were performed. In DSSAT, nitrogen stress is expressed by NSTD parameter, which ranges from 0 to 1, with values close to 0 meaning a good N status, while values close to 1 are indexes of severe nitrogen stress.

Fig. 7 shows the maps produced for the two crop seasons. The low N stress reported in both the year (≤ 0.28 in 2008 and ≤ 0.20 in 2009) is probably due to the high fertilization rates applied and the good weather conditions that probably favored N uptake. Indeed DSSAT didn't report any water stress until grain filling in both the years. NSTD variability, even if low, was driven by N fertilization: LI plots showed higher stress than HI, especially in 2009, when NSTD was almost 0 in all the polygons of high input treatment (Tab. 10).

Due to the lack of any N stress field measurements, the performance of the model on N stress prediction couldn't be tested. However, the model accuracy on LAI simulation can be considered an indirect proof of DSSAT sensibility to represent spatial variability of crop N status .

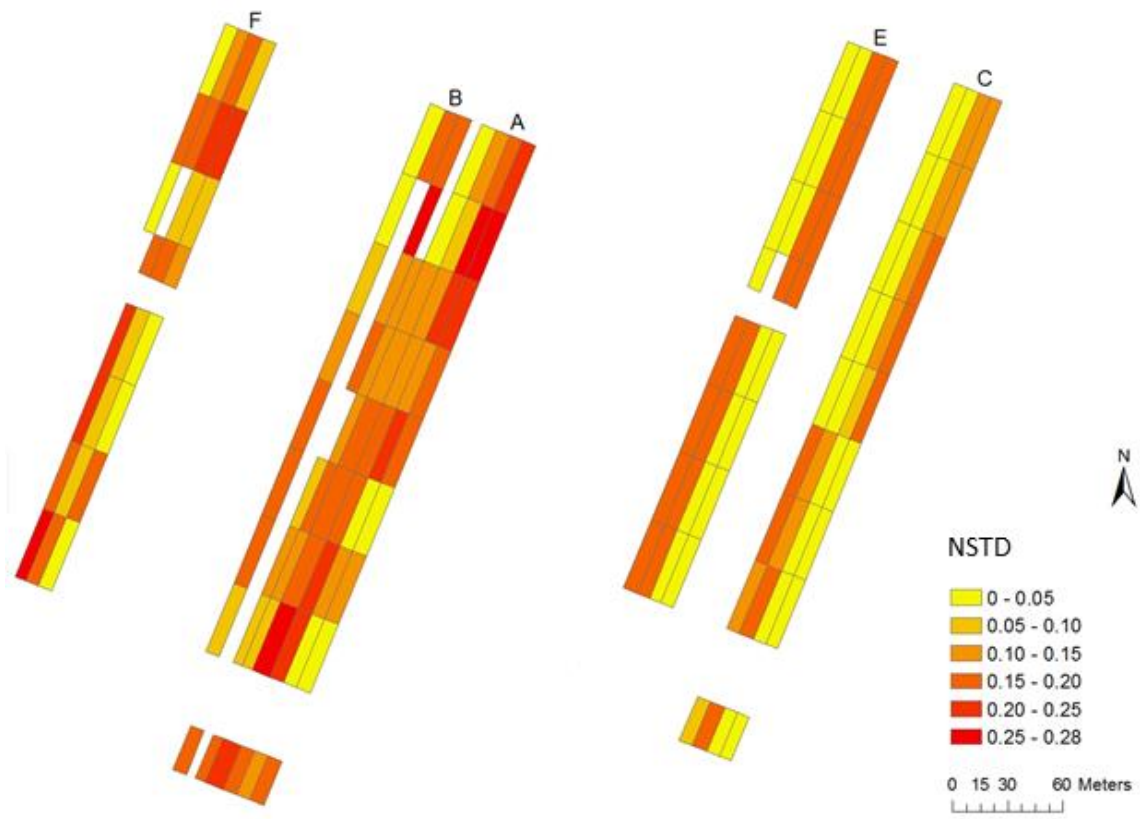


Figure 7. NSTD maps of 2008 (left) and 2009 (right).

Table 10. Simulated NSTD variability in different fields and treatment

Field	Average	St. Dev.	C.V.
2008			
A			
HI	0.09	0.06	0.67
LI	0.21	0.04	0.19
Tot	0.15	0.08	0.52
B			
HI	0.11	0.05	0.46
LI	0.15	0.06	0.36
Tot	0.13	0.06	0.43
F			
HI	0.09	0.07	0.80
LI	0.17	0.07	0.41
Tot	0.13	0.08	0.64
2009			
C			
HI	0.00	0.01	2.19
LI	0.14	0.03	0.23
Tot	0.07	0.07	1.02
E			
HI	0.00	0.00	0.00
LI	0.18	0.01	0.04
Tot	0.09	0.09	0.99

4.3.5 Evaluation of the optimum N rate

Minimization of N stress criteria simulated lower N input rates with respect to those effectively applied in the experiment. In HI and LI plots the average N rate was reduced of 87.55 kg ha⁻¹ and 76.62 kg ha⁻¹ in 2008, and 109.56 kg ha⁻¹ and 60.57 kg ha⁻¹ in 2009, respectively.

This strategy aimed to guarantee a good crop nutritional status based on N content in the biomass, but it didn't take into account the maximum achievable yield as a function of soil fertility. Indeed, the prescription map did not match the variability pattern reported by the soil texture maps (fig.2).

Maximization of crop yield criteria yielded to higher N input in 2008, as shown in fig 8. The average amount was 128.05 kg N ha⁻¹ in HI and 79.18 N kg ha⁻¹ in LI. High variability of N optimal rate was reported in all the fields, especially in HI plots, which had a standard deviation ≥ 45 kg ha⁻¹.

Especially in the central area of the experimental site, characterized by an inherit higher soil fertility ,higher N rates were requested to maximize the production. The average mineral N fertilizations amounted to 83.95 kg N ha⁻¹ for HI and 126.96 kg N ha⁻¹ for LI treatment. Similar N rates were simulated in 2009 (88.95 kg N ha⁻¹ in HI and 112.19 kg N ha⁻¹ LI (Tab. 11), with higher N input prescribed for the more fertile polygons (Fig. 8). Considering the previous undifferentiated fertilization, in 2008 the total mineral N amounted to 234.95 kg N ha⁻¹ in HI and 240.96 kg N ha⁻¹ in LI plots, while in the following crop season HI treatment reported 239.95 kg N ha⁻¹ and LI 226.19 kg N ha⁻¹.

This total rates did not substantially differ from the mineral N effectively provided in the experiment (266 kg N ha⁻¹ in HI and 240 kg N ha⁻¹ in LI). Apply such amount of N could be expensive for the farmer, indeed N fertilizations cost is one of the heaviest expenses of corn production, furthermore, high rates are not always related to adequate yield increases. On the other hand, high N rates could result in water nitrate pollution which can be a relevant issue in the Venice Lagoon watershed.

As suggested by Paz et al. (1999), a third strategy was applied to assess the optimum N rate able to optimize the gross margin. N optimum rate based on economic criteria resulted in lower N optimum rate that those aimed to maximize of crop yield. The average rate was reduced by 26% in 2008 and 43% in 2009 (tab. 11). As in the prescription maps aiming to optimize final production, optimum N rate is driven by soil fertility and previous uniform fertilization management in both the years. Polygons located in areas characterized by lower sand and higher soil organic matter reported higher N rates while on average LI plots requested to be fertilized almost the double than HI.

Eventually, the last approach aiming to minimize the N surplus according to the European Nitrate Directive resulted in very low or even null N rates for the majority of the polygons. In 2008 only LI plots required to be fertilized, although the average simulated rate is lower than 10 kg N ha⁻¹. In 2009 field E required almost a null fertilization (only two polygons reported an optimum rate of 10 kg N ha⁻¹), while field C required on average of 57.78 kg N

ha⁻¹ for LI treatment and 7.22 kg N ha⁻¹ for LI (Fig. 9). Furthermore, in some of the low fertility polygons even the 0 N input scenario resulted in N surplus > 0, demonstrating that in those areas even the previous uniform applied fertilizations caused over-fertilization. This criteria could be particularly useful for fields located in nitrate vulnerable zones, where farmers are allowed to fertilized with an average N amount established by the Action Plans of the European Nitrate Directive. With this approach, this average amount could be specifically managed for different zones across the field.

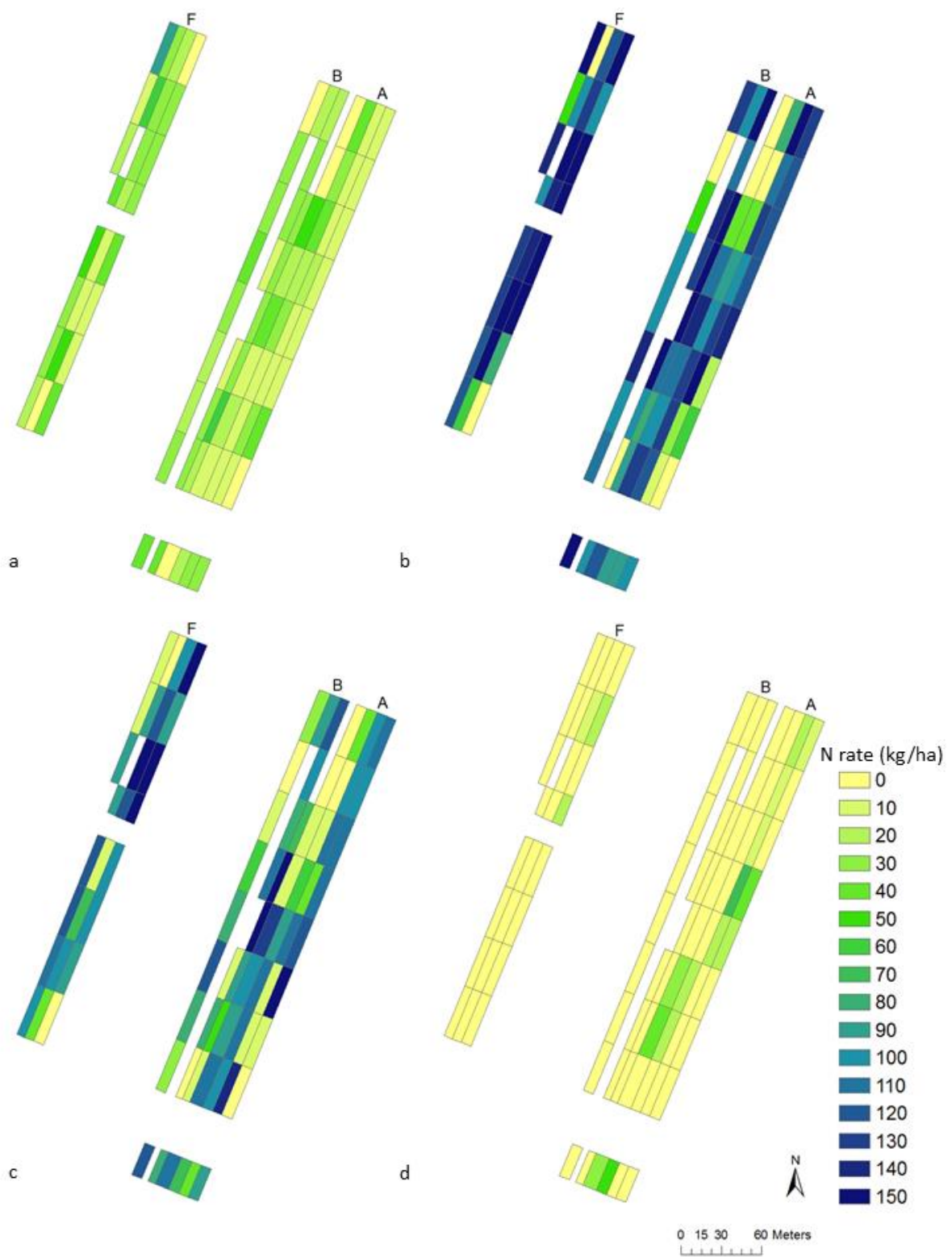


Figure 8. N fertilization prescription maps for 2008, based on N stress minimization (a); yield maximization (b); economic convenience (c) and N surplus minimization.

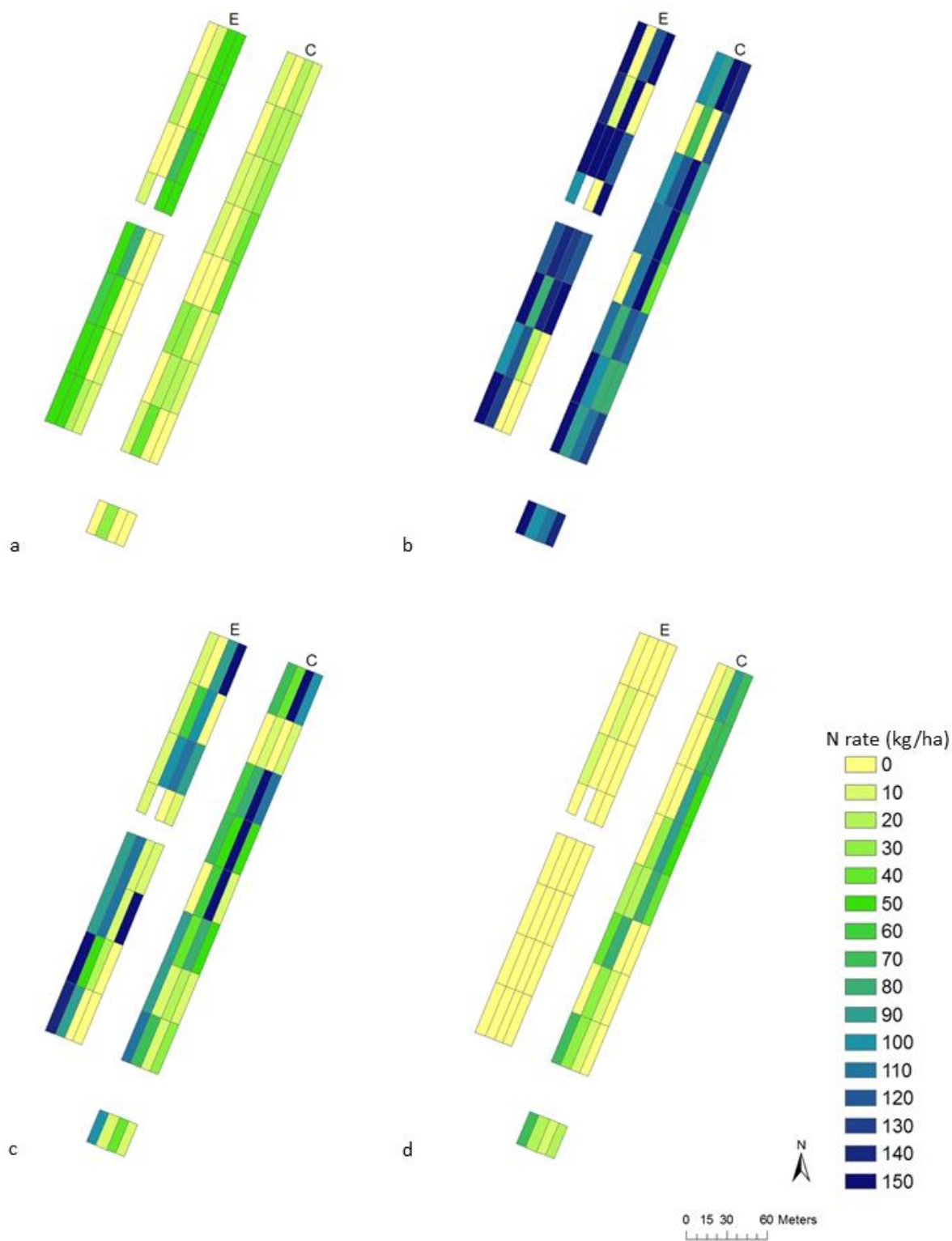


Figure 9. N fertilization prescription maps for 2009, based on N stress minimization (a); yield maximization (b); economic convenience (c) and N surplus minimization.

Tab. 11: N rates for the different fertilization strategies.

Field	N stress minimization				Yield maximization				Economic convenience				N surplus minimization			
	Average	Max	Min	St.dev.	Average	Max	Min	St.dev..	Average	Max	Min	St.dev.	Average	Max	Min	St.dev..
2008																
A																
HI	23.89	50	0	15.77	58.89	150	0	50.05	44.44	150	0	52.61	0	0	0	0
LI	11.11	20	0	4.71	121.11	150	90	14.91	100.56	120	40	18.62	21.67	70	0	19.17
Tot	17.5	50	0	13.17	90	150	0	48.17	72.5	150	0	48.19	10.83	70	0	17.3
B																
HI	28.46	60	0	15.73	91.54	150	0	49.13	50	120	0	43.01	0	0	0	0
LI	26.36	30	20	5.05	127.27	150	100	22.84	97.27	150	30	35.8	0	0	0	0
Tot	27.5	60	0	11.89	107.92	150	0	42.63	71.67	150	0	45.84	0	0	0	0
F																
HI	30	90	0	25.12	101.43	150	0	55.59	57.14	100	0	42.5	0	0	0	0
LI	26.67	50	0	11.55	132.5	150	100	16.03	123.33	150	90	21.88	4.17	20	0	7.93
Tot	28.46	90	0	19.74	115.77	150	0	44.38	87.69	150	0	47.78	1.92	20	0	5.67
2009																
C																
HI	5.56	20	0	7.05	93.89	140	0	38.37	38.33	80	0	27.92	7.22	30	0	9.58
LI	21.11	40	0	13.23	110	150	0	44.46	77.78	150	0	54.72	57.78	90	0	26.47
Tot	13.33	40	0	13.09	101.94	150	0	41.74	58.06	150	0	47.26	32.5	90	0	32.28
E																
HI	5.33	20	0	7.43	84	150	0	68.22	26.67	150	0	43.53	1.33	10	0	3.52
LI	53.75	80	50	8.85	114.38	150	0	49.12	86.25	150	0	48.29	0	0	0	0
Tot	30.32	80	0	25.88	99.68	150	0	60.14	57.42	150	0	54.47	0.65	10	0	2.5

4.4. Conclusions

When adopt model simulation for precision agriculture and site-specific application, it's essential to simulate crop growth and yield spatially. GeoSim was able to automate spatial simulations and facilitated the optimization of a point-based model for predicting yield and nitrogen stress across the fields, which makes it a very promising tool for precision agriculture applications.

Furthermore, the application of a model for precision agriculture purposes, is limited by the complexity of the input data, which are not often completely available. This appears to be particularly meaningful when running models as DSSAT, requiring a large input dataset. A lack or uncertainty on model input data could be partially overcome by the optimization of initial parameters.

GeoSim operated an optimization of soil initial water content and hydraulic parameters, providing accurate yield estimation, which was not negatively influenced by model optimization for LAI.

The incorporation of proximal sensed-derived data into the model guaranteed the accuracy of nitrogen stress simulation, due to the relationship between NDVI, LAI and N stress.

Simulating N stress could be useful in order to manage an in-season site-specific fertilization, increasing N efficiency but it could not guarantee to satisfy other criteria such as the maximum achievable yield, the economic convenience or the environmental impact of the fertilization.

4.5. References

- Basso, B., Ritchie J.T., Pierce, F.J. , Braga, R.P. and Jones, R.P. 2001. Spatial validation of crop models for precision agriculture. *Agr. Syst.* 68(2), 97-112.
- Batchelor, W.D., Basso, B. and Paz, J.O. 2002. Examples of strategies to analyze spatial and temporal yield variability using crop models. *Eu. J. Agron.* 18, 141-158.
- Carlson, T.N. and Ripley, D.A. 1997. On the relation between NDVI, fractional vegetation cover, and leaf area index. *Remote Sens. Environ.* 62, 241-256.
- Castrignanò, A., Katerji, N., Karam, F., Mastrorilli, M. and Hamdy, A. 1998. A modified version of CERES-Maize model for predicting crop response to salinity stress. *Ecol. Model.* 111, 107-120.
- Choudhury, J.K., Ahmed, N.U., Sherwood B., Idso, B.V., Reginato, R.J., and Daughtry, J.S.T. 1994. Relations between evaporation coefficients and vegetation indices studied by model simulations. *Remote Sens. Environ.* 50, 1-17.
- DeJonge, K.C., Kaleita, A.L. and Thorp, K. L. 2007. Simulating the effects of spatially variable irrigation on corn yields, costs, and revenue in Iowa. *Agric. Water Manage.* 92, 99- 109.
- Dente, A., Satalino, F.M. and Rinaldi, M. 2008. Assimilation of leaf area index derived from ASAR and MERIS data into CERES-Wheat model to map wheat yield. *Remote Sens. Environ.* 112, 1395–1407.
- DGR 1150/2011 Programma d'azione per le zone vulnerabili ai nitrati del Veneto.
- Dorigo, W.A., Zurita-Milla, R., de Wit, A.J.W., Brazile, J., Singh, R. and Schaepman, M.E. 2007. A review on reflective remote sensing and data assimilation techniques for enhanced agroecosystem modeling. *Int. J. Appl. Earth Obs. Geoinf.* 9 (2), 165–193.
- EC-Council Directive, 1991. Council Directive 91/676/EEC Concerning the Protection of Waters Against Pollution Caused by Nitrates from Agricultural Sources.
- Fang, H., Liang, S. and Hoogemboom, G. 2011. Integration of MODIS LAI and vegetation index products with the CSM–CERES–Maize model for corn yield estimation. *Int. J. Remote Sens.* 32, 1039-1065.

- Gitelson, A.A., Viña, A., Arkebauer, T.J., Rundquist, D.C., Keydan, G. and Leavitt, B. 2003. Remote estimation of leaf area index and green leaf biomass in maize canopies. *Geophys. Res. Lett.* 30, 1248.
- Godwin, R.J., Wood, G.A., Taylor, J.C., Knight, S.M. and Welsh, J.P. 2003. Precision farming of cereal crops: a review of a six year experiment to develop management guidelines. *Biosyst. Eng.* 84, 375-391.
- Goovaerts, P. 1997. *Geostatistics for Natural Resources Evaluation*. Oxford University Press, New York.
- Heege, H.J., Reush, S. and Thiessen, E. 2008. Prospects and results for optical systems for site-specific on-the-go control of nitrogen-top-dressing in Germany. *Precis. Agric.* 9, 115–131.
- Hodges, T., Botner, D., Sakamoto, C. and Hayshaung, J. 1987. Using the CERES-Maize model to estimate production for the U.S. Corn Belt. *Agric. Forest Meteorol.* 40, 293-303.
- Hong, N., White, J.G., Weisz, R., Crozier, C.R., Gumpertz, M.L. and Cassel, D. K. 2006. Remote sensing-informed variable-rate nitrogen management of wheat and corn: agronomic and groundwater outcomes. *Agron. J.* 98:,327-338.
- Hoogenboom, G., Jones, J. W., Wilkens, P.W., Porter, C.H., Boote, K. ., Hunt, L.A., Singh, U., Lizaso, J.L., White, J.W., Uryasev, O., Royce, F.S., Ogoshi, R., Gijisman, A.J., Tsuji, G.Y. and Koo, J. 2012. *Decision Support System for Agrotechnology Transfer (DSSAT) Version 4.5 [CD-ROM]*. University of Hawaii, Honolulu, Hawaii.
- Ines, A.V. M., Das. N.N., Hansen, J.W. and Njoku. E.J. 2013. Assimilation of remotely sensed soil moisture and vegetation with a crop simulation model for maize yield prediction. *Remote Sens. Environ.* 138, 149–164.
- Jones, D.D. and Barnes, E. M. 2000. Fuzzy composite programming to combine remote sensing and crop models for decision support in precision crop management. *Agric. Sys.* 65,137-158.
- Jones, C.A. and Kiniry, J.R. 1986. *CERES-Maize: A simulation model of maize growth and development*. Texas A&M University Press, College Station, Texas, USA.

- Launay, M. and Guerif, M. 2005. Assimilating remote sensing data into a crop model to improve predictive performance for spatial applications. *Agri. Ecosyst. Environ.* 111, 321-339.
- Ma, B.L., Morrison M.J. and Dwyer, L.M. 1996. Canopy light reflectance and field greenness to assess nitrogen fertilization and yield of corn. *Agron. J.* 88, 915-920.
- Ma, H., Huang, J., Zhu, D., Li, J., Su W., Zhang, C. and Fan, J. 2013. Estimating regional winter wheat yield by assimilation of time series of HJ-1 CCD NDVI into WOFOST-ACRM model with Ensemble Kalman Filter. *Math. Comput. Model.* 58, 753-764.
- Maas, S.J., 1988. Use of remotely-sensed information in agricultural crop growth models. *Ecol. Model.* 41, 247-268.
- Martin, K.L., Girma, K., Freeman, K.W., Teal, R.K., Tubana, B., Arnall, D.B., Chung, B., Walsh, O., Solie, J.B., Stone, M.L. and Raun., W.R. 2007. Expression of variability in corn as influenced by growth stage using optical sensor measurements. *Agron. J.* 99, 384-389.
- Miao, Y., Mulla, D.J., Batchelor, D.W., Paz, J. O., Robert, P. C and Wiebers, M. 2006. Evaluating management zone optimal nitrogen rates with a crop growth model. *Agron. J.* 98, 545-553.
- Mulla, D.J., Bhatti, A.U., Hammond, M.W. and Benson, J.A. 1992. A comparison of winter wheat yield and quality under uniform versus spatially variable fertilizer management. *Agric. Ecosyst. Environ.* 38, 301-311.
- Norman, J.M., Jarvis, P.G., 1975. Photosynthesis in Sitka Spruce *Picea sitchensis* (Bong.) Carr., V. Radiation penetration theory and a test case. *J. Appl. Ecol.* 12, 839-878.
- Ortiz-Monasterio, J.I. and Raun, W.R. 2007. Reduced nitrogen for improved farm income for irrigated spring wheat in the Yaqui Valley, Mexico, using sensor based nitrogen management. *J, Agr, Sci*, 145,215-222.
- Paz, J.O., Batchelor, W.D., Babcock, B.A., Colvin, T.S., Logsdon, S.D., Kaspar, T.C. and Kaler, D.L. 1999. Model-based technique to determine variable rate nitrogen for corn. *Agric. Syst.* 61, 69-75.

- Persson, T., Garcia, Y., Garcia, A., Paz, J, Jones, J. and Hoogenboom, G. 2009. Maize ethanol feedstock production and net energy value as affected by climate variability and crop management practices. *Agric, Syst.* 100.11-21.
- Raes, D., Steduto, P., Hsiao, T.C. and Fereres, E. 2009. AquaCrop—The FAO Crop Model to Simulate Yield Response to Water: II. Main Algorithms and Software Description. *Agron. J.* 101, 438–447.
- Raun, W.R., Solie, J.B., Stone, M.L., Martin, K.L., Freeman, K.W., Mullen, R.W. Zhang, H., Schepers, J.S. and Johnson, J.V. 2005. Optical sensor-based algorithm for crop nitrogen fertilization. *Commun. Soil Sci. Plan.* 36, 2759-2781.
- Raun, W.R., Solie, J. B., Johnson, J. ., Stone, M.L., Mullen, R.W., Freeman, K.W., Thomason, W.E., and Lukina, E.V. 2002. Improving nitrogen use efficiency in cereal grain production with optical sensing and variable rate application. *Agron. J.* 94, 815-820.
- Rouse, J.W., Haas, R.H., Schell, J.A., Deering, D.W. 1973. Monitoring vegetation systems in the Great Plains with ERTS. In: Third ERTS symposium. NASA SP-3 51, 309–317.
- Ruiz-Nogueira, B., Boote, K.J. and Sau, F. 2001. Calibration and use of CROPGRO-soybean model for improving soybean management under rainfed conditions. *Agric. Syst.* 68,151-173.
- Seidl, M.S., Paz, J.O. and Batchelor, W.D. 2000. Integrating remotely sensed images to improve spatial crop model calibration. Paper No. 00-3039, ASAE, St Joseph, USA.
- Solie, J.B., Monore, A.D., Raun, W.R. and Stone, M.L. 2012. Generalized algorithm for variable-rate nitrogen application in cereal grains. *Agron. J.* 104, 878-387.
- Steduto, P., Hsiao, T.C., Dirk, R. and Fereres, E. 2009. AquaCrop-the FAO crop model to simulate yield response to water: I. Concepts and underlying principles. *Agron. J.* 101, 426–437.
- Teal, R.K., Tubana, B., Girma, K., Freeman, K. W., Arnall, D. B., Walsh, O. and Raun, W.R 2006. In-season prediction of corn grain yield potential using normalized difference vegetation index. *Agron. J.* 98, 1488-1494.

- Thorp, K.R., Batchelor, W.D., Paz, J.O., Steward, B.L. and Caragea, P.C. 2006. Methodology to link production and environmental risks of precision nitrogen management strategies in corn. *Agric. Syst.* 89, 272–298.
- Thorp, K.R., DeJonge, K.C., Kaleita, A., Batchelor, W.D and Paz, J.O. 2008. Methodology for the use of DSSAT models for precision agriculture decision support. *Comput. Electron. Agric.* 64, 276–285.
- Thorp, K.R. and Bronson, K.F. 2013. A model-independent open-source geospatial tool for managing point-based environmental model simulations at multiple spatial locations. *Environmental Modelling & Software* 50:26-35.
- Thorp, K.R., Hunsaker, D.J. and French, A.N. 2010. Assimilating leaf area index estimates from remote sensing into a simulation of a cropping system model. *Trans ASABE* 53:251-262.
- Thorp, K.R., Hunsaker, D.J., French, A.N., Bautista, E. and Bronson, K. F. 2014. Intregrating geospatial data and cropping system simulation within a geographic information system to analyze spatial seed cotton yield, water use, and irrigation requirements. *Precision Agric.* 16, 532-557.
- Tojo Soler, C.M., Sentelhas, P.C. and Hoogenboom, G. 2007. Application of the CSM-CERES-Maize model for planting date evaluation and yield forecasting for maize grown off-season in a subtropical environment. *Eu. J. Agron.* 27,165-177.

Cited Website

www.agerborsamerici.it

Chapter V

Overall conclusions

A drawback in applying N VRA arises from the difficulties to predict precisely final crop yield at the time of fertilizing (Heege, 2013). This could have negative effect in case of both fertilization based on management zones (MZ) and on the go proximal sensing. Indeed unexpected weather conditions affect the yield potential and result in over- or under-fertilization, with economic and environmental negative consequences. The incapacity of exploit N resources could result in a largely positive N balance in the soil and subsequently in N leaching. This represents a serious risk of nitrate water pollution, especially in fields located in nitrate vulnerable zones, such as the Venice Lagoon watershed.

The ability of predict final production could be particularly relevant for crops grown in areas which represent limits for their cultivation, as durum wheat grown in North Italy. There irregular rainfall and high temperatures could highly and unexpectedly impacted grain quality and quantity.

In the first experiment N-VRA based on management zones was managed in a two-years durum wheat experiment. High N input confirmed to be a leverage to reach high grain yield with satisfactory quality levels, but with risks for the environment, especially in case of unexpected weather condition. VRA was able to mitigate only partially the impact of weather, indeed the sever water stress occurred during the first year resulted in low production levels and subsequently high N surplus in the soil. Furthermore, the uncertainty in weather conditions negatively influence the temporal stability of the MZs between the two seasons, both in term of quantity and quality indicators.

Coupling medium- weather forecasts and crop modelling allows to predict crop yield and modulate N input accordingly. After running simulations optimum N rate can be evaluated on order to maximize the yield or the profit, or minimize N losses in the environment.

In Chapter III a new approach for integration of proximal sensing (NDVI), medium weather forecast and crop modelling on durum wheat was proposed. The algorithm developed is a break-through in respect to traditional N VRA algorithms, because it takes into account, along with spatial variation of crop nutritional status at NDVI sensing time and early N uptake, also crop response to weather conditions after sensing. The model, previously calibrated with data collected in the previous two years, was run in each MZ with weather forecast to evaluate economic N optimum rate. NDVI was able to capture spatial variability of crop nutritional status and correct predicted optimum N rate, accordingly. This N-VRA allowed to level off spatial variability of grain yield and protein content, but the high N leaching caused by high precipitation amount occurred was not correctly predicted by the model, and resulted in an over-estimation of the yield and optimum N rate. Consequently, N surplus in the soil was higher than expected. Nevertheless, N VRA still showed higher environmental sustainability than a High N uniform rate application.

Coupling spectral sensing data and crop modelling could also be useful to improve model simulations for N-VRA. In Chapter IV an approach of integration of proximal sensing and crop modelling to improve estimation of N stress on corn was evaluated. After being optimize across the field to correctly simulate corn yield, the model was optimize to optimized to match simulated LAI with LAI derived from NDVI measurements. The well known relationship between NDVI, LAI and crop N status ensured to accurately estimated crop N stress. A model able to accurately predict crop N stress could be apply using weather forecasts in order to evaluate N rates able to minimize it, to maximize farmers' income, or minimize the environmental impact of fertilization.

The application of crop modelling for N VRA purposes demonstrated its potential in increase fertilization efficiency its environmental sustainability, but some limits were underlined. Firstly, crop models need to be able to simulate crop growth and yield over different locations and weather conditions, which required an adequate calibration with data previously collected.

In addition, it is essential to predict crop growth and yield spatially. Traditional crop models are point-based, and they require independent calibrations and simulations for each

homogeneous zone. GeoSim confirmed to be an useful tool to automate the process of model optimization, calibration and simulation.

An other limitation is related to the complexity level of the input data, which are not often completely available. This appears to be particularly meaningful when running models as DSSAT, requiring a large input dataset. A lack on model input data could be partially overcome by an optimization of the initial parameters, or further elaborations and assumptions, but this increase the level of uncertainty of the model.

5.1 References

Heege, H.J. 2013. Precision in Crop Farming. Site specific concepts and sensing methods: application and results. Hernan J. Heege ed.